Chapter 2
Component Modeling with State-Space Method

2.1 Basic Knowledge About State-Space Modeling Method

A state-space representation, also known as the 'time-domain approach', is a mathematical model of a physical system as a set of input, output, and state variables related to first-order differential equations. To abstract from the number of inputs, outputs, and states, these variables are expressed as vectors. Additionally, if the dynamical system is linear, time-invariant, and finite-dimensional, then the differential and algebraic equations may be written in matrix form [1]. The state-space representation provides a convenient and compact way to model and analyze systems with multiple inputs and outputs. With p inputs and q outputs, we can encode all the information about a system instead of $q \times p$ Laplace transforms. Unlike the frequency-domain approach, the use of the state-space representation is not limited to systems with linear components and zero initial conditions [2].

The most general state-space representation of a linear system with m inputs, n outputs, and p state variables is written in the following form [3]:

$$\dot{X}(\tau) = A \cdot X(\tau) + B \cdot U(\tau) \tag{2.1}$$

$$Y(\tau) = C \cdot X(\tau) + D \cdot U(\tau) \tag{2.2}$$

where

$U(\tau)$ is input variable vector, $U(\tau) = [u_1(\tau), u_2(\tau), \ldots, u_{\mathrm{m}}(\tau)]^T$;
$Y(\tau)$ is output variable vector, $Y(\tau) = [y_1(\tau), y_2(\tau), \cdots, y_{\mathrm{n}}(\tau)]^T$;
$X(\tau)$ is state variable vector, $X(\tau) = \left[x_1(\tau), x_2(\tau), \cdots, x_{\mathrm{p}}(\tau)\right]^T$;
A is the state (or system) matrix, $\dim[A] = p \times p$;
B is the input matrix, $\dim[B] = p \times m$;
C is the output matrix, $\dim[C] = n \times p$;
D is the feed-forward matrix, $\dim[D] = n \times m$;

Y. Yao and Y. Yu, *Modeling and Control in Air-conditioning Systems*,
Energy and Environment Research in China, DOI 10.1007/978-3-662-53313-0_2

The internal state variables are the smallest possible subset of system variables that can represent the entire state of the system at any given time. The minimum number of state variables required to represent a given system is usually equal to the order of the system's defining differential equation. If the system is represented in transfer function form, the minimum number of state variables is equal to the order of the transfer function's denominator after it has been reduced to a proper fraction [4].

In this chapter, the state-space method is firstly employed to develop dynamic models of the main components in a general HVAC system including water-to-air heat exchanger, refrigeration system, cooling tower, air-conditioned space, air duct, water pipe, and valves (or dampers). Afterward, the method of component models' integration is introduced and an example of HVAC system modeling based on the component models is given.

2.2 Modeling for HVAC Components

2.2.1 Water-to-Air Heat Exchanger

Water-to-air heat exchanger is used for air cooling with or without accompanying dehumidification. They work under dry conditions (without dehumidification) when the external surface temperature is lower than the air dew-point temperature or otherwise under wet conditions (with dehumidification). For general comfort conditioning, cooling, and dehumidifying, the extended-surface (finned) heat exchanger design is the most popular. In finned heat exchanger, the external surface of the tubes is primary and the fin surface is secondary. The primary surface generally consists of rows of round tubes or pipes that may be staggered or placed in line with respect to the airflow. The inside surface of the tubes is usually smooth and plain, but some heat exchanger designs have various forms of internal fins or turbulence promoters to enhance the performance. The individual tube passes in a heat exchanger are usually interconnected by return bends to form the serpentine arrangement of multi-pass tube circuits [5]. Heat exchangers for water, aqueous glycol, or halocarbon refrigerants usually have aluminum fins on copper tubes, or copper fins on copper tubes, or aluminum fins on aluminum tubes. The outside diameters of core tube are commonly 8, 10, 12.5, 16, 20, and 25 mm, with fins spaced 1.4–6.4 apart. Tube spacing ranges from 15 to 75 mm, depending on the width of individual fins and on the other performance considerations.

Figure 2.1 shows the physical map of a water-to-air heat exchanger which is taken as the modeling object. The objective of the modeling is to study the dynamic characteristics of the water-to-air heat exchanger when subjected to perturbations of different inlet variables including entering air temperature and humidity, entering water temperature, and flow rate of the two fluids.

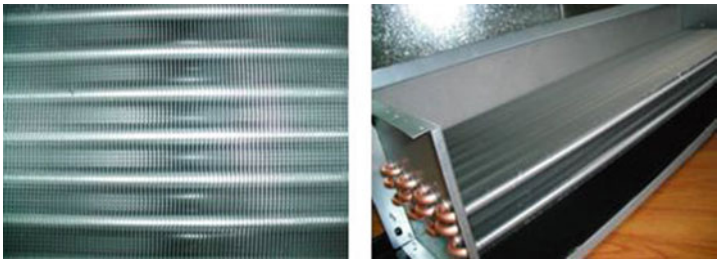

Fig. 2.1 Physical map of a water-to-air heat exchanger

2.2.1.1 Model Development [6]

1) Assumptions and basic equations

Figure 2.2 shows the schematic diagram of water-to-air heat exchanger for modeling. Further, the following assumptions are necessary to be made for the convenience of modeling.

(1) Moisture air is treated as a mixture of ideal gases. The specific heat and density of air are considered as constants in the process of heat and mass transfer;
(2) Air-side heat transfer coefficient includes the additional thermal resistance due to the presence of partially or completely wet extended surfaces;
(3) Under wet-condition mode, the air on the surface of coils and fins is considered as saturated state;
(4) Temperature and humidity of the air change linearly from the inlet to the outlet of the heat exchanger. So does temperature of the water [7].

Thus, a series of equations can be established according to the law of energy and mass conservation.

(1) *Mass and energy equation for water passing through coils*:

$$G_{\mathrm{w,E}} = G_{\mathrm{w,L}} = G_{\mathrm{w}} \tag{2.3}$$

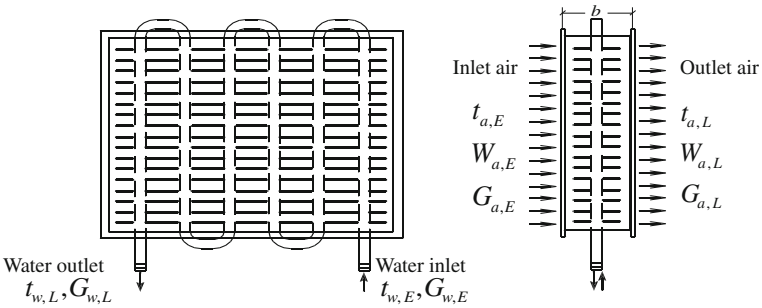

Fig. 2.2 Schematic diagram of water-to-air heat exchanger for modeling

$$\frac{1}{2}\rho_{\mathrm{w}}c_{\mathrm{w}}A_{\mathrm{w}}l\frac{\mathbf{d}(t_{\mathrm{w,L}}+t_{\mathrm{w,E}})}{\mathbf{d}\tau}=G_{\mathrm{w,E}}c_{\mathrm{w}}(t_{\mathrm{w,E}}-t_{\mathrm{w,L}})+a_{\mathrm{gw}}A_{\mathrm{i}}\left(t_{\mathrm{g}}-\frac{t_{\mathrm{w,E}}+t_{\mathrm{w,L}}}{2}\right) \tag{2.4}$$

(2) *Mass and energy equation for air passing through heat exchanger*:

$$G_{\mathrm{a,E}}=G_{\mathrm{a,L}}=G_{\mathrm{a}} \tag{2.5}$$

• Dry-condition process:

$$W_{\mathrm{a,E}}=W_{\mathrm{a,L}} \tag{2.6a}$$

$$\frac{1}{2}\varepsilon_{\mathrm{a}}\rho_{\mathrm{a}}c_{\mathrm{a}}A_{\mathrm{a}}b\frac{\mathbf{d}(t_{\mathrm{a,L}}+t_{\mathrm{a,E}})}{\mathbf{d}\tau}=G_{\mathrm{a,E}}c_{\mathrm{a}}(t_{\mathrm{a,E}}-t_{\mathrm{a,L}})+a_{\mathrm{ga}}A_{\mathrm{o}}\left(t_{\mathrm{m}}-\frac{t_{\mathrm{a,E}}+t_{\mathrm{a,L}}}{2}\right) \tag{2.6b}$$

• Wet-condition process:

$$\frac{1}{2}\varepsilon_{\mathrm{a}}\rho_{\mathrm{a}}bA_{\mathrm{a}}\frac{\mathbf{d}(W_{\mathrm{a,L}}+W_{\mathrm{a,E}})}{\mathbf{d}\tau}=G_{\mathrm{a,E}}(W_{\mathrm{a,E}}-W_{\mathrm{a,L}})+\lambda_{\mathrm{m}}A_{\mathrm{o}}\left(W_{\mathrm{gb}}-\frac{W_{\mathrm{a,E}}+W_{\mathrm{a,L}}}{2}\right) \tag{2.7a}$$

$$\frac{1}{2}\varepsilon_{\mathrm{a}}\rho_{\mathrm{a}}bA_{\mathrm{a}}\frac{\mathbf{d}(h_{\mathrm{a,L}}+h_{\mathrm{a,E}})}{\mathbf{d}\tau}=G_{\mathrm{a,E}}(h_{\mathrm{a,E}}-h_{\mathrm{a,L}})+a_{\mathrm{ga}}A_{\mathrm{o}}\left(t_{\mathrm{m}}-\frac{t_{\mathrm{a,E}}+t_{\mathrm{a,L}}}{2}\right)+q_{\mathrm{r}}A_{\mathrm{o}}\lambda_{\mathrm{m}}\left(W_{\mathrm{gb}}-\frac{W_{\mathrm{a,E}}+W_{\mathrm{a,L}}}{2}\right) \tag{2.7b}$$

(3) *Energy equation for coils and fins*

• Dry-condition process:

$$M_{\mathrm{g}}c_{\mathrm{g}}\frac{\mathbf{d}t_{\mathrm{g}}}{\mathbf{d}\tau}=a_{\mathrm{gw}}A_{\mathrm{i}}\left(\frac{t_{\mathrm{w,E}}+t_{\mathrm{w,L}}}{2}-t_{\mathrm{g}}\right)+a_{\mathrm{ga}}A_{\mathrm{o}}\left(\frac{t_{\mathrm{a,E}}+t_{\mathrm{a,L}}}{2}-t_{\mathrm{m}}\right) \tag{2.8a}$$

• Wet-condition process:

$$M_{\mathrm{g}}c_{\mathrm{g}}\frac{\mathbf{d}t_{\mathrm{g}}}{\mathbf{d}\tau}=a_{\mathrm{gw}}A_{\mathrm{i}}\left(\frac{t_{\mathrm{w,E}}+t_{\mathrm{w,L}}}{2}-t_{\mathrm{g}}\right)+a_{\mathrm{ga}}A_{\mathrm{o}}\left(\frac{t_{\mathrm{a,E}}+t_{\mathrm{a,L}}}{2}-t_{\mathrm{m}}\right)+q_{\mathrm{r}}A_{\mathrm{o}}\lambda_{\mathrm{m}}\left(\frac{W_{\mathrm{w,E}}+W_{\mathrm{w,L}}}{2}-W_{\mathrm{gb}}\right) \tag{2.8b}$$

In Eqs. (2.3) through (2.8), the symbol 'G' stands for flow rate, kg/s; 'c' for mass specific heat, J/(kg °C); 'A' for area, m^2; 'h' for enthalpy, J/kg; 'l' for length of coiled tube, m; 'b' for width of heat exchanger, m; 't' for temperature, °C; 'W' for

air humidity, kg/(kg dry air); 'M' for mass, kg; 'q_r' for latent heat of condensation of water vapor, J/kg; 'a_{gw}' for heat transfer coefficient on the water side, W/(m^2 °C); 'a_{ga}' for heat transfer coefficient on the air side, W/(m^2 °C); 'λ_m' for mass transfer coefficient, kg/ (m^2/s); 'τ' for time, s; 'ρ' for density, kg/m^3; and 'ε_a' for air volume ratio in heat exchanger. The subscript 'a' stands for air; 'w' for water; 'g' for shell wall of heat exchanger; 'E' for inlet; 'L' for outlet; 'm' fins of coil; 'gb' for saturated air near external surface of heat exchanger; 'o' for air-side surface of heat exchanger; and 'i' for water-side surface of heat exchanger.

2) Parameter determination and linearization

Two kinds of variables are considered in the equations: the fundamental and the lumped. The fundamental variables include the temperature and humidity of inlet and exit air ($t_{a,E}$, $W_{a,E}$, $t_{a,L}$, $W_{a,L}$), the temperature of inlet and exit water ($t_{w,E}$, $t_{w,L}$), and the air and water flow rates (G_a and G_w). These variables can be considered as the summation of initial value (θ_o) and a small increment ($\Delta\theta$):

$$\theta = \theta_o + \Delta\theta \tag{2.9}$$

where θ denotes, $t_{a,E}$, $W_{a,E}$, $t_{a,L}$, $W_{a,L}$, $t_{w,E}$, $t_{w,L}$, G_a, and G_w, respectively.

The lumped variables include the coefficients of heat and mass transfer between fluids and heat exchanger (i.e., a_{gw}, a_{ga} and λ_m), which are usually expressed as an equation dependent on the fluid flow rate (G_a or u_a, G_w or u_w), respectively, as below:

$$Nu_w = C_1 Re_w^{n_1} \tag{2.10}$$

$$Nu_a = C_2 Re_a^{n_2} \tag{2.11}$$

$$Nu_d = C_3 Re_a^{n_3} \tag{2.12}$$

where $C_1, C_2, C_3, n_1, n_2, n_3$ are empirical constants that can be determined with experimental data; $Nu_w = \frac{2a_{gw}r_i}{\lambda_w}$; $Re_w = \frac{2u_w r_i}{v_w}$; $Re_a = \frac{2u_a r_d}{v_a}$; $Nu_d = \frac{2\lambda_m r_d}{\rho_a D_{w,a}}$. $Re_a = \frac{2u_a r_d}{v_a} = \frac{2G_a r_d}{v_a \rho_a A_a}$; $r_d = \frac{(S-2r_i)(e-\delta_c)}{(S-2r_i)+(e-\delta_c)}$. The symbol '$\lambda_w$' is heat conductivity coefficient of water, W/ (m °C); 'r_i' is inner radius of coil, m; 'u_w' and 'u_a' are velocities of water and air, respectively, m/s; 'v_w' and 'v_a' are kinematic viscosity coefficients of water and air, respectively, m^2/s; '$D_{w,a}$' is mass diffusivity of water vapor in the air, *m^2/s;* 'S' is finned tube center spacing of surface of heat exchanger, *m;* 'e' is fin spacing of heat exchanger, *m;* and 'δ_c' is fin thickness of heat exchanger, m.

Thus, the lumped variables can be linearized by using the first-order Taylor series:

$$\sigma = \sigma_o + \left(\frac{\partial\sigma}{\partial\theta'}\right)_o \Delta\theta' \tag{2.13}$$

where σ stands for a_{gw}, a_{ga} and λ_m, respectively; θ' for u_a (G_a) or u_w (G_w); and Δ for increment of variables.

The efficiency of sensible heat exchange, η_s, is defined as follows:

$$\eta_s = \frac{\left(t_m - \frac{t_{a,E} + t_{a,L}}{2}\right)}{\left(t_g - \frac{t_{a,E} + t_{a,L}}{2}\right)} \tag{2.14}$$

where t_m is the average surface temperature of fins. η_s is mainly related to the structure of finned heat exchanger. For a specific water-to-air heat exchanger, η_s can be considered as a constant, normally as 0.7–0.8.

According to Eq. (2.14), t_m can be expressed as follows:

$$t_m = \eta_s t_g - (1 - \eta_s)\frac{t_{a,E} + t_{a,L}}{2} \tag{2.15}$$

The humidity of saturated air, W_{gb}, on the fins can be expressed by Eq. (2.16).

$$W_{gb} = a_1 t_m^3 + a_2 t_m^2 + a_3 t_m + a_4 \tag{2.16}$$

where the coefficients, a_1, a_2, a_3 and a_4, are obtained as 0.0008, −0.0190, 0.7287, and 1.6910, respectively, through data fitting of the thermodynamic properties of moist air. The maximum relative error of Eq. (2.16) compared with the data in ASHRAE Handbook [8] is less than 3.5 % when the temperature changes from 5 to 40 °C.

By using the first-order Taylor series, Eq. (2.16) can be converted into a linear one as below:

$$W_{gb} = (W_{gb})_o + \left(3a_1 t_m^2 + 2a_2 t_m + a_3\right)_o \Delta t_m \tag{2.17}$$

Let $\beta_1 = \left(3a_1 t_m^2 + 2a_2 t_m + a_3\right)_o$, Eq. (2.17) can be written as:

$$W_{gb} = (W_{gb})_o + \beta_1 \Delta t_m \tag{2.18}$$

The enthalpy of moisture air, h_a, can be calculated by:

$$h_a = c_a t_a + (2501 + 1.84 t_a) \cdot W_a \tag{2.19}$$

Let $\beta_2 = (2501 + 1.84 t_a)$, Eq. (2.19) can be simplified as follows:

$$h_a = c_a t_a + \beta_2 W_a \tag{2.20}$$

Since the value of $1.84 t_a$ is very small compared with 2501, β_2 can be considered as a constant dependent on the initial air temperature.

The latent heat of condensation of water vapor (q_r: J/kg) can be calculated by Eq. (2.21).

$$q_r = (2501 - 2.35t_a) \times 10^3 \tag{2.21}$$

Since the air temperature (t_a) changes in a small range, q_r can be similarly equal to a constant as well, i.e., q_r = 2,441,250.

3) State-space representation

Through parameter linearization and removing the high-order item (product of two increment items), Eqs. (2.3) through (2.8) can be transformed as follows:

For dry-condition process

$$T_w \frac{\mathbf{d}\Delta t_{w,L}}{\mathbf{d}\tau} = X_1\Delta t_{w,L} + X_2\Delta t_g + X_3\Delta t_{w,E} + X_4\Delta G_{w,E} + \xi_{\Delta t_{w,L,dry}} \tag{2.22}$$

$$T_a \frac{\mathbf{d}\Delta t_{a,L}}{\mathbf{d}\tau} = Y_{dry,1}\Delta t_{a,L} + Y_{dry,2}\Delta t_g + Y_{dry,3}\Delta t_{a,E} + Y_{dry,4}\Delta G_{a,E} + \xi_{\Delta t_{a,L,dry}} \tag{2.23}$$

$$\begin{aligned} T_g \frac{\mathbf{d}\Delta t_g}{\mathbf{d}\tau} = {} & Z_{dry,1}\Delta t_{w,L} + Z_{dry,2}\Delta t_{a,L} + Z_{dry,3}\Delta t_g + Z_{dry,4}\Delta t_{a,E} \\ & + Z_{dry,5}\Delta t_{w,E} + Z_{dry,6}\Delta G_{w,E} + Z_{dry,7}\Delta G_{a,E} \end{aligned} \tag{2.24}$$

$$\Delta G_{w,L} = \Delta G_{w,E} \tag{2.25}$$

$$\Delta G_{a,L} = \Delta G_{a,E} \tag{2.26}$$

$$\Delta W_{a,L} = \Delta W_{a,E} \tag{2.27}$$

For wet-condition process

$$T_w \frac{\mathbf{d}\Delta t_{w,L}}{\mathbf{d}\tau} = X_1\Delta t_{w,L} + X_2\Delta t_g + X_3\Delta t_{w,E} + X_4\Delta G_{w,E} + \xi_{\Delta t_{w,L,wet}} \tag{2.28}$$

$$\begin{aligned} T_a \frac{\mathbf{d}\Delta t_{a,L}}{\mathbf{d}\tau} = {} & Y_{wet,1}\Delta t_{a,L} + Y_{wet,2}\Delta W_{a,L} + Y_{wet,3}\Delta t_g + Y_{wet,4}\Delta t_{a,E} \\ & + Y_{wet,5}\Delta G_{a,E} + Y_{wet,6}\Delta W_{a,E} + \xi_{\Delta t_{a,L,wet}} \end{aligned} \tag{2.29}$$

$$\begin{aligned} T_m \frac{\mathbf{d}\Delta W_{a,L}}{\mathbf{d}\tau} = {} & M_{wet,1}\Delta t_{a,L} + M_{wet,2}\Delta W_{a,L} + M_{wet,3}\Delta t_g + M_{wet,4}\Delta t_{a,E} \\ & + M_{wet,5}\Delta G_{a,E} + M_{wet,6}\Delta W_{a,E} + \xi_{\Delta W_{a,L,wet}} \end{aligned} \tag{2.30}$$

$$\begin{aligned} T_g \frac{\mathbf{d}\Delta t_g}{\mathbf{d}\tau} = {} & Z_{wet,1}\Delta t_{w,L} + Z_{wet,2}\Delta t_{a,L} + Z_{wet,4}\Delta t_g + Z_{wet,5}\Delta t_{a,E} + Z_{wet,6}\Delta t_{w,E} \\ & + Z_{wet,7}\Delta G_{w,E} + Z_{wet,8}\Delta G_{a,E} + Z_{wet,9}\Delta W_{a,E} \end{aligned} \tag{2.31}$$

$$\Delta G_{w,L} = \Delta G_{w,E} \tag{2.32}$$

$$\Delta G_{a,L} = \Delta G_{a,E} \tag{2.33}$$

All coefficients in Eqs. (2.22) through (2.31) are listed in Table 2.1. Combining Eqs. (2.22) through (2.33), the state-space equation for water-to-air heat exchanger can be expressed by Eq. (2.34):

$$\dot{x}_{coil} = A_{coil} \cdot x_{coil} + B_{coil} \cdot u_{coil} + \xi_{coil} \tag{2.34}$$

And the corresponding output equation is written as follows:

$$y_{coil} = C_{coil} \cdot x_{coil} + D_{coil} \cdot u_{coil} \tag{2.35}$$

To transform into the standard form of state-space representation, Eq. (2.34) can be written as follows:

$$\dot{x}_{coil} = A_{coil}(x_{coil} + A_{coil}^{-1}\xi_{coil}) + B_{coil}u_{coil} \tag{2.36}$$

Let $X_{coil} = x_{coil} + A_{coil}^{-1}\xi_{coil}$, we have $x_{coil} = X_{coil} - A_{coil}^{-1}\xi_{coil}$. Thus, the standard state-space model for water-to-air heat exchanger can be obtained as follows:

$$\dot{X}_{coil} = A_{coil}X_{coil} + B_{coil}u_{coil} \tag{2.37}$$

$$y_{coil} = c_{coil}X_{coil} + D_{coil}u_{coil} - C_{coil}A_{coil}^{-1}\xi_{coil} \tag{2.38}$$

For the dry-condition process:

$$x_{coil} = [\Delta t_{w,L}, \Delta t_{a,L}, \Delta t_g]^T;\ y_{coil} = [\Delta t_{w,L}, \Delta G_{w,L}, \Delta t_{a,L}, \Delta W_{a,L}, \Delta G_{a,L}]^T;$$

$$u_{coil} = [\Delta t_{w,E}, \Delta G_{w,E}, \Delta t_{a,E}, \Delta W_{a,E}, \Delta G_{a,E}]^T;\ \xi = \left[\xi_{\Delta t_{w,L,dry}}, \xi_{\Delta t_{a,L,dry}}, 0\right]^T;$$

$$A_{coil} = \begin{bmatrix} \frac{X_1}{T_w} & 0 & \frac{X_2}{T_w} \\ 0 & \frac{Y_{dry,1}}{T_a} & \frac{Y_{dry,2}}{T_a} \\ \frac{Z_{dry,1}}{T_g} & \frac{Z_{dry,2}}{T_g} & \frac{Z_{dry,3}}{T_g} \end{bmatrix};\ B_{coil} = \begin{bmatrix} \frac{X_3}{T_w} & \frac{X_4}{T_w} & 0 & 0 & 0 \\ 0 & 0 & \frac{Y_{dry,3}}{T_a} & 0 & \frac{Y_{dry,4}}{T_a} \\ \frac{Z_{dry,5}}{T_g} & \frac{Z_{dry,6}}{T_g} & \frac{Z_{dry,4}}{T_g} & 0 & \frac{Z_{dry,7}}{T_g} \end{bmatrix};$$

$$C_{coil} = \begin{bmatrix} 1 & 0 & 0 \\ 0 & 0 & 0 \\ 0 & 1 & 0 \\ 0 & 0 & 0 \\ 0 & 0 & 0 \end{bmatrix};\ D_{coil} = \begin{bmatrix} 0 & 0 & 0 & 0 & 0 \\ 0 & 1 & 0 & 0 & 0 \\ 0 & 0 & 0 & 0 & 0 \\ 0 & 0 & 0 & 1 & 0 \\ 0 & 0 & 0 & 0 & 1 \end{bmatrix}.$$

Table 2.1 Coefficients in Eqs. (2.22) through (2.31)

Equation No.	Coefficient expression
Eq. (2.22)	$T_{\mathrm{w}} = \frac{1}{2}\rho_{\mathrm{w}} c_{\mathrm{w}} A_{\mathrm{w}} l;\ X_{\mathrm{dry},1} = -c_{\mathrm{w}}(G_{\mathrm{w,E}})_{\mathrm{o}} - \frac{A_{\mathrm{i}}}{2}(a_{\mathrm{gw}})_{\mathrm{o}};$ $X_{\mathrm{dry},2} = A_{\mathrm{i}}(a_{\mathrm{gw}})_{\mathrm{o}};\ X_{\mathrm{dry},3} = c_{\mathrm{w}}(G_{\mathrm{w,E}})_{\mathrm{o}} - \frac{A_{\mathrm{i}}}{2}(a_{\mathrm{gw}})_{\mathrm{o}};$ $X_{\mathrm{dry},4} = c_{\mathrm{w}}(t_{\mathrm{w,E}} - t_{\mathrm{w,L}})_{\mathrm{o}} + A_{\mathrm{i}}\left(\frac{\partial a_{\mathrm{gw}}}{\partial G_{\mathrm{w,E}}}\right)_{\mathrm{o}}\left(t_{\mathrm{g}} - \frac{t_{\mathrm{w,L}} + t_{\mathrm{w,E}}}{2}\right)_{\mathrm{o}};$ $\xi_{\Delta t_{\mathrm{w,L,dry}}} = -\frac{1}{2}\rho_{\mathrm{w}} c_{\mathrm{w}} A_{\mathrm{w}} l \frac{\partial \Delta t_{\mathrm{w,E}}}{\partial \tau}$
Eq. (2.23)	$T_{\mathrm{a}} = \frac{1}{2}\varepsilon_{\mathrm{a}}\rho_{\mathrm{a}} c_{\mathrm{a}} A_{\mathrm{a}} b_{\mathrm{a}};\ Y_{\mathrm{dry},1} = -c_{\mathrm{a}}(G_{\mathrm{a,E}}) - \frac{A_{\mathrm{o}}\eta_{\mathrm{s}}}{2}(a_{\mathrm{ga}})_{\mathrm{o}};$ $Y_{\mathrm{dry},2} = A_{\mathrm{o}}\eta_{\mathrm{s}}(a_{\mathrm{ga}})_{\mathrm{o}};\ Y_{\mathrm{dry},3} = c_{\mathrm{a}}(G_{\mathrm{a,E}})_{\mathrm{o}} - \frac{A_{\mathrm{o}}\eta_{\mathrm{s}}}{2}(a_{\mathrm{ga}})_{\mathrm{o}};$ $Y_{\mathrm{dry},4} = c_{\mathrm{a}}\left(t_{\mathrm{a,E}} - t_{\mathrm{a,L}}\right)_{\mathrm{o}} + \left(\frac{\partial a_{\mathrm{ga}}}{\partial G_{\mathrm{a,E}}}\right)_{\mathrm{o}}\eta_{\mathrm{s}} A_{\mathrm{o}}\left(t_{\mathrm{g}} - \frac{t_{\mathrm{a,E}} + t_{\mathrm{a,L}}}{2}\right);$ $\xi_{\Delta t_{\mathrm{a,L,dry}}} = \frac{1}{2}\varepsilon_{\mathrm{a}}\rho_{\mathrm{a}} c_{\mathrm{a}} A_{\mathrm{a}} b \frac{\partial \Delta t_{\mathrm{a,E}}}{\partial \tau}$
Eq. (2.24)	$T_{\mathrm{g}} = c_{\mathrm{g}} M_{\mathrm{g}};\ Z_{\mathrm{dry},1} = Z_{\mathrm{dry},5} = \frac{A_{\mathrm{i}}}{2}(a_{\mathrm{g,w}})_{\mathrm{o}};$ $Z_{\mathrm{dry},2} = Z_{\mathrm{dry},4} = \frac{A_{\mathrm{o}}\eta_{\mathrm{s}}}{2}(a_{\mathrm{ga}})_{\mathrm{o}};\ Z_{\mathrm{dry},3} = -A_{\mathrm{i}}(a_{\mathrm{gw}})_{\mathrm{o}} - A_{\mathrm{o}}\eta_{\mathrm{s}}(a_{\mathrm{ga}})_{\mathrm{o}};$ $Z_{\mathrm{dry},6} = Z_{\mathrm{wet},7} = \frac{A_{\mathrm{i}}}{2}\left(\frac{\partial a_{\mathrm{gw}}}{\partial G_{\mathrm{w,E}}}\right)_{\mathrm{o}}(t_{\mathrm{w,L}} + t_{\mathrm{w,E}} - 2t_{\mathrm{g}})_{\mathrm{o}};$ $Z_{\mathrm{dry},7} = \frac{A_{\mathrm{o}}\eta_{\mathrm{s}}}{2}\left(\frac{\partial a_{\mathrm{ga}}}{\partial G_{\mathrm{a,E}}}\right)_{\mathrm{o}}\left[\frac{1}{2}(t_{\mathrm{a,L}} + t_{\mathrm{a,E}}) - (t_{\mathrm{g}})_{\mathrm{o}}\right].$
Eq. (2.28)	$T_{\mathrm{w}} = \frac{1}{2}\rho_{\mathrm{w}} c_{\mathrm{w}} A_{\mathrm{w}} l\ X_{\mathrm{wet},1} = -c_{\mathrm{w}}(G_{\mathrm{w,E}})_{\mathrm{o}} - \frac{A_{\mathrm{i}}}{2}(a_{\mathrm{gw}})_{\mathrm{o}};$ $X_{\mathrm{wet},2} = A_{\mathrm{i}}(a_{\mathrm{gw}})_{\mathrm{o}};\ X_{\mathrm{wet},3} = c_{\mathrm{w}}(G_{\mathrm{w,E}})_{\mathrm{o}} - \frac{A_{\mathrm{i}}}{2}(a_{\mathrm{gw}})_{\mathrm{o}};$ $X_{\mathrm{wet},4} = c_{\mathrm{w}}(t_{\mathrm{w,E}} - t_{\mathrm{w,L}})_{\mathrm{o}} + A_{\mathrm{i}}\left(\frac{\partial a_{\mathrm{gw}}}{\partial G_{\mathrm{w,E}}}\right)_{\mathrm{o}}\left(t_{\mathrm{g}} - \frac{t_{\mathrm{w,L}} - t_{\mathrm{w,E}}}{2}\right)_{\mathrm{o}};$ $\xi_{\Delta t_{\mathrm{w,L,wet}}} = -\frac{1}{2}\varepsilon_{\mathrm{a}}\rho_{\mathrm{w}} c_{\mathrm{w}} A_{\mathrm{w}} \frac{\partial \Delta t_{\mathrm{w,E}}}{\partial \tau}.$
Eq. (2.29)	$T_{\mathrm{a}} = \frac{1}{2}\varepsilon_{\mathrm{a}}\rho_{\mathrm{a}} c_{\mathrm{a}} A_{\mathrm{a}} b;$ $Y_{\mathrm{wet},1} = -c_{\mathrm{a}}(G_{\mathrm{a,E}}) - \frac{A_{\mathrm{o}}}{2}\left[(a_{\mathrm{ga}})_{\mathrm{o}}\eta_{\mathrm{s}} + \beta_1(q_{\mathrm{r}} - \beta_2)(1 - \eta_{\mathrm{s}})(\lambda_{\mathrm{m}})_{\mathrm{o}}\right];$ $Y_{\mathrm{wet},2} = Y_{\mathrm{wet},6} = \frac{A_{\mathrm{o}}(\beta_2 - q_{\mathrm{r}})}{2}(\lambda_{\mathrm{m}});$ $Y_{\mathrm{wet},3} = A_{\mathrm{o}}\eta_{\mathrm{s}}(a_{\mathrm{ga}})_{\mathrm{o}} + (q_{\mathrm{r}} - \beta_2)A_{\mathrm{o}}\beta_1\eta_{\mathrm{s}}(\lambda_{\mathrm{m}})_{\mathrm{o}};$ $Y_{\mathrm{wet},4} = c_{\mathrm{a}}(G_{\mathrm{a,E}})_{\mathrm{o}} - \frac{A_{\mathrm{o}}}{2}\left[2(a_{\mathrm{ga}})_{\mathrm{o}} - (a_{\mathrm{ga}})_{\mathrm{o}}\eta_{\mathrm{s}} + \beta_1(q_{\mathrm{r}} - \beta_2)(1 - \eta_{\mathrm{s}})(\lambda_{\mathrm{m}})_{\mathrm{o}}\right].$ $Y_{\mathrm{wet},5} = c_{\mathrm{a}}(t_{\mathrm{a,E}} - t_{\mathrm{a,L}})_{\mathrm{o}} - \frac{A_{\mathrm{o}}}{2}\left[\left(\frac{\partial a_{\mathrm{ga}}}{\partial G_{\mathrm{a,E}}}\right)_{\mathrm{o}}\eta_{\mathrm{s}} + \beta_1(q_{\mathrm{r}} - \beta_2)(1 - \eta_{\mathrm{s}})\left(\frac{\partial \lambda_{\mathrm{m}}}{\partial G_{\mathrm{a,E}}}\right)_{\mathrm{o}}\right](t_{\mathrm{a,E}} + t_{\mathrm{a,L}})_{\mathrm{o}}$ $+ A_{\mathrm{o}}(t_{\mathrm{g}})_{\mathrm{o}}\left[\left(\frac{\partial a_{\mathrm{ga}}}{\partial G_{\mathrm{a,E}}}\right)_{\mathrm{o}}\eta_{\mathrm{s}} + \beta_1(q_{\mathrm{r}} - \beta_2)\eta_{\mathrm{s}}\left(\frac{\partial \lambda_{\mathrm{m}}}{\partial G_{\mathrm{a,E}}}\right)_{\mathrm{o}}\right] + \frac{A_{\mathrm{o}}(\beta_2 - q_{\mathrm{r}})}{2}\left(\frac{\partial \lambda_{\mathrm{m}}}{\partial G_{\mathrm{a,E}}}\right)(W_{\mathrm{a,E}} + W_{\mathrm{a,L}})_{\mathrm{o}};$ $\xi_{\Delta t_{\mathrm{w,L,wet}}} = -\frac{1}{2}\varepsilon_{\mathrm{a}}\rho_{\mathrm{a}} A_{\mathrm{a}} c_{\mathrm{a}} \frac{\partial \Delta t_{\mathrm{a,E}}}{\partial \tau}.$
Eq. (2.30)	$T_{\mathrm{m}} = \frac{1}{2}\varepsilon_{\mathrm{a}}\rho_{\mathrm{a}} A_{\mathrm{a}} b;\ M_{\mathrm{wet},1} = M_{\mathrm{wet},4} = -\frac{\beta_1(1-\eta_{\mathrm{s}})A_{\mathrm{o}}}{2}(\lambda_{\mathrm{m}})_{\mathrm{o}};$ $M_{\mathrm{wet},2} = -(G_{\mathrm{a,E}})_{\mathrm{o}} - \frac{A_{\mathrm{o}}}{2}(\lambda_{\mathrm{m}})_{\mathrm{o}};\ M_{\mathrm{wet},3} = \beta_1\eta_{\mathrm{s}}A_{\mathrm{o}}(\lambda_{\mathrm{m}})_{\mathrm{o}};$ $M_{\mathrm{wet},6} = (G_{\mathrm{a,E}})_{\mathrm{o}} - \frac{A_{\mathrm{o}}}{2}(\lambda_{\mathrm{m}})_{\mathrm{o}};$ $M_{\mathrm{wet},6} = \begin{bmatrix} \beta_1\eta_{\mathrm{s}}A_{\mathrm{o}}(t_{\mathrm{g}})_{\mathrm{o}} - \frac{A_{\mathrm{o}}}{2}(W_{\mathrm{a,E}} + W_{\mathrm{a,L}})_{\mathrm{o}} \\ -\frac{\beta_1 A_{\mathrm{o}}(1-\eta_{\mathrm{s}})}{2}(t_{\mathrm{a,E}} + t_{\mathrm{a,L}})_{\mathrm{o}} \end{bmatrix}\left(\frac{\partial \lambda_{\mathrm{m}}}{\partial G_{\mathrm{a,E}}}\right) + (W_{\mathrm{a,E}} - W_{\mathrm{a,L}})_{\mathrm{o}};$ $\xi_{\Delta t_{\mathrm{a,L,wet}}} = -\frac{1}{2}\varepsilon_{\mathrm{a}}\rho_{\mathrm{a}} b A_{\mathrm{a}} \frac{\partial \Delta W_{\mathrm{a,E}}}{\partial \tau}.$
Eq. (2.31)	$T_{\mathrm{g}} = c_{\mathrm{g}} M_{\mathrm{g}};\ Z_{\mathrm{wet},1} = Z_{\mathrm{wet},6} = \frac{A_{\mathrm{i}}}{2}(a_{\mathrm{gw}})_{\mathrm{o}};$ $Z_{\mathrm{wet},2} = Z_{\mathrm{wet},5} = \frac{A_{\mathrm{o}}\eta_{\mathrm{s}}}{2}(a_{\mathrm{ga}})_{\mathrm{o}} + \frac{1}{2}\beta_1(1 - \eta_{\mathrm{s}})q_{\mathrm{r}}A_{\mathrm{o}}(\lambda_{\mathrm{m}})_{\mathrm{o}};$ $Z_{\mathrm{wet},3} = Z_{\mathrm{wet},9} = \frac{A_{\mathrm{o}}q_{\mathrm{r}}}{2}(\lambda_{\mathrm{m}})_{\mathrm{o}};$ $Z_{\mathrm{wet},4} = -A_{\mathrm{i}}(a_{\mathrm{gw}})_{\mathrm{o}} - A_{\mathrm{o}}\eta_{\mathrm{s}}(a_{\mathrm{ga}})_{\mathrm{o}} - q_r\beta_1\eta_s A_o(\lambda_{\mathrm{m}})_{\mathrm{o}};$ $Z_{\mathrm{wet},7} = -A_{\mathrm{i}}\left(t_{\mathrm{g}} - \frac{t_{\mathrm{w,E}} + t_{\mathrm{w,L}}}{2}\right)_{\mathrm{o}}\left(\frac{\partial a_{\mathrm{gw}}}{\partial G_{\mathrm{w,E}}}\right)_{\mathrm{o}};$ $Z_{\mathrm{wet},8} = \eta_{\mathrm{s}}A_{\mathrm{o}}\left(\frac{\partial a_{\mathrm{ga}}}{\partial G_{\mathrm{a,E}}}\right)_{\mathrm{o}}\left[\frac{1}{2}(t_{\mathrm{a,L}} + t_{\mathrm{a,E}})_{\mathrm{o}} - (t_{\mathrm{g}})_{\mathrm{o}}\right]$ $+ A_{\mathrm{o}}q_{\mathrm{r}}\left(\frac{\partial \lambda_{\mathrm{m}}}{\partial G_{\mathrm{a,E}}}\right)_{\mathrm{o}}\left[\frac{1}{2}\beta_1(1 - \eta_{\mathrm{s}})(t_{\mathrm{a,E}} + t_{\mathrm{a,L}})_{\mathrm{o}} - \beta_1\eta_{\mathrm{s}}(t_{\mathrm{g}})_{\mathrm{o}} + \frac{1}{2}(W_{\mathrm{a,E}} + W_{\mathrm{a,L}})_{\mathrm{o}}\right]$

For the wet-condition process:

$$x_{\text{coil}} = [\Delta t_{\text{w,L}}, \Delta t_{\text{a,L}}, \Delta W_{\text{a,L}}, \Delta t_{\text{g}}]^T;\ y_{\text{coil}} = [\Delta t_{\text{w,L}}, \Delta G_{\text{w,L}}, \Delta t_{\text{a,L}}, \Delta W_{\text{a,L}}, \Delta G_{\text{a,L}}]^T;$$

$$u_{\text{coil}} = [\Delta t_{\text{w,E}}, \Delta G_{\text{w,E}}, \Delta t_{\text{a,E}}, \Delta W_{\text{a,E}}, \Delta G_{\text{a,E}}]^T;\ \xi = \left[\xi_{\Delta t_{\text{w,L,wet}}}, \xi_{\Delta t_{\text{a,L,wet}}}, \xi_{\Delta t_{\text{g,wet}}}, 0\right]^T;$$

$$A_{\text{coil}} = \begin{bmatrix} \frac{X_1}{T_{\text{w}}} & 0 & 0 & \frac{X_2}{T_{\text{w}}} \\ 0 & \frac{Y_{\text{wet},1}}{T_{\text{a}}} & \frac{Y_{\text{wet},2}}{T_{\text{a}}} & \frac{Y_{\text{wet},3}}{T_{\text{a}}} \\ 0 & \frac{M_{\text{wet},1}}{T_{\text{m}}} & \frac{M_{\text{wet},2}}{T_{\text{m}}} & \frac{M_{\text{wet},3}}{T_{\text{m}}} \\ \frac{Z_{\text{wet},1}}{T_{\text{g}}} & \frac{Z_{\text{wet},2}}{T_{\text{g}}} & \frac{Z_{\text{wet},3}}{T_{\text{g}}} & \frac{Z_{\text{wet},4}}{T_{\text{g}}} \end{bmatrix};\ B_{\text{coil}} = \begin{bmatrix} \frac{X_3}{T_{\text{w}}} & \frac{X_4}{T_{\text{w}}} & 0 & 0 & 0 \\ 0 & 0 & \frac{Y_{\text{wet},4}}{T_{\text{a}}} & \frac{Y_{\text{wet},6}}{T_{\text{a}}} & \frac{Y_{\text{wet},5}}{T_{\text{a}}} \\ 0 & 0 & \frac{M_{\text{wet},4}}{T_{\text{m}}} & \frac{M_{\text{wet},6}}{T_{\text{m}}} & \frac{M_{\text{wet},5}}{T_{\text{m}}} \\ \frac{Z_{\text{wet},6}}{T_{\text{g}}} & \frac{Z_{\text{wet},7}}{T_{\text{g}}} & \frac{Z_{\text{wet},5}}{T_{\text{g}}} & \frac{Z_{\text{wet},9}}{T_{\text{g}}} & \frac{Z_{\text{wet},8}}{T_{\text{g}}} \end{bmatrix}$$

$$C_{\text{coil}} = \begin{bmatrix} 1 & 0 & 0 & 0 \\ 0 & 0 & 0 & 0 \\ 0 & 1 & 0 & 0 \\ 0 & 0 & 1 & 0 \\ 0 & 0 & 0 & 0 \end{bmatrix};\ D_{\text{coil}} = \begin{bmatrix} 0 & 0 & 0 & 0 & 0 \\ 0 & 1 & 0 & 0 & 0 \\ 0 & 0 & 0 & 0 & 0 \\ 0 & 0 & 0 & 0 & 0 \\ 0 & 0 & 0 & 0 & 1 \end{bmatrix}.$$

In Eq. (2.34), the variables, $\Delta t_{\text{w,E}}, \Delta G_{\text{w,E}}, \Delta t_{\text{a,E}}, \Delta W_{\text{a,E}}$ and $\Delta G_{\text{a,E}}$, are input perturbations, and the variables, $\Delta t_{\text{w,L}}, \Delta G_{\text{w,L}}, \Delta t_{\text{a,L}}, \Delta W_{\text{a,L}}$ and $\Delta G_{\text{a,L}}$, are the response ones. The state variables are $\Delta t_{\text{w,L}}, \Delta t_{\text{a,L}}, \Delta t_{\text{g}}$ for the dry-condition process and $\Delta t_{\text{w,L}}, \Delta t_{\text{a,L}}, \Delta W_{\text{a,L}}, \Delta t_{\text{g}}$ for the wet-condition process.

2.2.1.2 Model Validation

An experimental setup has been built for validating the state-space model of water-to-air heat exchanger. The schematic diagram of the experimental setup is shown in Fig. 2.3. A grid board is placed in the upstream of the test section to reduce the influence of turbulence of inlet air on the test. A louvered mixer is placed after the heat exchanger to guarantee a uniform temperature profile of outlet air. The test instruments and relevant equipments in the experimental system are listed in Table 2.2, and the detailed information of structure about the water-to-air heat exchanger is given in Fig. 2.4 and Table 2.3.

Three experimental cases with the validation time of 1200 s are investigated to verify the heat exchanger's transient behaviors including the transient responses of the exit air temperature and humidity as well as the exit water temperature subjected to different sudden perturbations. These cases are as follows: ① Start up the chiller at the beginning of the system's running; ② the water flow rate has a sudden increase of 0.058 kg/s during the system's running; and ③ Stop the chiller at the end of the system's running. The initial conditions corresponding to these cases (see Table 2.4), which are used for the model simulation, are obtained under the steady state before the perturbations began to apply to the heat exchanger. During the

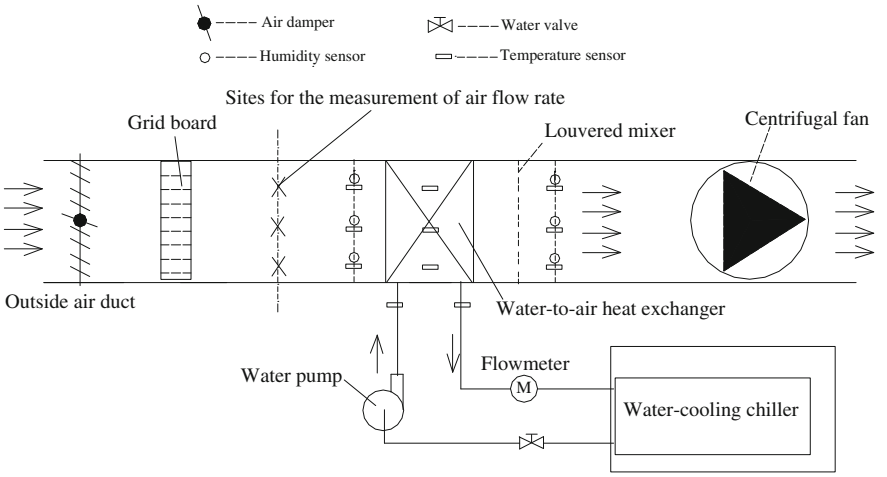

Fig. 2.3 Schematic diagram of experimental setup for water-to-air heat exchanger model validation

Table 2.2 Specific details about the apparatus in the experimental system

Items	Properties or features
Temperature sensor	Copper-constantan thermocouples: ±0.2 °C
Temperature and humidity sensor	Type: HHC2-S; ±0.008 for air humidity ratio and ±0.1 °C for air temperature
Digital anemometer	Type: T425; precision: ±(0.03 + 5 %) m/s
Electromagnetic flowmeter	Type: ETFM-20; precision: ±0.5 %
Water pump	Type: 50T5WA-3; nominal water flow: 4.2 m^3/h; power: 1.7 kW
Ventilator	Type: KT40-2.5; nominal airflow rate: 2000 m^3/h; power: 0.75 kW
Chiller	Nominal cooling capacity: 6.0 kW; power: 2.0 kW

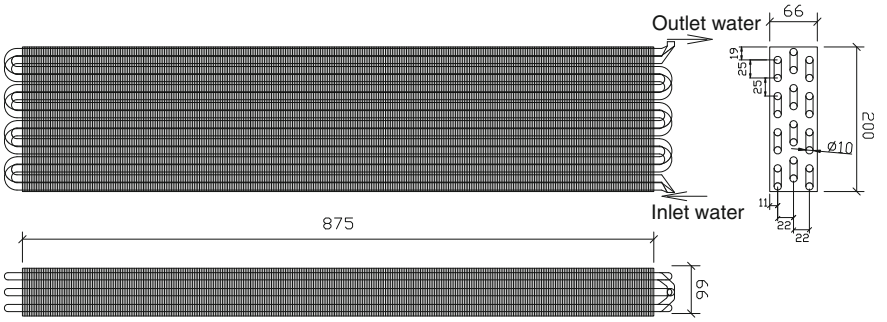

Fig. 2.4 Structure of the water-to-air heat exchanger

Table 2.3 Structural information of the water-to-air heat exchanger

Length of the coil: l (m)	21.0	Area of windward side A_a (m^2)	0.175
Inner diameter of the coil: r_i (m)	0.004	Length along airflow: b (m)	0.66
Inner surface area of the coil: A_i (m^2)	0.5287	Thickness of fin: δ_c (m)	0.0002
External surface area of the coil: A_o (m^2)	8.8065	Total mass: M_g (kg)	17.52
Mean specific heat: c_g [J/(kg °C)]	625	Fin spacing e (m)	0.0024

Table 2.4 Initial conditions for model validation and simulation

Cases	Case I	Case II	Case III
Initial conditions			
$(t_{a,E})_o$ (°C)	29.8 ± 0.1	28.3 ± 0.1	28.2 ± 0.1
$(t_{a,L})_o$ (°C)	28.8 ± 0.1	21.3 ± 0.1	20.7 ± 0.1
$(W_{a,E})_o$ (g/kg dry air)	20.1 ± 0.2	18.7 ± 0.2	16.1 ± 0.2
$(W_{a,L})_o$ (g/kg dryair)	20.1 ± 0.2	17.0 ± 0.2	14.3 ± 0.2
$(G_a)_o$ (kg/s)	0.2000 ± 0.01	0.2000 ± 0.01	0.2000 ± 0.01
$(t_{w,E})_o$ (°C)	28.2 ± 0.1	16.7 ± 0.1	15.7 ± 0.1
$(t_{w,L})_o$ (°C)	28.4 ± 0.1	18.9 ± 0.1	18.6 ± 0.1
$(G_w)_o$ (kg/s)	0.2587 ± 0.005	0.2387 ± 0.005	0.1964 ± 0.005
$(t_g)_o$ (°C)	29.3 ± 0.1	19.5 ± 0.1	18.9 ± 0.1

Note: Case I: ***Start-up the chiller***; Case II: $G_w \uparrow$ ***0.058 kg/s***; Case III: ***Stop the chiller***

simulation, the dew-point temperature of inlet air is compared with the heat exchanger's wall surface temperature to judge whether the wet-cooling model or the dry-cooling model is used for the calculation.

The average error (AE) is used to evaluate the goodness of the calculated results by the model compared with the experimental data during the transient response process, which is defined by Eq. (2.39).

$$\mathrm{AE}(\text{Average error}) = \frac{1}{N}\sum_{i=1}^{N}\left(\frac{\left|\Delta Y_{m,i} - \Delta Y_{exp,i}\right|}{\left|\Delta Y_{exp,i}\right|} \times 100\,\%\right) \tag{2.39}$$

where ΔY stands for the variation of the response parameters comparing with the initial value; the subscripts 'm' and 'exp' stand, respectively, for the model result and the experimental ones; i denotes the ith calculated or experimental result at the same time point; and N stands for the total number of the calculated or experimental result during the transient response process.

(1) Experimental case I

For the experimental case I, only changes were made on inlet air temperature and humidity as well as inlet water temperature of the water-to-air heat exchanger. As

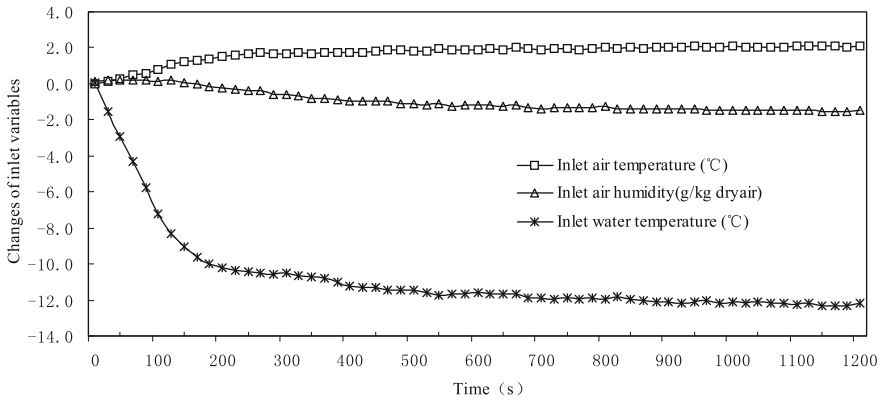

Fig. 2.5 Changes of inlet variables in the case I (measured data)

shown in Fig. 2.5, the inlet air temperature increases gradually till to the steady value; the inlet air humidity increases a little in the beginning (last for about 120 s) and decreases afterward; and the inlet water temperature drops quickly in the first 180 s and then tends to be steady. The ultimate change of the inlet air temperature, the inlet air humidity, and the inlet water temperature is about +2.1 °C, −1.6 g/(kg dry air), and −12.3 °C, respectively. The flow rates of air and water passing through the water-to-air heat exchanger were kept stable as much as possible during the experiment, and they are considered as zero in the model simulation.

Figure 2.6 shows the comparisons of the model results with the experimental data on transient responses of the exit air temperature, the exit air humidity, and the exit water temperature for the case I, and the corresponding average error [AE, calculated by Eq. (2.39)] is estimated as 8.7, 8.8, and 10.3 %, respectively. It is reasonable to see that the exit air temperature and humidity will decrease when subjected to a big decrease in the inlet water temperature while the other inlet variables have small change. The exit water temperature decreases with the decrease in the inlet one, and the ultimate change of the exit water temperature is lower than that of the inlet one. This is because decreasing the inlet water temperature will increase heat transfer quantity of the water-to-air heat exchanger.

(2) Experimental case II

For the experimental case II, the water flow rate had a sudden increase of 0.058 kg/s while the other inlet variables were kept unchanged. The comparisons between model results and experimental data on transient responses of the exit variables are given in Fig. 2.7. The model results are shown to have a good agreement with the experimental data, and the average errors of the simulated results for the case II are all less than 12 %. It is obvious that a larger water flow rate will bring about a larger cooling and dehumidification capacity of the water-to-air heat exchanger and cause the exit air temperature and humidity to

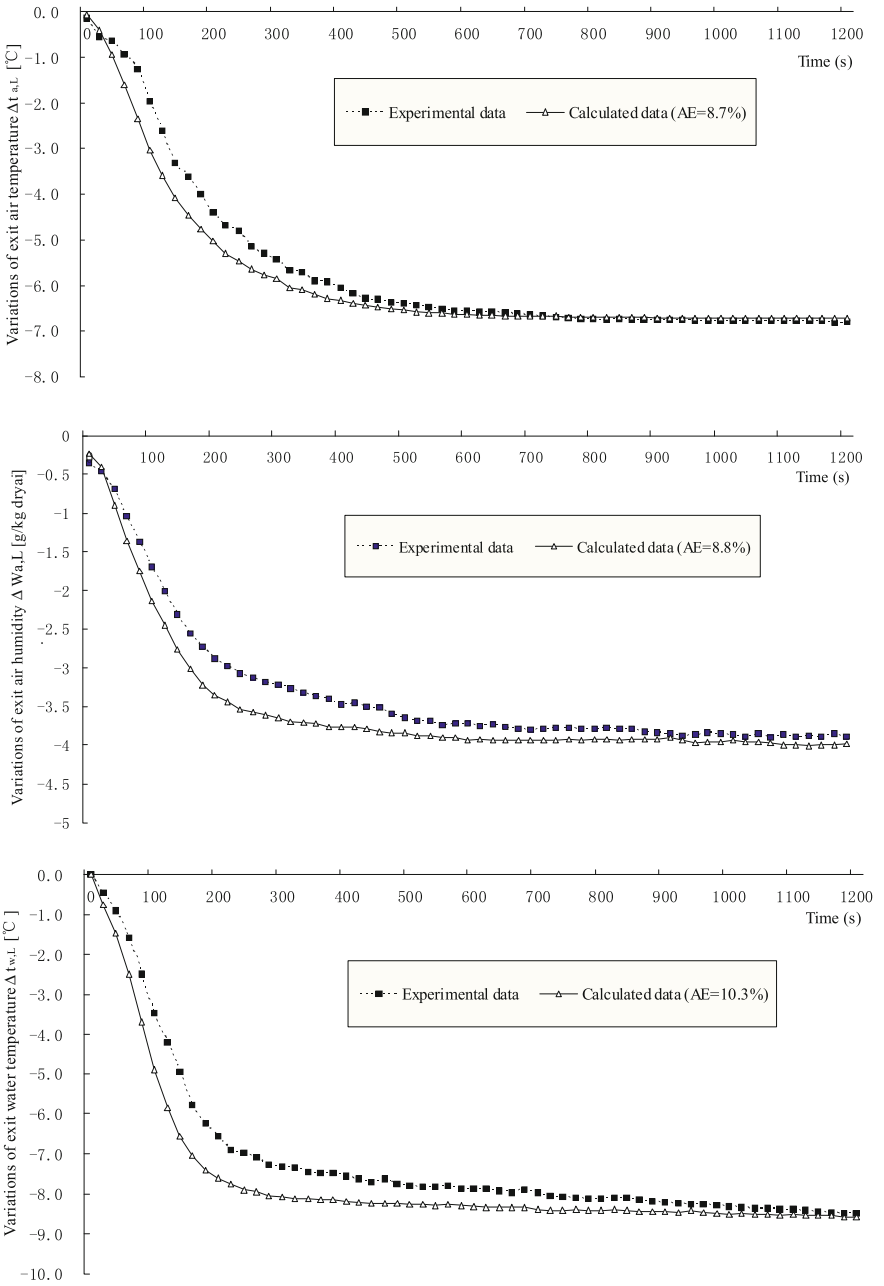

Fig. 2.6 Responses of exit variables to the changes of inlet ones (case I)

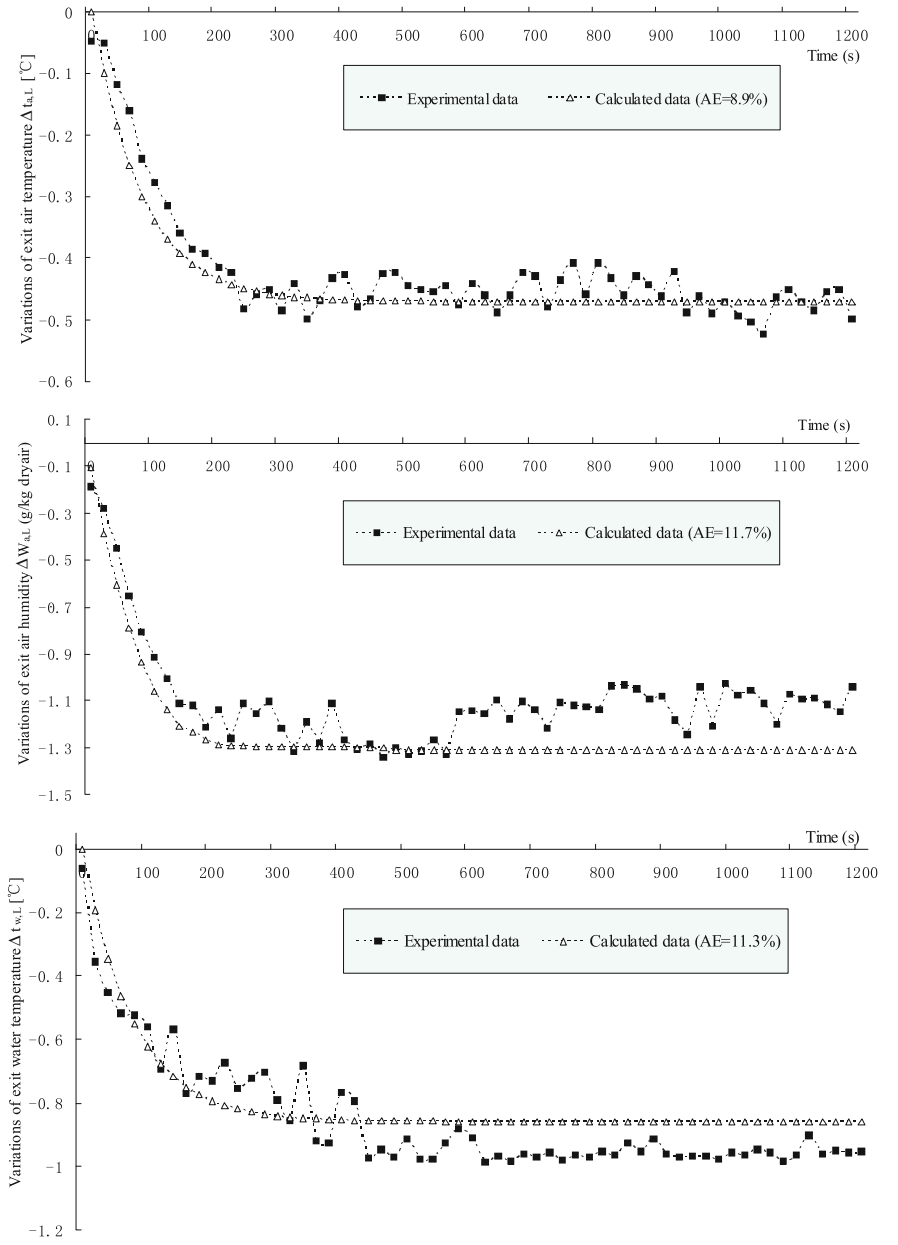

Fig. 2.7 Responses of exit variables to a sudden increase in water flow rate by 0.058 kg/s (case II)

decrease. Meanwhile, the water flow rate affects as well the exit water temperature of water-to-air heat exchanger. In this case, the exit water temperature gradually decreased after the water flow rate had a sudden increase.

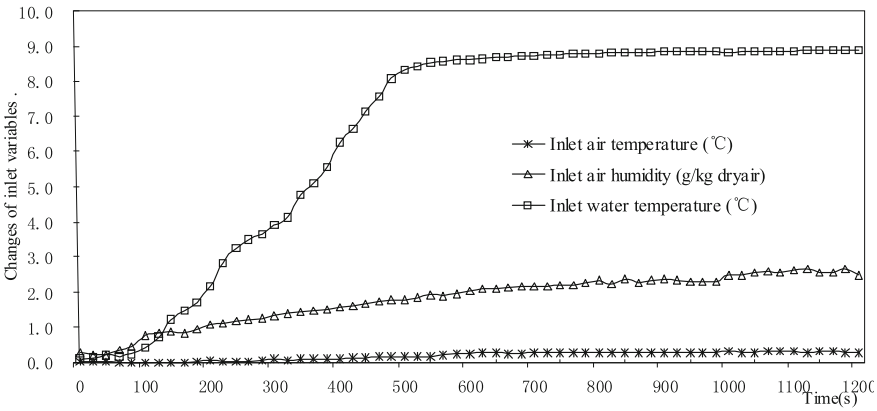

Fig. 2.8 Changes of inlet variables in the case III (measured data)

(3) Experimental case III

In the case III, the inlet air temperature and humidity and the inlet water temperature all gradually increase (see Fig. 2.8), while the water and the airflow rates are kept unchanged. Figure 2.9 shows the calculated and experimental results on the transient responses of exit variables to the changes of inlet variables under initial conditions in the case III. Comparing with the experimental data, the average error of the model results on the transient responses of the exit air temperature and humidity as well as the exit water temperature is estimated as 14.2, 8.9, and 8.2 %, respectively.

As seen from the three study cases (case I, case II, and case III), the simulation errors compared with the experimental data are all less than 15 %, which indicates that the dynamic model developed in this study is capable of predicting well-transient performances of water-to-air heat exchanger under wet conditions.

2.2.2 Chiller

Vapor-compression packaged liquid chillers are often employed to provide chilled media for space thermal environment control purposes in commercial and industrial applications. As well known, the space-cooling load often changes and the refrigeration system needs to operate in an unsteady manner and adjust its capacity to guarantee an anticipated space thermal conditions. Usually, a refrigeration system adjusts its capacity mainly through modulating compressor speed with input frequency control. To obtain better control effect of the space thermal conditions, we need to have the knowledge of the dynamic performance of the refrigeration system under different conditions, and a dynamic model for refrigeration system is very necessary for that objective.

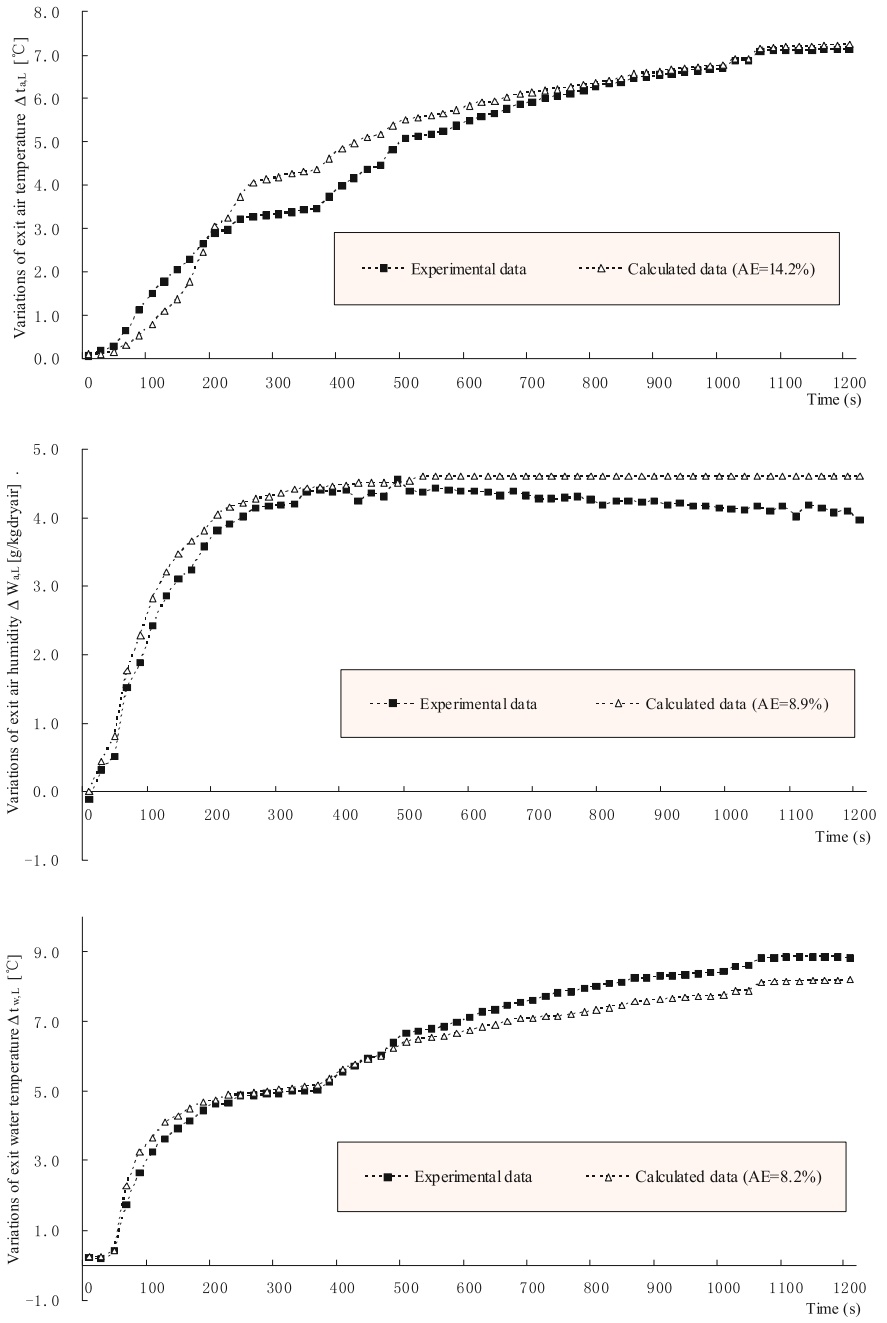

Fig. 2.9 Responses of exit variables to the changes of inlet ones (case III)

2.2.2.1 Model Development [9]

Basically, a conventional refrigeration system mainly consists of four key components (i.e., compressor, condenser, expander, and evaporator) and other accessories. Figure 2.10 shows the theoretical single-stage cycle used as a model for actual vapor-compression chiller. Heat is added to the refrigerant from state '4' to state '1.' The heat capacity of the refrigerant fluid is assumed to be constant in this process. The refrigerant temperature is increased in process from state '1' to state '2'. Process from state '2' to state '3' is a heat rejection process in which the refrigerant temperature decreases linearly with heat transfer. The cycle ends with expansion between states '3' and '4.'

1) Assumptions and fundamental equations

For the convenience of modeling, some assumptions are necessary to be made as below:

(1) The compression (from state '1' to state '2') is assumed to be a isentropic process, and the expansion from state '3' to state '4' is considered to be isenthalpic;
(2) Mass flow rate of refrigerant is uniform throughout the cycle;
(3) Mass of refrigerant in the condenser and evaporator is unchanged during the dynamic response simulation;
(4) Working performance of the compressor is kept invariable during the dynamic response simulation;
(5) Temperature of chilled liquid (passing through the evaporator) and cooling liquid (passing through the condenser) change linearly from the inlet to the outlet of the corresponding heat exchanger. And shell temperature of the heat

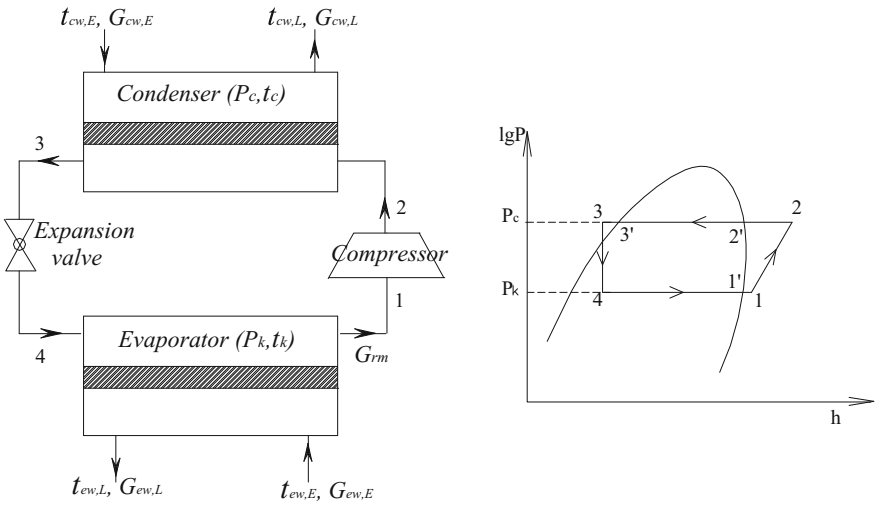

Fig. 2.10 Schematic diagram for the working cycle of vapor-compression chiller

exchangers (i.e., the condenser and the evaporator) is represented by a lumped parameter;

(6) Superheated temperature of gaseous refrigerant after evaporator and subcooled temperature of liquid refrigerant after condenser are assumed to be constant (equal to initial conditions) during the transient response simulation.

Based on the above assumptions, the fundamental equations can be established according to the principle of energy and mass conservation.

Energy equation for refrigerant in the condenser

$$c_{\mathrm{cr}} M_{\mathrm{cr}} \frac{\mathbf{d}t_{\mathrm{c}}}{\mathbf{d}\tau} = G_{\mathrm{rm}}(h_{\mathrm{r},2} - h_{\mathrm{r},3}) + a_{\mathrm{co}} A_{\mathrm{co}}(t_{\mathrm{cg}} - t_{\mathrm{c}}) \tag{2.40}$$

Mass equation for cooling liquid passing through the condenser

$$G_{\mathrm{cw,L}} = G_{\mathrm{cw,E}} = G_{\mathrm{cw}} \tag{2.41}$$

Energy equation for cooling liquid passing through the condenser

$$\frac{1}{2} c_{\mathrm{cw}} M_{\mathrm{cw}} \frac{\mathbf{d}(t_{\mathrm{cw,L}} + t_{\mathrm{cw,E}})}{\mathbf{d}\tau} = c_{\mathrm{cw}} G_{\mathrm{cw,E}}(t_{\mathrm{cw,E}} - t_{\mathrm{cw,L}}) + a_{\mathrm{cw}} A_{\mathrm{cw}} \left(t_{\mathrm{cg}} - \frac{t_{\mathrm{cw,E}} + t_{\mathrm{cw,L}}}{2} \right) \tag{2.42}$$

Energy equation for shell of the condenser

$$c_{\mathrm{cg}} M_{\mathrm{cg}} \frac{\mathbf{d}t_{\mathrm{cg}}}{\mathbf{d}\tau} = a_{\mathrm{co}} A_{\mathrm{co}}(t_{\mathrm{c}} - t_{\mathrm{cg}}) + a_{\mathrm{cw}} A_{\mathrm{cw}} \left(\frac{t_{\mathrm{cw,E}} + t_{\mathrm{cw,L}}}{2} - t_{\mathrm{cg}} \right) \tag{2.43}$$

Energy equation for refrigerant in the evaporator

$$c_{\mathrm{er}} M_{\mathrm{er}} \frac{\mathbf{d}t_{\mathrm{k}}}{\mathbf{d}\tau} = G_{\mathrm{rm}}(h_{\mathrm{r},3} - h_{\mathrm{r},1}) + a_{\mathrm{eo}} A_{\mathrm{eo}}(t_{\mathrm{eg}} - t_{\mathrm{k}}) \tag{2.44}$$

Mass equation for chilled liquid passing through the evaporator

$$G_{\mathrm{ew,L}} = G_{\mathrm{ew,E}} = G_{\mathrm{ew}} \tag{2.45}$$

Energy equation for chilled liquid passing through the evaporator

$$\frac{1}{2} c_{\mathrm{ew}} M_{\mathrm{ew}} \frac{\mathbf{d}(t_{\mathrm{ew,L}} + t_{\mathrm{ew,E}})}{\mathbf{d}\tau} = c_{\mathrm{ew}} G_{\mathrm{ew,E}}(t_{\mathrm{ew,E}} - t_{\mathrm{ew,L}}) + a_{\mathrm{ew}} A_{\mathrm{ew}} \left(t_{\mathrm{eg}} - \frac{t_{\mathrm{ew,E}} + t_{\mathrm{ew,L}}}{2} \right) \tag{2.46}$$

Energy equation for shell of the evaporator

$$c_{\mathrm{eg}} M_{\mathrm{eg}} \frac{\mathbf{d}t_{\mathrm{eg}}}{\mathbf{d}\tau} = a_{\mathrm{eo}} A_{\mathrm{eo}}(t_{\mathrm{k}} - t_{\mathrm{eg}}) + a_{\mathrm{ew}} A_{\mathrm{ew}} \left(\frac{t_{\mathrm{ew,E}} + t_{\mathrm{ew,L}}}{2} - t_{\mathrm{eg}} \right) \tag{2.47}$$

Electric power of compressor

$$N_{\text{com}} = \frac{G_{\text{rm}}}{\eta_{\text{com}}}\frac{R_{\text{r}}T_1}{\kappa_{\text{s}}-1}\left[\left(\frac{p_{\text{c}}}{p_{\text{k}}}\right)^{\frac{\kappa_{\text{s}}-1}{\kappa_{\text{s}}}}-1\right] = \frac{G_{\text{rm}}}{\eta_{\text{com}}}\frac{R_{\text{r}}(t_{\text{k}}+\Delta t_{\text{e,shr}}+273.15)}{\kappa_{\text{s}}-1}\left[\left(\frac{f_{\text{p}}(t_{\text{c}})}{f_{\text{p}}(t_{\text{k}})}\right)^{\frac{\kappa_{\text{s}}-1}{\kappa_{\text{s}}}}-1\right] = G_{\text{rm}}f_{N_{\text{com}}}(t_{\text{k}},t_{\text{c}}) \tag{2.48}$$

Energy equation for refrigerant in the expansion process

$$h_{\text{r},3} = h_{\text{r},4} \tag{2.49}$$

Cooling capacity of chiller

$$\begin{aligned} Q_{\text{c}} &= G_{\text{rm}}(h_{\text{r},1}-h_{\text{r},4}) = G_{\text{rm}}(f_{\text{h}}(t_{\text{k}})-f_{\text{h}}(t_{\text{c}})) \\ &= G_{\text{rm}}f_{Q_{\text{c}}}(t_{\text{k}},t_{\text{c}}) \end{aligned} \tag{2.50}$$

Coefficient of performance (COP) of chiller

$$\text{COP} = \frac{Q_{\text{c}}}{N_{\text{com}}} = \frac{f_{Q_{\text{C}}}(t_{\text{k}},t_{\text{c}})}{f_{N_{\text{com}}}(t_{\text{k}},t_{\text{c}})} = f_{\text{COP}}(t_{\text{k}},t_{\text{c}}) \tag{2.51}$$

In Eqs. (2.40) through (2.51), the symbol '*G'* stands for flow rate, kg/s; '*c*' for mass specific heat, J/ (kg °C); '*A*' for area, m^2; '*h*' for enthalpy, J/kg; 't_c' for condensing temperature, °C; 't_k' for evaporating temperature, °C; '*M*' for mass, kg; '*a*' for heat transfer coefficient, W/(m^2 °C); and 'τ' for time, s. The subscript 'cg' for shell wall of condenser; '*eg*' for shell wall of evaporator; 'co' for refrigerant-side surface of condenser; 'cr' for refrigerant in condenser; '*cw*' for cooling liquid in condenser; '*cr*' for refrigerant in condenser; 'eo' for refrigerant-side surface of evaporator; 'er' for refrigerant in evaporator; '*ew*' for coolant liquid in evaporator; '*er*' for refrigerant in evaporator; '*rm*' for circulating refrigerant in refrigeration system; 'N_{com}' for power of compressor, W; 'η_{com}' for working efficient of compressor; 'R_r' for gas constant of gaseous refrigerant, J/kg.K; 'κ_s' for adiabatic compression index of compressor; 'T_1' for inlet temperature of compressor, K; 'p_c' and 'p_k' are pressure in condenser and evaporator, respectively, Pa; '$\Delta t_{e,shr}$' for superheat degree of gaseous refrigerant, °C; 'Q_c' for cooling capacity, W; and '*f* ' denotes function.

2) Key parameters determination

(1) *Heat transfer coefficients*

Four coefficients of heat transfer are concerned in the model equations. They include condensation heat transfer coefficient in condenser (a_{co}), boiling heat transfer coefficient in evaporator (a_{eo}), convective heat transfer coefficient between liquid coolant and condenser (a_{cw}), and that between cold carrier liquid and

evaporator (a_{ew}). These coefficients can be usually modeled by Eqs. (2.52) through (2.54), respectively [10] .

$$a_{co} = C_1\left(t_c - t_{cg}\right)^{n_1} \tag{2.52}$$

$$a_{eo} = C_2\left(t_{eg} - t_k\right)^{n_2} \tag{2.53}$$

$$Nu_d = C_3 {Re_d}^{n_3} \tag{2.54}$$

For condenser: $Nu_d = \frac{a_{cw} d_{ci}}{\lambda_w}$, $Re_d = \frac{u_{cw} d_{ci}}{\nu_w}$; For evaporator: $Nu_d = \frac{a_{ew} d_{ei}}{\lambda_w}$, $Re_d = \frac{u_{ew} d_{ei}}{\nu_w}$. $C_1, C_2, C_3, n_1, n_2, n_3$ are empirical coefficients determined by field test data.

(2) *Enthalpy calculation for refrigerant at key state in the refrigeration cycle*

According to the diagram of refrigeration cycle (Fig. 2.19), the refrigerant often exists in the form of superheated vapor at the states '1' and '2' and subcooled liquid at states '3' and '4'. For a real refrigerant, the state equations are often expressed by semiempirical ones. The famous Martin-Hou equations are often used to calculate the thermophysical properties of refrigerants [11, 12], based on which the enthalpy of refrigerant at different states can be obtained.

The enthalpy of refrigerant in the gaseous state (h_{vapor}, kJ/kg) can be calculated by:

$$\begin{aligned} h_{vapor} = h_0 + (p_{r,g} v_{r,g} - R_r T_{r,g}) + \sum_{n=1}^{4} \frac{c_n T_{r,g}^n}{n} + c_5 \ln T_{r,g} - \frac{c_6}{T_{r,g}} + \sum_{n=2}^{5} \frac{A_n}{(n-1)(v_{r,g} - b)^{n-1}} \\ + e^{-K_1 T_{r,g}/T_{cc}} (1 + K_1 T_{r,g}/T_{cc}) \times \sum_{n=2}^{5} \frac{C_n}{(n-1)(v_{r,g} - b)^{n-1}} \end{aligned} \tag{2.55}$$

The state equation for the gaseous refrigerant can be expressed as follows:

$$p_{r,g} = \frac{R_r T_{r,g}}{v_{r,g} - b} + \sum_{n=2}^{5} \frac{A_n + B_n T_{r,g} + C_n e^{-K_1 T_{r,g}/T_{cc}}}{(v_{r,g} - b)^n} \tag{2.56}$$

The saturated vapor pressure of refrigerant ($p_{r,bg}$, kPa) can be computed by

$$\ln p_{r,bg} = A + \frac{B}{T_{r,bg}} + \mathrm{C} T_{r,bg} + \mathrm{D} T_{r,bg}^2 + \frac{E(F - T_{r,bg})}{T_{r,bg}} \ln(F - T_{r,bg}) + G \ln T_{r,bg} \tag{2.57}$$

The enthalpy of subcooled liquid refrigerant ($h_{r,l\Delta t}$, kJ/kg) can be calculated by Eq. (2.58).

$$h_{\mathrm{r,l}\Delta\mathrm{t}} = h_{\mathrm{r,bl}} - \frac{p_{\mathrm{r,bl}} - p_{\mathrm{atm}}}{q_{\mathrm{r}}} \tag{2.58}$$

In Eq. (2.58), the heat of vaporization (q_{r}, kJ/kg) can be obtained by the Clausius-Clapeyron equation as follows:

$$q_{\mathrm{r}} = T_{\mathrm{r,q}}(v_{\mathrm{r,bl}} - v_{\mathrm{r,bg}})p_{\mathrm{r,q}} \left[-\frac{B}{T_{\mathrm{r,q}}^2} + C + 2\mathrm{DT}_{\mathrm{r,q}} - \frac{\mathrm{EF}}{T_{\mathrm{r,q}}^2} \times \ln(F - T_{\mathrm{r,q}}) - \frac{\mathrm{EF}}{T_{\mathrm{r,q}}} \times \frac{1}{F - T_{\mathrm{r,q}}} + E \times \frac{1}{F - T_{\mathrm{r,q}}} + \frac{G}{T_{\mathrm{r,q}}} \right] \tag{2.59}$$

The enthalpy of saturated liquid refrigerant ($h_{\mathrm{r,bl}}$, kJ/kg) is written as follows:

$$h_{\mathrm{r,bl}} = h_{\mathrm{r,bg}} - q_{\mathrm{r}} \tag{2.60}$$

The density of saturated liquid refrigerant can be counted by Eq. (2.61).

$$\rho_{\mathrm{r,bl}} = \rho_{\mathrm{cc}} + \sum_{n=1}^{6} D_{\mathrm{n}} \left(1 - T_{\mathrm{r,bl}}/T_{\mathrm{cc}}\right)^{\frac{n}{3}} \tag{2.61}$$

In Eqs. (2.55)–(2.61), h stands for enthalpy, kJ/kg; p for pressure, kPa; T for temperature, K; ρ for density, kg/m^3; v for specific volume, m^3/kg; h_{o} for reference enthalpy, kJ/kg; R_{o} gas constant of gaseous refrigerant, kJ/kg.K; q_{r} for vaporization heat of refrigerant, kJ/kg; the subscript 'r, bg' for saturated gaseous refrigerant; the subscript 'r, bl' for saturated liquid refrigerant; the subscript 'r, q' for gaseous refrigerant; the subscript '$r, l\Delta t$' for subcooled liquid refrigerant; the subscript 'atm' for standard atmospheric pressure; and the subscript 'cc' for critical state; the rest parameters including A, B, C, D, E, F, G, K_1, b, $c_1 \sim c_6$, $A_2 \sim A_5$, $B_2 \sim B_5$, $C_2 \sim C_5$, and $D_1 \sim D_6$ are undetermined coefficients.

The enthalpy of refrigerant at states '1' (h_1) and '2' (h_2) can be calculated by using Eqs. (2.55) and (2.56) with respect to temperature and pressure. The pressure at states '1' (p_1) and '2' (p_2) corresponds, respectively, to saturated evaporating pressure and saturated condensation pressure. Known from Eq. (2.57), the saturated evaporating pressure is dependent on the evaporating temperature (T_{k}), and the saturated condensation one is dependent on the condensing temperature (T_{c}). Assuming the influence of small perturbations on the superheated temperature of vapor refrigerant is negligible, the variations of h_1 and h_2 are only dependent upon T_{k} and T_{c}, respectively. The enthalpy of refrigerant at states '3' (h_3) and '4' (h_4) can be computed by Eqs. (2.56), (2.58), (2.59), (2.60), and (2.61). Likewise, h_3 and h_4 are both dependent upon the condensing temperature (T_{c}).

(3) *Adiabatic compression process index (κ_{s})*

The adiabatic compression process index for the real gaseous refrigerant can be expressed by Eq. (2.63) [13].

$$\kappa_s = \frac{Z}{Z_p - \frac{R_r Z_T^2}{c_{r,p}}} \tag{2.62}$$

where$Z_p = Z - p\left(\frac{\partial Z}{\partial p}\right)_T$; $Z_T = Z + T\left(\frac{\partial Z}{\partial T}\right)_p$. Z is the compressibility factor; the subscripts 'p' and 'T' stand, respectively, for the isobaric process and isothermal process. During the dynamic simulation, the adiabatic compression process index (κ_s) can be assumed to be constant.

3) State-space model formulation

Through parameter linearization, Eqs. (2.40) through (2.51) can be transformed as follows:

$$T_{cr}\frac{\mathbf{d}\Delta t_c}{\mathbf{d}\tau} = X_{cr,1}\Delta t_c + X_{cr,2}\Delta t_{cg} + X_{cr,3}\Delta G_{rm} \tag{2.63}$$

$$T_{cw}\frac{\mathbf{d}\Delta t_{cw,L}}{\mathbf{d}\tau} = X_{cw,1}\Delta t_{cw,L} + X_{cw,2}\Delta t_{cg} + X_{cw,3}\Delta t_{cw,E} + X_{cw,4}\Delta G_{cw,E} + \xi_{\Delta t_{cw,L}} \tag{2.64}$$

$$T_{cg}\frac{\mathbf{d}\Delta t_{cg}}{\mathbf{d}\tau} = X_{cg,1}\Delta t_c + X_{cg,2}\Delta t_{cw,L} + X_{cg,3}\Delta t_{cg} + X_{cg,4}\Delta t_{cw,E} + X_{cg,5}\Delta G_{cw,E} \tag{2.65}$$

$$T_{er}\frac{\mathbf{d}\Delta t_k}{\mathbf{d}\tau} = X_{er,1}\Delta t_k + X_{er,2}\Delta t_{eg} + X_{er,3}\Delta G_{rm} \tag{2.66}$$

$$T_{ew}\frac{\mathbf{d}\Delta t_{ew,L}}{\mathbf{d}\tau} = X_{ew,1}\Delta t_{ew,L} + X_{ew,2}\Delta t_{eg} + X_{ew,3}\Delta t_{ew,E} + X_{ew,4}\Delta G_{ew,E} + \xi_{\Delta t_{ew,L}} \tag{2.67}$$

$$T_{eg}\frac{\mathbf{d}\Delta t_{eg}}{\mathbf{d}\tau} = X_{e.g.,1}\Delta t_k + X_{e.g.,2}\Delta t_{ew,L} + X_{e.g.,3}\Delta t_{eg} + X_{e.g.,4}\Delta t_{ew,E} + X_{e.g.,5}\Delta G_{ew,E} \tag{2.68}$$

$$\Delta G_{cw,L} = \Delta G_{cw,E} = \Delta G_{cw} \tag{2.69}$$

$$\Delta G_{ew,L} = \Delta G_{ew,E} = \Delta G_{ew} \tag{2.70}$$

$$\Delta N_{com} = X_{Ew,1}\Delta t_c + X_{Ew,2}\Delta t_k + X_{Ew,3}\Delta G_{rm} \tag{2.71}$$

$$\Delta Q_c = X_{Q,1}\Delta t_c + X_{Q,2}\Delta t_k + X_{Q,3}\Delta G_{rm} \tag{2.72}$$

$$\Delta COP = X_{cop,1}\Delta t_c + X_{cop,2}\Delta t_k \tag{2.73}$$

Table 2.5 Coefficients in Eqs. (2.63) through (2.73)

Equation No.	Coefficient expression
Eq. (2.63)	$T_{cr} = (c_{cr}M_{cr})_o$; $X_{cr,1} = \left[\left(\frac{\partial h_{r,2}}{\partial t_c}\right)_o - \left(\frac{\partial h_{r,3}}{\partial t_c}\right)_o\right](G_{rm})_o + A_{co}(t_{cg} - t_c)_o\left(\frac{\partial a_{co}}{\partial t_c}\right)_o - (a_{co}A_{co})_o$; $X_{cr,2} = A_{co}(t_{cg} - t_c)_o\left(\frac{\partial a_{co}}{\partial t_{cg}}\right)_o + (a_{co}A_{co})_o$; $X_{cr,3} = (h_{r,2} - h_{r,3})_o$
Eq. (2.64)	$T_{cw} = c_wM_{cw}/2$; $X_{cw,1} = -c_w(G_{cw,E})_o - A_{cw}(a_{cw})_o/2$; $X_{cw,2} = A_{cw}(a_{cw})_o$; $X_{cw,3} = c_w(G_{cw,E})_o - A_{cw}(a_{cw})_o/2$; $X_{cw,4} = c_w(t_{cw,E} - t_{cw,L})_o + A_{cw}(t_{cg} - \frac{t_{cw,E}+t_{cw,L}}{2})_o\left(\frac{\partial a_{cw}}{\partial G_{cw,E}}\right)_o$; $\xi_{\Delta t_{cw,L}} = -\frac{1}{2}c_wM_{cw}\frac{\partial \Delta t_{cw,E}}{\partial \tau}$
Eq. (2.65)	$T_{cg} = c_{cg}M_{cg}$; $X_{cg,1} = A_{co}(t_c - t_{cg})_o\left(\frac{\partial a_{co}}{\partial t_c}\right)_o + (a_{co}A_{co})_o$; $X_{cg,2} = X_{cg,4} = A_{cw}(a_{cw})/2_o$; $X_{cg,3} = A_{co}(t_c - t_{cg})_o\left(\frac{\partial a_{co}}{\partial t_{cg}}\right)_o - (a_{cw}A_{cw} + a_{co}A_{co})_o$; $X_{cg,5} = -A_{cw}(t_{cg} - \frac{t_{cw,E}+t_{cw,L}}{2})_o\left(\frac{\partial a_{cw}}{\partial G_{cw,E}}\right)_o$
Eq. (2.66)	$T_{er} = (c_{er}M_{er})_o$; $X_{er,1} = -\left(\frac{\partial h_{r,1}}{\partial t_k}\right)_o(G_{rm})_o + A_{eo}(t_{eg} - t_k)_o\left(\frac{\partial a_{eo}}{\partial t_k}\right)_o - (a_{eo}A_{eo})_o$; $X_{er,2} = A_{eo}(t_{eg} - t_k)_o\left(\frac{\partial a_{eo}}{\partial t_{eg}}\right)_o + (a_{eo}A_{eo})_o$; $X_{er,3} = (h_{r,4} - h_{r,1})_o$;
Eq. (2.67)	$T_{ew} = c_wM_{ew}/2$; $X_{ew,1} = -c_w(G_{ew,E})_o - \frac{A_{ew}}{2}(a_{ew})_o$; $X_{ew,2} = A_{ew}(a_{ew})_o$; $X_{ew,3} = c_w\rho_w(G_{ew,E})_o - \frac{A_{ew}}{2}(a_{ew})_o$; $X_{ew,4} = c_w(t_{ew,E} - t_{ew,L})_o + A_{ew}(t_{eg} - \frac{t_{ew,E}+t_{ew,L}}{2})_o\left(\frac{\partial a_{ew}}{\partial G_{ew,E}}\right)_o$; $\xi_{\Delta t_{ew,L}} = -\frac{1}{2}c_wM_{ew}\frac{\partial \Delta t_{ew,E}}{\partial \tau}$
Eq. (2.68)	$T_{eg} = c_{eg}M_{eg}$; $X_{e.g.,1} = A_{eo}(t_k - t_{eg})_o\left(\frac{\partial a_{eo}}{\partial t_k}\right)_o + (a_{eo}A_{eo})_o$; $X_{e.g.,2} = X_{e.g.,4} = \frac{A_{ew}}{2}(a_{ew})_o$; $X_{e.g.,3} = A_{eo}(t_k - t_{eg})_o\left(\frac{\partial a_{eo}}{\partial t_{eg}}\right)_o - (a_{ew}A_{ew} + a_{eo}A_{eo})_o$; $X_{e.g.,5} = -A_{ew}(t_{eg} - \frac{t_{ew,E}+t_{ew,L}}{2})_o\left(\frac{\partial a_{ew}}{\partial G_{ew,E}}\right)_o$
Eq. (2.71)	$X_{Ew,1} = (G_{rm})_o\left(\frac{\partial f_{N_{wom}}(t_k,t_c)}{\partial t_c}\right)_o$; $X_{Ew,2} = (G_{rm})_o\left(\frac{\partial f_{N_{com}}(t_k,t_c)}{\partial t_k}\right)_o$; $X_{Ew,3} = (f_{N_{com}}(t_k,t_c))_o$
Eq. (2.72)	$X_{Q,1} = (G_{rm})_o\left(\frac{\partial f_{Q_c}(t_k,t_c)}{\partial t_c}\right)_o$; $X_{Q,2} = (G_{rm})_o\left(\frac{\partial f_{Q_c}(t_k,t_c)}{\partial t_k}\right)_o$; $X_{Q,3} = (f_{Q_c}(t_k,t_c))_o$
Eq. (2.73)	$X_{cop,1} = \left[\frac{\partial f_{COP}(t_k,t_c)}{\partial t_c}\right]_o$; $X_{cop,2} = \left[\frac{\partial f_{COP}(t_k,t_c)}{\partial t_k}\right]_o$

All coefficients in the above equations are listed in Table 2.5. Combining Eqs. (2.63) through (2.73), the state-space equation for the vapor-compression packaged liquid chiller can be expressed as follows:

$$\Delta \dot{x}_{chiller} = A_{chiller} \cdot \Delta x_{chiller} + B_{chiller} \cdot \Delta u_{chiller} + \xi \tag{2.74}$$

$$\Delta y_{\text{chiller}} = C_{\text{chiller}} \cdot \Delta x_{\text{chiller}} + D_{\text{chiller}} \cdot \Delta u_{\text{chiller}} \tag{2.75}$$

Let $\Delta X_{\text{chiller}} = \Delta x_{\text{chiller}} + A_{\text{chiller}}^{-1} \xi_{\text{chiller}}$, then Eqs. (2.74) and (2.75) can be converted into a standard state-space form as follows:

$$\Delta \dot{X}_{\text{chiller}} = A_{\text{chiller}} \Delta X_{\text{chiller}} + B_{\text{chiller}} \Delta u_{\text{chiller}} \tag{2.76}$$

$$\Delta y_{\text{chiller}} = C_{\text{chiller}} \Delta X_{\text{chiller}} + D_{\text{chiller}} \Delta u_{\text{chiller}} - C_{\text{chiller}} A_{\text{chiller}}^{-1} \xi_{\text{chiller}} \tag{2.77}$$

where

$$\Delta x_{\text{chiller}} = [\Delta t_{\text{c}}, \Delta t_{\text{cw,L}}, \Delta t_{\text{cg}}, \Delta t_{\text{k}}, \Delta t_{\text{ew,L}}, \Delta t_{\text{eg}}]^T;$$

$$\Delta y_{\text{chiller}} = [\Delta t_{\text{cw,L}}, \Delta G_{\text{cw,L}}, \Delta t_{\text{ew,L}}, \Delta G_{\text{ew,L}}, \Delta N_{\text{com}}, \Delta Q_{\text{c}}, \Delta \text{COP}]^T;$$

$$\Delta u_{\text{chiller}} = [\Delta t_{\text{cw,E}}, \Delta G_{\text{cw,E}}, \Delta t_{\text{ew,E}}, \Delta G_{\text{ew,E}}, \Delta G_{\text{rm}}]^T;$$

$$\xi = [0, \xi_{\Delta t_{\text{cw,L}}}, 0, 0, \xi_{\Delta t_{\text{ew,L}}}, 0]^T;$$

$$A_{\text{chiller}} = \begin{bmatrix} \frac{X_{\text{cr},1}}{T_{\text{cr}}} & 0 & \frac{X_{\text{cr},2}}{T_{\text{cr}}} & 0 & 0 & 0 \\ 0 & \frac{X_{\text{cw},1}}{T_{\text{cw}}} & \frac{X_{\text{cw},2}}{T_{\text{cw}}} & 0 & 0 & 0 \\ \frac{X_{\text{cg},1}}{T_{\text{cg}}} & \frac{X_{\text{cg},2}}{T_{\text{cg}}} & \frac{X_{\text{cg},3}}{T_{\text{cg}}} & 0 & 0 & 0 \\ \frac{X_{\text{er},4}}{T_{\text{er}}} & 0 & 0 & \frac{X_{\text{er},1}}{T_{\text{er}}} & 0 & \frac{X_{\text{er},2}}{T_{\text{er}}} \\ 0 & 0 & 0 & 0 & \frac{X_{\text{ew},1}}{T_{\text{ew}}} & \frac{X_{\text{ew},2}}{T_{\text{ew}}} \\ 0 & 0 & 0 & \frac{X_{\text{e.g.},1}}{T_{\text{eg}}} & \frac{X_{\text{e.g.},2}}{T_{\text{eg}}} & \frac{X_{\text{e.g.},3}}{T_{\text{eg}}} \end{bmatrix}; B_{\text{chiller}} = \begin{bmatrix} 0 & 0 & 0 & 0 & \frac{X_{\text{cr},3}}{T_{\text{cr}}} \\ \frac{X_{\text{cw},3}}{T_{\text{cw}}} & \frac{X_{\text{cw},4}}{T_{\text{cw}}} & 0 & 0 & 0 \\ \frac{X_{\text{cg},4}}{T_{\text{cg}}} & \frac{X_{\text{cg},5}}{T_{\text{cg}}} & 0 & 0 & 0 \\ 0 & 0 & 0 & 0 & \frac{X_{\text{er},3}}{T_{\text{er}}} \\ 0 & 0 & \frac{X_{\text{ew},3}}{T_{\text{ew}}} & \frac{X_{\text{ew},4}}{T_{\text{ew}}} & 0 \\ 0 & 0 & \frac{X_{\text{e.g.},4}}{T_{\text{eg}}} & \frac{X_{\text{e.g.},5}}{T_{\text{eg}}} & 0 \end{bmatrix};$$

$$C_{\text{chiller}} = \begin{bmatrix} 0 & 1 & 0 & 0 & 0 & 0 \\ 0 & 0 & 0 & 0 & 0 & 0 \\ 0 & 0 & 0 & 0 & 1 & 0 \\ 0 & 0 & 0 & 0 & 0 & 0 \\ X_{\text{Ew},1} & 0 & 0 & X_{\text{Ew},2} & 0 & 0 \\ X_{\text{Q},1} & 0 & 0 & X_{\text{Q},2} & 0 & 0 \\ X_{\text{cop},1} & 0 & 0 & X_{\text{cop},2} & 0 & 0 \end{bmatrix}; D_{\text{chiller}} = \begin{bmatrix} 0 & 0 & 0 & 0 & 0 \\ 0 & 1 & 0 & 0 & 0 \\ 0 & 0 & 0 & 0 & 0 \\ 0 & 0 & 0 & 1 & 0 \\ 0 & 0 & 0 & 0 & X_{\text{Ew},3} \\ 0 & 0 & 0 & 0 & X_{\text{Q},3} \\ 0 & 0 & 0 & 0 & 0 \end{bmatrix}.$$

By solving the state-space model as in Eqs. (2.76) and (2.77), the response characteristics of evaporating and condensing temperature (Δt_{k} and Δt_{c}), exit coolant temperature of evaporator and condenser ($\Delta t_{\text{ew,L}}$ and $\Delta t_{\text{cw,L}}$), shell wall temperature of evaporator and condenser (Δt_{eg} and Δt_{cg}), input electric power (ΔN_{com}), and cooling output (ΔQ_{c}) as well as COP of chiller can be obtained under different initial conditions and perturbations.

2.2.2.2 Model Validation

(1) Experimental setup

An experimental refrigeration system has been built to validate the state-space dynamic model of chiller, whose schematic diagram is shown in Fig. 2.11. The

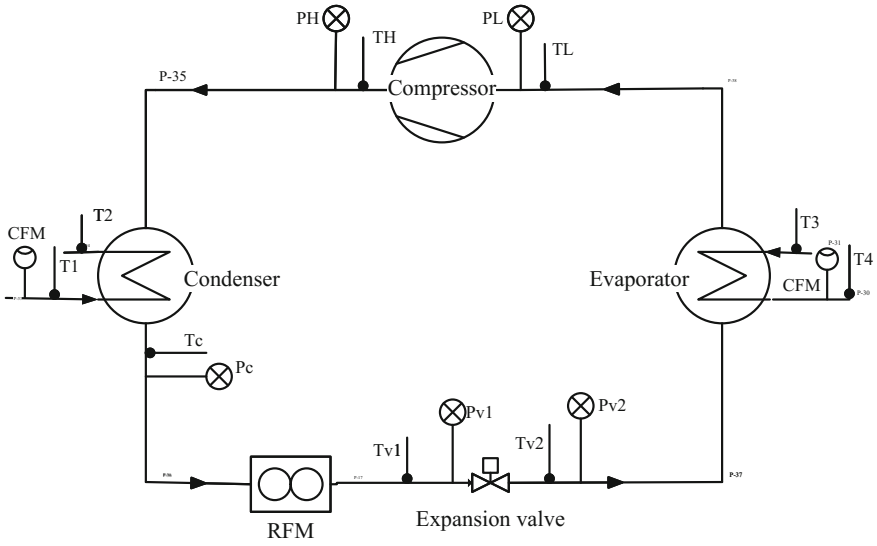

Fig. 2.11 Schematic diagram of experimental setup for the model validation of refrigeration system. *PH* Compressor exhaust pressure sensor; *PL* Compressor inlet pressure sensor; *Pv*1 Expansion valve inlet pressure sensor; *Pv*2 Expansion valve outlet pressure sensor; *Pc* Condenser outlet pressure sensor; *TH* Compressor exhaust temperature sensor; *TL* Compressor inlet temperature sensor; *Tv*1 Expansion valve inlet temperature sensor; *Tv*2 Expansion valve outlet temperature sensor; *Tc* Condenser outlet temperature sensor; *T*1 Condenser inlet coolant temperature sensor; *T*2 Condenser outlet coolant temperature sensor; *T*3 Evaporator inlet cold carrier temperature sensor; *T*4 Evaporator outlet cold carrier temperature sensor; *RFM* Refrigerant flowmeter; *CFM* Coolant or cold carrier flowmeter

condenser and evaporator of the system are of plate-type heat exchanger, and the main structural parameters are listed in Table 2.6. The system uses R-134a (which is admitted to be environmentally friendly) as the working refrigerant. The model coefficients for calculating the thermal properties of the refrigerant R-134a are determined based on the REFPROP 7.01 (a popular calculation program for the refrigerants), which are listed in Table 2.7 [14]. A kind of heat conduction oil is employed as the coolant of the condenser and the cold carrier of the evaporator. The thermal conductivity and the specific heat of the oil versus its temperature ranging from −40 to +60 °C are shown in Fig. 2.12. The density and kinematics viscosity of the heat conduction oil change very small within the temperature range of −40 to +60 °C, which is assumed to be constant (1084 kg/m^3 and 6.5×10^{-6} m^2/s, respectively) in the dynamic response simulation.

The measurement parameters are mainly the refrigerant temperature and pressure at key states of the refrigerant cycle, the inlet and exit coolant (or cold carrier) temperature of the condenser (or the evaporator), the shell wall temperatures of the condenser, and evaporator as well as the corresponding mass flow rate (see Fig. 2.11 for detail). The fluid temperatures are measured by Pt1000 sensors (measurement precision: ±0.1 °C), and the shell wall temperatures are measured by

Table 2.6 Basic information about structural parameters of condenser and evaporator in the experimental chiller system

Structural parameters for the condenser			
Equivalent diameter of channel for coolant (m)	0.0008	Heat transfer area on the coolant side (m^2)	18.33
Heat transfer area on the refrigerant side (m^2)	12.15	Total cross-sectional area of channel for coolant (m^2)	0.006
Coolant volume in the condenser (m^3)	0.0085	Liquid refrigerant volume in the condenser (m^3)	0.0071
Mass of the condenser (kg)	10.86	Specific heat of the condenser (J/(kg °C))	880
Structural parameters for the evaporator			
Equivalent diameter of channel for cold carrier (m)	0.0008	Heat transfer area on the cold carrier side (m^2)	8.87
Heat transfer area on the refrigerant side (m^2)	6.24	Total cross-sectional area of channel for cold carrier (m^2)	0.004
Cold carrier volume in the evaporator (m^3)	0.0038	Liquid refrigerant volume in the evaporator (m^3)	0.0025
Mass of the evaporator (kg)	5.42	Specific heat of the evaporator (J/(kg °C))	880

Table 2.7 Model coefficients for the calculation of thermal properties of the refrigerant R-134a

A	24.8033908	c_3	−0.00000202
A_2	−0.1195051	c_4	0
A_3	0.00014478	c_5	15.8217
A_4	−0.000000105	D	0.0000225
A_5	−6.95E−12	D_1	819.6183
B	−3980.408	D_2	1023.582
B_2	0.000113759	D_3	−1156.757
B_3	−0.0000000894	D_4	789.7191
B_4	0	D_5	0
B_5	1.27E−13	D_6	0
b	0.000345547	E	0.1995548
C	−0.02405332	F	374.8473
C_2	−3.531592	G	0
C_3	0.006469248	K_1	5.475
C_4	0	h_0 (kJ/kg)	209.092133
C_5	−2.05E−9	p_{atm} (kPa)	101.325
c_1	−0.005257455	R (kJ/kg)	0.081488163
c_2	0.00329657	T_c (K)	374.25

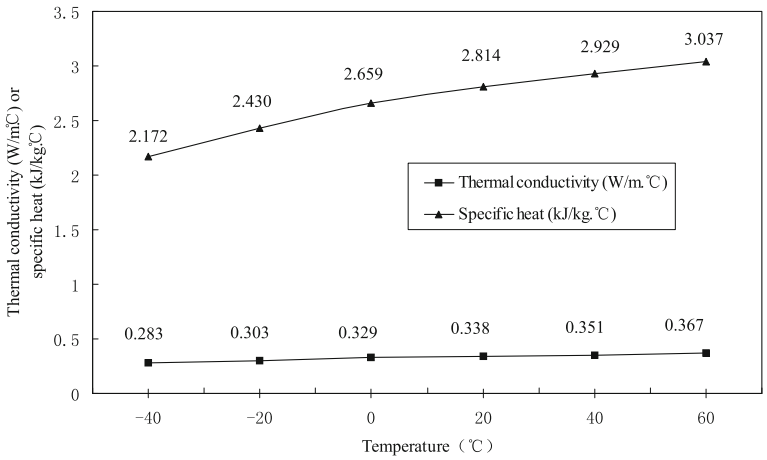

Fig. 2.12 Thermal properties versus temperature of the cooling and cold carrier fluid

copper-constantan thermocouples (measurement precision: ±0.2 °C) which have a direct contact with the exterior surface of the heat exchangers. The pressure sensors are of AKS32 type (measurement precision: (20 ± 0.3 % full scale) Pa). The meter for the measurement of refrigerant mass flow rate is of LSLW type (measurement precision: 0.5 % of full scale) and that for the coolant and cold carrier mass flow rate is of FVC one (measurement precision: 0.5 % of full scale). All the measured parameters were collected automatically by the Keithley 2700 data acquisition system connected with a computer, and the sampling interval was set as 2 s.

(2) Methods for experimental validation

In real situations, the exit cold carrier temperature of evaporator is the key control parameter we care the most. Therefore, the state-space model of chiller is experimentally validated mainly in terms of the transient responses of the exit cold carrier temperature of evaporator under certain initial conditions and perturbations that are chosen arbitrarily.

To begin with, the empirical constants in Eqs. (2.52)–(2.54) need to be determined through experiments by using the following equations:

$$G_{\mathrm{rm}}(h_2 - h_3) = a_{\mathrm{co}}A_{\mathrm{co}}(t_{\mathrm{c}} - t_{\mathrm{cg}}) = C_1A_{\mathrm{co}}(t_{\mathrm{c}} - t_{\mathrm{cg}})^{n_1+1} \tag{2.78}$$

$$G_{\mathrm{rm}}(h_4 - h_1) = a_{\mathrm{eo}}A_{\mathrm{eo}}(t_{\mathrm{eg}} - t_{\mathrm{k}}) = C_2A_{\mathrm{eo}}(t_{\mathrm{eg}} - t_{\mathrm{k}})^{n_2+1} \tag{2.79}$$

$$\begin{aligned} c_{\mathrm{cw}}G_{\mathrm{cw}}(t_{\mathrm{cw,L}} - t_{\mathrm{cw,E}}) &= a_{\mathrm{cw}}A_{\mathrm{cw}}\left[t_{\mathrm{cg}} - \left(t_{\mathrm{cw,L}} + t_{\mathrm{cw,E}}\right)/2\right] \\ &= A_{\mathrm{cw}}\frac{C_3\lambda_{\mathrm{w}}}{d_{\mathrm{ci}}}\left[t_{\mathrm{cg}} - \left(t_{\mathrm{cw,L}} + t_{\mathrm{cw,E}}\right)/2\right]Re_{\mathrm{d}}{}^{n_3} \end{aligned} \tag{2.80}$$

As shown in Eqs. (2.78)–(2.80), the measured parameters include the temperature and pressure of refrigerant at the key states (states '1,' '2,' '3,' and '4'), the inlet and exit coolant temperature of condenser ($t_{cw,E}, t_{cw,L}$), the inlet and exit cold carrier temperature of evaporator ($t_{ew,E}, t_{ew,L}$), and the shell wall temperature of condenser and evaporator (t_{eg}, t_{cg}) as well as the mass flow rate of refrigerant, coolant, and cold carrier (G_{rm}, G_{cw}, G_{ew}). All these parameters are measured under different steady conditions in which G_{rm} and G_{cw} ranges, respectively, from 0.05 to 0.30 kg/s and from 1.0 to 2.5 kg/s.

To obtain the empirical constants, C_1, C_2, C_3, n_1, n_2 *and* n_3, Eqs. (2.78)–(2.80) can be written, respectively, as follows:

$$Ln[G_{rm}(h_2 - h_3)] = Ln(C_1 A_{co}) + (n_1 + 1)Ln(t_c - t_{cg}) \tag{2.81}$$

$$Ln[G_{rm}(h_4 - h_1)] = Ln(C_2 A_{eo}) + (n_2 + 1)Ln(t_{eg} - t_k) \tag{2.82}$$

$$Ln\left[c_{cw}G_{cw}(t_{cw,L} - t_{cw,E})\right] = Ln\left[A_{cw}\frac{C_3\lambda_w}{d_{ci}}\left[t_{cg} - \left(t_{cw,L} + t_{cw,E}\right)/2\right]\right] + n_3 LnRe_d \tag{2.83}$$

The constants, C_1, C_2, C_3, n_1, n_2 *and* n_3, can be determined, respectively, according to the slope and intercept of the straight line of $Ln[G_{rm}(h_2 - h_3)]$ versus $Ln(t_c - t_{cg})$, $Ln[G_{rm}(h_4 - h_1)]$ versus $Ln(t_{eg} - t_k)$ and $Ln\left[c_{cw}G_{cw}(t_{cw,L} - t_{cw,E})\right]$ versus $LnRe_d$ fitting to the experimental data. The results are listed as follows: $C_1 = 2558$; $C_2 = 3056$; $n_1 = -0.25$; $n_2 = 0.25$; $C_3 = 0.05$; $n_3 = 0.8$.

Similarly, the average error (AE, Eq. (2.39)) is employed as well to evaluate the validity of the model results compared with the experimental data during the transient response process.

(3) Experimental results

Three experimental cases have been performed for the model validation. The initial conditions of the three cases are listed in Table 2.8, which were measured under the steady states before the input perturbations began. The perturbations corresponding to the three experimental cases are shown in Fig. 2.13, respectively. The perturbations on the inlet cold carrier temperature of evaporator were achieved through adjusting the heat load simulated by an electric heating box, and that on the inlet coolant temperature of condenser were done through changing the cooling capacity of the cooling tower. The refrigerant mass flow rate is closely related to the compressor rotation speed which can be adjusted by a compatible frequency converter.

Figure 2.14 shows the comparisons of the theoretical simulations with the experimental data on the transient responses of the exit cold carrier temperature of evaporator under the perturbations of case *I* (see Fig. 2.13). It is easily understood that the exit cold carrier temperature of evaporator will increase with the inlet cold

Table 2.8 Initial conditions for model validation and simulation

Initial conditions	Experimental cases		
	Case I	Case II	Case III
Evaporating temperature $(t_k)_o$ (°C)	14.5	15.9	14.5
Inlet cold carrier temperature of evaporator $(t_{ew,E})_o$ (°C)	24.8	24.8	25.4
Outlet cold carrier temperature of evaporator $(t_{ew,L})_o$ (°C)	19.5	19.9	19.7
Shell wall temperature of evaporator $(t_{eg})_o$ (°C)	22.5	22.9	22.6
Cold carrier flow rate of evaporator $(G_{ew})_o$ (kg/s)	1.45	1.45	1.45
Condensing temperature $(t_c)_o$ (°C)	36.3	50.1	48.2
Inlet coolant temperature of condenser $(t_{cw,E})_o$ (°C)	29.5	42.2	39.9
Outlet cold carrier temperature of condenser $(t_{cw,L})_o$ (°C)	37.2	49.7	49.4
Coolant flow rate of condenser $(G_{cw})_o$ (kg/s)	1.16	1.05	1.51
Shell wall temperature of condenser $(t_{cg})_o$ (°C)	33.9	42.5	40.9
Compressor inlet temperature $(t_{com,E})_o$ (°C)	24.1	20.2	23.4
Compressor exhaust temperature $(t_{com,L})_o$ (°C)	58.1	51.2	81.5
Refrigerant flow rate $(G_{rm})_o$ (kg/s)	0.116	0.17	0.26

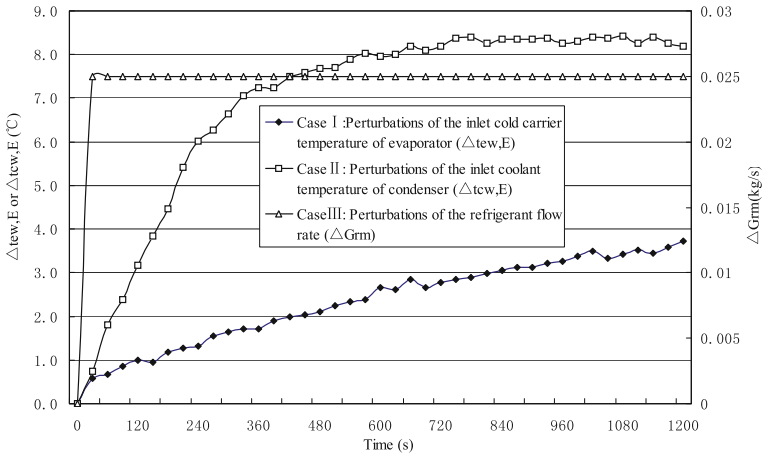

Fig. 2.13 Perturbations for the experimental cases (measured data)

carrier temperature rising. The experimental results manifest that the model can predict well the transient responses of the exit cold carrier temperature of evaporator (the average error (AE) is estimated about 6.4 %) under perturbations of the inlet cold carrier temperature.

Figure 2.15 shows the calculated and experimental data on the transient responses of the exit cold carrier temperature of evaporator under the perturbations of case *II* (see Fig. 2.13). Clearly, the increase in the inlet coolant temperature of

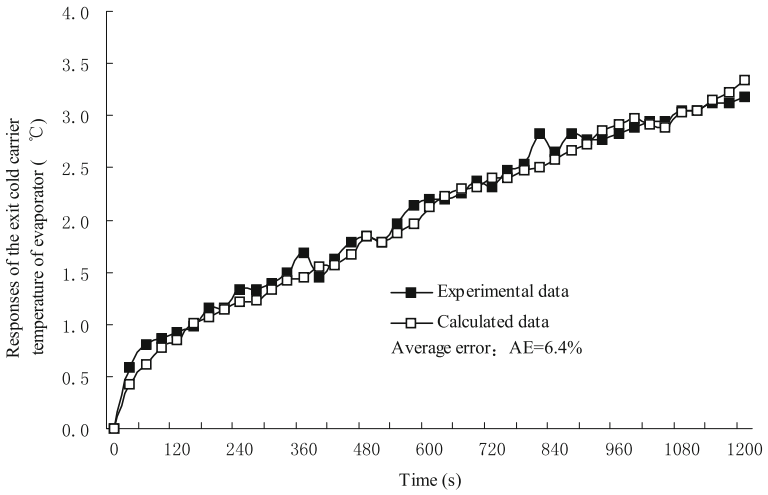

Fig. 2.14 Responses of the exit cold carrier temperature of evaporator ($\Delta t_{ew,L}$) under the perturbations of case I (calculated results vs. experimental data)

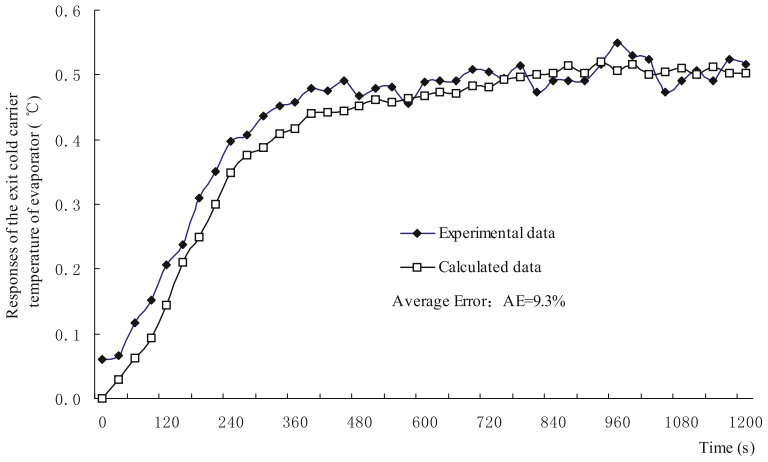

Fig. 2.15 Responses of the exit cold carrier temperature of evaporator ($\Delta t_{ew,L}$) under the perturbations of case II (calculated results vs. experimental data)

condenser will cause the condensing temperature to rise and decrease the chiller's cooling capacity. As a result, the exit cold carrier temperature of evaporator will increase. The average error (AE) of the model results compared with the experimental data for the experimental case *II* is about 9.3 %, which also verifies the

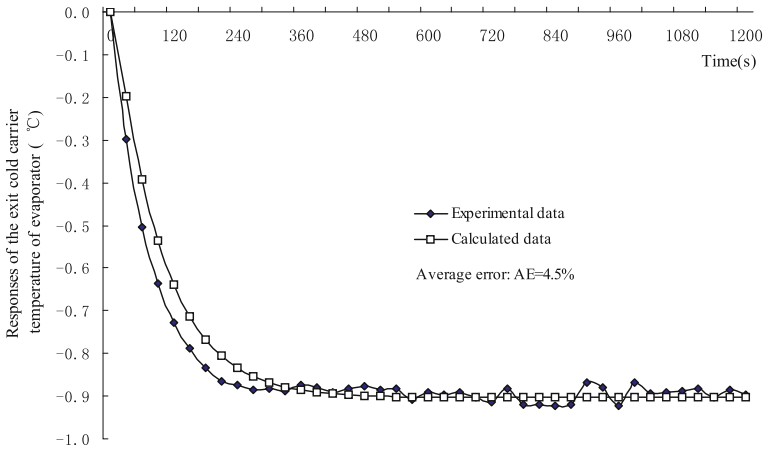

Fig. 2.16 Responses of the exit cold carrier temperature of evaporator ($\Delta t_{ew,L}$) under the perturbations of case III (calculated results vs. experimental data)

effectiveness of the model in predicting the transient responses of the exit cold carrier temperature of evaporator under perturbations of the inlet coolant temperature of condenser.

Figure 2.16 shows the calculated and experimental data on the transient responses of the exit cold carrier temperature of evaporator under the perturbations of case *III* (see Fig. 2.13). It is reasonable to see that the exit cold carrier temperature of evaporator will decrease with the increase in the refrigerant flow rate since the chiller's output cooling capacity increases under such circumstance. The average error (AE) of the model simulation in the experimental case *III* is about 4.5 %, which validates as well the goodness of the proposed model for predicting the transient responses of the exit cold carrier temperature of evaporator under perturbations of the refrigerant flow rate.

As seen from the experimental study cases illustrated above, the errors of model simulation compared with the experimental data are all less than 10 %. Therefore, we can safely conclude that the proposed state-space model is capable of studying the transient response characteristics and dynamic performance of the vapor-compression liquid refrigeration system under different ambient perturbations.

2.2.3 Cooling Tower

A HVAC (heating, ventilating, and air-conditioning) cooling tower is used to dispose of ('reject') unwanted heat from a chiller. Water-cooled chillers are normally more energy efficient than air-cooled chillers due to heat rejection to tower

water at or near wet-bulb temperatures. With respect to the heat transfer mechanism employed, the main types are as follows: ① dry-cooling towers operate by heat transfer through a surface that separates the working fluid from ambient air, such as in a tube to air heat exchanger, utilizing convective heat transfer. They do not use evaporation; ② fluid coolers (or closed-circuit cooling towers) are hybrids that pass the working fluid through a tube bundle, upon which clean water is sprayed and a fan-induced draft applied;③ wet-cooling towers (or open-circuit cooling towers) operate on the principle of evaporative cooling. Since the wet-cooling towers have the highest heat transfer performance, and the warm water can be cooled to a temperature lower than the ambient air dry-bulb temperature, the wet-cooling towers are used in a HVAC system more frequently. To achieve better performance (more cooling), a medium called 'fill' is used to increase the surface area and the time of contact between the air and water flows to improve heat transfer.

There are two types of configurations for the wet-cooling tower, one is cross-flow and the other is counterflow. Cross-flow is a design in which the airflow is directed perpendicular to the water flow. Airflow enters one or more vertical faces of the cooling tower to meet the fill material. Water flows (perpendicular to the air) through the fill by gravity. The air continues through the fill and thus past the water flow into an open plenum volume. Lastly, a fan forces the air out into the atmosphere. In a counterflow design, the airflow is directly opposite to the water flow. Airflow first enters an open area beneath the fill media and is then drawn up vertically. The water is sprayed through pressurized nozzles near the top of the tower and then flows downward through the fill, opposite to the airflow. Advantages of the counterflow design include the following: ① Spray water distribution makes the tower more freeze-resistant and ② breakup of water in spray makes heat transfer more efficient. In the following section, the counterflow wet-cooling tower is taken as an example for the state-space modeling.

2.2.3.1 Model Development

1) Assumptions and fundamental equations

As shown in Fig. 2.17, a counterflow wet-cooling tower normally consists of two sections: The upper is fill and the lower is sink. The main assumptions for modeling are as follows:

(1) Moisture air is treated as a mixture of ideal gases;
(2) The exterior wall of the cooling tower is thermally adiabatic;
(3) The single-film theory is applied to the heat and mass transfer between the air and the water film on the fill;
(4) Air temperature and humidity as well as water temperature change linearly from inlet to outlet of the cooling tower, and they are, respectively, mean value of inlet and outlet.

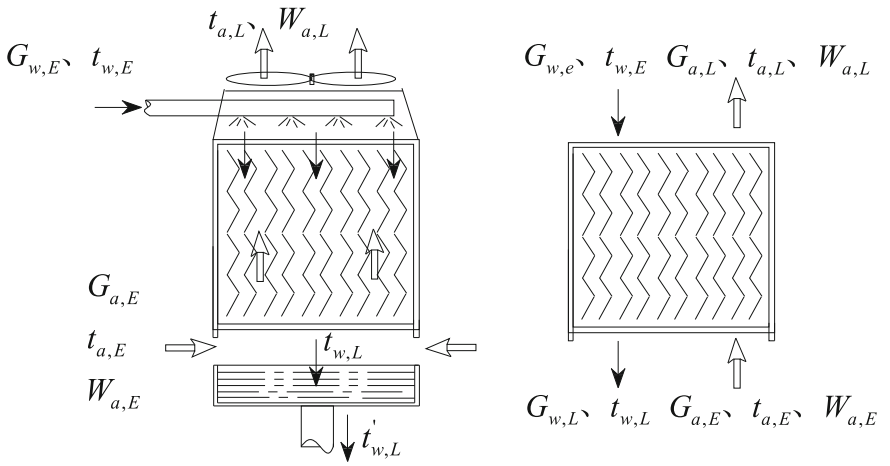

Fig. 2.17 Schematic diagram for counterflow wet-cooling tower

By using the first law of energy and mass conservation, the following equations can be obtained for the counterflow wet-cooling tower.

(1) *Mass and energy equation for air passing through fill of cooling tower*

$$G_{\mathrm{a,E}} = G_{\mathrm{a,L}} = G_{\mathrm{a}} \tag{2.84}$$

$$\frac{1}{2}\rho_{\mathrm{a}}\varepsilon_{\mathrm{a}}A_{\mathrm{ta}}H_{\mathrm{t}}\frac{\mathbf{d}(h_{\mathrm{a,E}}+h_{\mathrm{a,L}})}{\mathbf{d}\tau} = G_{\mathrm{a,E}}(h_{\mathrm{a,E}}-h_{\mathrm{a,L}}) + a_{\mathrm{wa}}A_{\mathrm{t}}\left(\frac{t_{\mathrm{w,E}}+t_{\mathrm{w,L}}}{2}-\frac{t_{\mathrm{a,E}}+t_{\mathrm{a,L}}}{2}\right) + q_{\mathrm{r}}\lambda_{\mathrm{m}}A_{\mathrm{t}}\left(W_{\mathrm{tb}}-\frac{W_{\mathrm{a,E}}+W_{\mathrm{a,L}}}{2}\right) \tag{2.85}$$

(2) *Mass equation for air moisture*

$$\frac{1}{2}\rho_{\mathrm{a}}\varepsilon_{\mathrm{a}}A_{\mathrm{ta}}H_{\mathrm{t}}\frac{\mathbf{d}(W_{\mathrm{a,L}}+W_{\mathrm{a,E}})}{\mathbf{d}\tau} = G_{\mathrm{a,E}}(W_{\mathrm{a,E}}-W_{\mathrm{a,L}}) + \lambda_{\mathrm{m}}A_{\mathrm{t}}\left(W_{\mathrm{tb}}-\frac{W_{\mathrm{a,E}}+W_{\mathrm{a,L}}}{2}\right) \tag{2.86}$$

(3) *Mass and energy equation for water passing through fill of cooling tower*

$$G_{\mathrm{w,E}} = G_{\mathrm{w,L}} = G_{\mathrm{w}} \tag{2.87}$$

$$\frac{1}{2}c_{\mathrm{w}}G_{\mathrm{w,E}}\frac{H_{\mathrm{t}}}{u_{\mathrm{w}}}\frac{\mathbf{d}(t_{\mathrm{w,L}}+t_{\mathrm{w,E}})}{\mathbf{d}\tau}=c_{\mathrm{w}}G_{\mathrm{w,E}}(t_{\mathrm{w,E}}-t_{\mathrm{w,L}})+a_{\mathrm{wa}}A_{\mathrm{t}}\left(\frac{t_{\mathrm{a,E}}+t_{\mathrm{a,L}}}{2}-\frac{t_{\mathrm{w,E}}+t_{\mathrm{w,L}}}{2}\right)+q_{\mathrm{r}}\lambda_{\mathrm{m}}A_{\mathrm{t}}\left(\frac{W_{\mathrm{a,E}}+W_{\mathrm{a,L}}}{2}-W_{\mathrm{tb}}\right) \tag{2.88}$$

(4) *Mass equation for water in sink of cooling tower*

$$M_{\mathrm{w,pt}}\frac{\mathbf{d}t'_{\mathrm{w,L}}}{\mathbf{d}\tau}=G_{\mathrm{w,E}}(t_{\mathrm{w,L}}-t'_{\mathrm{w,L}}) \tag{2.89}$$

In Eqs. (2.84) through (2.89), the symbol 'G' stands for flow rate, kg/s; 'ε_{a}'for air volume ratio in cooling tower; 'A_{ta}' for cross-sectional area of cooling tower, m^2; 'A_{t}' for surface area between air and water film in cooling tower, m^2; 'H_{t}' for height of cooling tower, m; 'u_{w}' for falling velocity of water, m/s; 'λ_{m}' for mass transfer coefficient, kg/ (m^{2}/s); and 'a_{wa}' for heat transfer coefficient between air and water film in cooling tower, W/(m^2 °C);

2) Key parameters

According to the single-film theory, the saturated humidity of air on the water film surface of fill (W_{tb}) can be expressed by Eq. (2.90), a function dependent on the average temperature of the water film.

$$W_{\mathrm{tb}}\approx\beta_1\frac{t_{\mathrm{w,E}}+t_{\mathrm{w,L}}}{2} \tag{2.90}$$

The convective heat transfer coefficient (a_{wa}) and convective mass transfer coefficient (λ_{m}) can refer to the correlation equation of heat and mass transfer for plate flow as follows [15]:

$$Nu_{\mathrm{a}}=\frac{a_{\mathrm{wa}}H_{\mathrm{t}}}{\lambda_{\mathrm{a}}}=0.648Re_{\mathrm{a}}^{0.5}\mathrm{Pr}_{\mathrm{a}}^{1/3} \tag{2.91}$$

$$Sh_{\mathrm{m}}=\frac{\lambda_{\mathrm{m}}H_{\mathrm{t}}}{\rho_{\mathrm{a}}D_{\mathrm{w,a}}}=0.648Re_{\mathrm{a}}^{0.5}Sc_{\mathrm{j}}^{1/3} \tag{2.92}$$

where $Re_{\mathrm{a}}=\frac{H_{\mathrm{t}}(u_{\mathrm{a}}+u_{\mathrm{w}})}{\nu_{\mathrm{a}}}$; H_{t} is height of film in cooling tower, m; u_{w} is mean gliding speed of water film on the fill, which can be calculated by Eq. (2.93)

$$u_{\mathrm{w}}=\frac{1}{H_{\mathrm{t}}}\int_0^{H_{\mathrm{t}}}\sqrt{u_{\mathrm{o}}^2+2gH_{\mathrm{t}}}dy \tag{2.93}$$

where u_o is spraying velocity at the spray nozzle, *m/s*. Please note that drag forces of water film is neglected in Eq. (2.93).

3) State-space representation

Through linearization, Eqs. (2.84) through (2.89) can be written as follows:

$$\begin{aligned} T_{\mathrm{t,ta}} \frac{\mathbf{d}\Delta t_{\mathrm{a,L}}}{\mathbf{d}\tau} = {} & X_{\mathrm{t},1}\Delta t_{\mathrm{a,L}} + X_{\mathrm{t},2}\Delta W_{\mathrm{a,L}} + X_{\mathrm{t},3}\Delta t_{\mathrm{w,L}} + X_{\mathrm{t},4}\Delta t_{\mathrm{a,E}} \\ & + X_{\mathrm{t},5}\Delta t_{\mathrm{w,E}} + X_{\mathrm{t},6} W_{\mathrm{a,E}} + X_{\mathrm{t},7}\Delta G_{\mathrm{a,E}} + \xi_{t_{\mathrm{a,L}}} \end{aligned} \tag{2.94}$$

$$T_{\mathrm{t,wa}} \frac{\mathbf{d}\Delta W_{\mathrm{a,L}}}{\mathbf{d}\tau} = Y_{\mathrm{t},1}\Delta W_{\mathrm{a,L}} + Y_{\mathrm{t},2}\Delta t_{\mathrm{w,L}} + Y_{\mathrm{t},3}\Delta t_{\mathrm{w,E}} + Y_{\mathrm{t},4}\Delta W_{\mathrm{a,E}} + Y_{\mathrm{t},5}\Delta G_{\mathrm{a,E}} + \xi_{W_{\mathrm{a,L}}} \tag{2.95}$$

$$\begin{aligned} T_{\mathrm{t,tw}} \frac{\mathbf{d}\Delta t_{\mathrm{w,L}}}{\mathbf{d}\tau} = {} & Z_{\mathrm{t},1}\Delta t_{\mathrm{a,L}} + Z_{\mathrm{t},2}\Delta W_{\mathrm{a,L}} + Z_{\mathrm{t},3}\Delta t_{\mathrm{w,L}} + Z_{\mathrm{t},4}\Delta t_{\mathrm{a,E}} \\ & + Z_{\mathrm{t},5}\Delta t_{\mathrm{w,E}} + Z_{\mathrm{t},6} W_{\mathrm{a,E}} + Z_{\mathrm{t},7}\Delta G_{\mathrm{a,E}} + Z_{\mathrm{t},8}\Delta G_{\mathrm{w,E}} + \xi_{t_{\mathrm{w,L}}} \end{aligned} \tag{2.96}$$

$$M_{\mathrm{w,pt}} \frac{\mathbf{d}\Delta t'_{\mathrm{w,L}}}{\mathbf{d}\tau} = M_{\mathrm{t},1}\Delta t_{\mathrm{w,L}} + M_{\mathrm{t},2}\Delta t'_{\mathrm{w,L}} + M_{\mathrm{t},3}\Delta G_{\mathrm{w,E}} \tag{2.97}$$

$$\Delta G_{\mathrm{a,L}} = \Delta G_{\mathrm{a,E}} \tag{2.98}$$

$$\Delta G_{\mathrm{w,L}} = \Delta G_{\mathrm{w,E}} \tag{2.99}$$

The coefficients in Eqs. (2.94)–(2.97) are described in Table 2.9.

Choosing the variables, $\Delta t_{\mathrm{a,L}}, \Delta W_{\mathrm{a,L}}, \Delta t_{\mathrm{w,L}}, \Delta t'_{\mathrm{w,L}}$, in the differential term as state ones, the variables, $\Delta t_{\mathrm{a,E}}, \Delta W_{\mathrm{a,E}}, \Delta G_{\mathrm{a,E}}, \Delta t_{\mathrm{w,E}}, \Delta G_{\mathrm{w,E}}$, as input ones, and the variables, $\Delta t_{\mathrm{a,L}}, \Delta W_{\mathrm{a,L}}, \Delta G_{\mathrm{a,L}}, \Delta t'_{\mathrm{w,L}}, \Delta G_{\mathrm{w,L}}$, as output ones, Eqs. (2.94)–(2.99) can be expressed in the form of state-space representation as follows:

$$\dot{x}_{\mathrm{tower}} = A_{\mathrm{tower}} \cdot x_{\mathrm{tower}} + B_{\mathrm{tower}} \cdot u_{\mathrm{tower}} + \xi_{\mathrm{tower}} \tag{2.100}$$

$$y_{\mathrm{tower}} = C_{\mathrm{tower}} \cdot x_{\mathrm{tower}} + D_{\mathrm{tower}} \cdot u_{\mathrm{tower}} \tag{2.101}$$

Similarly, the standard state-space form can be deduced from Eqs. (2.100) and (2.101) as follows:

$$\dot{X}_{\mathrm{tower}} = A_{\mathrm{tower}} X_{\mathrm{tower}} + B_{\mathrm{tower}} u_{\mathrm{tower}} \tag{2.102}$$

$$y_{\mathrm{tower}} = C_{\mathrm{tower}} X_{\mathrm{tower}} + D_{\mathrm{tower}} u_{\mathrm{tower}} - C_{\mathrm{tower}} A_{\mathrm{tower}}^{-1} \xi_{\mathrm{tower}} \tag{2.103}$$

Table 2.9 Coefficients in Eqs. (2.95)–(2.98)

Equation No.	Coefficient expression
Eq. (2.94)	$T_{\mathrm{t,ta}} = \frac{1}{2}\varepsilon_{\mathrm{a}} c_{\mathrm{a}} \rho_{\mathrm{a}} A_{\mathrm{t,a}} H_{\mathrm{t}}$; $X_{\mathrm{t},1} = -c_{\mathrm{a}}(G_{\mathrm{a,E}})_{\mathrm{o}} - A_{\mathrm{t}}(a_{\mathrm{wa}})_{\mathrm{o}}/2$; $X_{\mathrm{t},2} = X_{\mathrm{t},6} = -\frac{A_{\mathrm{t}}(q_{\mathrm{r}}-\beta_2)}{2}(\lambda_{\mathrm{m}})_{\mathrm{o}}$; $X_{\mathrm{t},3} = X_{\mathrm{t},5} = \frac{A_{\mathrm{t}}}{2}\left[(a_{\mathrm{wa}})_{\mathrm{o}} + \beta_1(q_{\mathrm{r}}-\beta_2)(\lambda_{\mathrm{m}})_{\mathrm{o}}\right]$; $X_{\mathrm{t},4} = c_{\mathrm{a}}(G_{\mathrm{a,E}})_{\mathrm{o}} - A_{\mathrm{t}}(a_{\mathrm{wa}})_{\mathrm{o}}/2$; $X_{\mathrm{t},7} = c_{\mathrm{a}}(t_{\mathrm{a,E}} - t_{\mathrm{a,L}})_{\mathrm{o}} + \frac{A_{\mathrm{t}}}{2}\left(\frac{\partial a_{\mathrm{wa}}}{\partial G_{\mathrm{a,E}}}\right)_{\mathrm{o}}(t_{\mathrm{w,L}} + t_{\mathrm{w,E}} - t_{\mathrm{a,L}} - t_{\mathrm{a,E}})_{\mathrm{o}} - \frac{A_{\mathrm{t}}(q_{\mathrm{r}}-\beta_2)}{2}\left(\frac{\partial \lambda_{\mathrm{m}}}{\partial G_{\mathrm{a,E}}}\right)_{\mathrm{o}}[\beta_1(t_{\mathrm{w,E}} + t_{\mathrm{w,L}})_{\mathrm{o}} - (W_{\mathrm{a,E}} + W_{\mathrm{a,L}})_{\mathrm{o}}]$; $\xi_{t_{\mathrm{a,L}}} = -T_{\mathrm{t,ta}}\frac{d\Delta t_{\mathrm{a,E}}}{d\tau}$;
Eq. (2.95)	$T_{\mathrm{t,wa}} = \frac{1}{2}\varepsilon_{\mathrm{a}}\rho_{\mathrm{a}} A_{\mathrm{t,a}} H_{\mathrm{t}}$; $Y_{\mathrm{t},1} = -(G_{\mathrm{a,E}})_{\mathrm{o}} - \frac{A_{\mathrm{t}}}{2}(\lambda_{\mathrm{m}})_{\mathrm{o}}$; $Y_{\mathrm{t},2} = Y_{\mathrm{t},3} = \frac{A_{\mathrm{t}}\beta_1}{2}(\lambda_{\mathrm{m}})_{\mathrm{o}}$; $Y_{\mathrm{t},4} = (G_{\mathrm{a,E}})_{\mathrm{o}} - \frac{A_{\mathrm{t}}}{2}(\lambda_{\mathrm{m}})_{\mathrm{o}}$; $Y_{\mathrm{t},5} = (W_{\mathrm{a,E}} - W_{\mathrm{a,L}})_{\mathrm{o}} + \frac{A_{\mathrm{t}}}{2}\left(\frac{\partial \lambda_{\mathrm{m}}}{\partial G_{\mathrm{a,E}}}\right)_{\mathrm{o}}[\beta_1(t_{\mathrm{w,L}} + t_{\mathrm{w,E}})_{\mathrm{o}} - (W_{\mathrm{a,E}} + W_{\mathrm{a,L}})_{\mathrm{o}}]$; $\xi_{W_{\mathrm{a,L}}} = -T_{\mathrm{t,wa}}\frac{d\Delta W_{\mathrm{a,E}}}{d\tau}$
Eq. (2.96)	$T_{\mathrm{t,tw}} = \frac{1}{2}c_{\mathrm{w}}\frac{H_{\mathrm{t}}}{u_{\mathrm{w}}}$; $Z_{\mathrm{t},1} = Z_{\mathrm{t},4} = \frac{A_{\mathrm{t}}}{2(G_{\mathrm{w,E}})_{\mathrm{o}}}(a_{\mathrm{wa}})_{\mathrm{o}}$; $Z_{\mathrm{t},2} = Z_{\mathrm{t},6} = \frac{A_{\mathrm{t}}q_{\mathrm{r}}}{2(G_{\mathrm{w,E}})_{\mathrm{o}}}(\lambda_{\mathrm{m}})_{\mathrm{o}}$; $Z_{\mathrm{t},3} = -\frac{1}{(G_{\mathrm{w,E}})_{\mathrm{o}}}\left(\frac{\beta_1 A_{\mathrm{t}} q_{\mathrm{r}}}{2}(\lambda_{\mathrm{m}})_{\mathrm{o}} + \frac{A_{\mathrm{t}}}{2}(a_{\mathrm{wa}})_{\mathrm{o}}\right) - c_{\mathrm{w}}$; $Z_{\mathrm{t},5} = -\frac{1}{(G_{\mathrm{w,E}})_{\mathrm{o}}}\left(\frac{\beta_1 A_{\mathrm{t}} q_{\mathrm{r}}}{2}(\lambda_{\mathrm{m}})_{\mathrm{o}} + \frac{A_{\mathrm{t}}}{2}(a_{\mathrm{wa}})_{\mathrm{o}}\right) + c_{\mathrm{w}}$; $Z_{\mathrm{t},7} = \frac{1}{(G_{\mathrm{w,E}})_{\mathrm{o}}}\left[\frac{A_{\mathrm{t}}}{2}\left(\frac{\partial a_{\mathrm{wa}}}{\partial G_{\mathrm{a,E}}}\right)_{\mathrm{o}}(t_{\mathrm{a,E}} + t_{\mathrm{a,L}} - t_{\mathrm{w,E}} - t_{\mathrm{w,L}})_{\mathrm{o}} + \frac{q_{\mathrm{r}}A_{\mathrm{t}}}{2}\left(\frac{\partial \lambda_{\mathrm{m}}}{\partial G_{\mathrm{a,E}}}\right)_{\mathrm{o}}[(W_{\mathrm{a,E}} + W_{\mathrm{a,L}})_{\mathrm{o}} - \beta_1(t_{\mathrm{w,E}} + t_{\mathrm{w,L}})_{\mathrm{o}}]\right]$; $Z_{\mathrm{t},8} = -\frac{1}{2G_{\mathrm{w,E}}^2}\left[(a_{\mathrm{wa}})_{\mathrm{o}}A_{\mathrm{t}}\left((t_{\mathrm{a,E}} + t_{\mathrm{a,L}})_{\mathrm{o}} - (t_{\mathrm{w,E}} + t_{\mathrm{w,L}})_{\mathrm{o}}\right) + q_{\mathrm{r}}(\lambda_{\mathrm{m}})_{\mathrm{o}}A_{\mathrm{t}}\left((W_{\mathrm{a,E}} + W_{\mathrm{a,L}})_{\mathrm{o}} - \beta_1(t_{\mathrm{w,E}} + t_{\mathrm{w,L}})_{\mathrm{o}}\right)\right]$; $\xi_{t_{\mathrm{w,L}}} = -T_{\mathrm{t,tw}}\frac{d\Delta t_{\mathrm{w,E}}}{d\tau}$;
Eq. (2.97)	$M_{\mathrm{t},1} = -M_{\mathrm{t},2} = (G_{\mathrm{w,E}})_{\mathrm{o}}$; $M_{\mathrm{t},3} = (t_{\mathrm{w,L}} - t'_{\mathrm{w,L}})_{\mathrm{o}}$;

where

$$
\begin{aligned}
X_{\mathrm{tower}} &= x_{\mathrm{tower}} + A_{\mathrm{tower}}^{-1}\xi_{\mathrm{tower}};\\
x_{\mathrm{tower}} &= \left[\Delta t_{\mathrm{a,L}}, \Delta W_{\mathrm{a,L}}, \Delta t_{\mathrm{w,L}}, \Delta t'_{\mathrm{w,L}}\right]^T;\\
y_{\mathrm{tower}} &= \left[\Delta t_{\mathrm{a,L}}, \Delta W_{\mathrm{a,L}}, \Delta G_{\mathrm{a,L}}, \Delta t'_{\mathrm{w,L}}, \Delta G_{\mathrm{w,L}}\right]^T;\\
u_{\mathrm{tower}} &= \left[\Delta t_{\mathrm{a,E}}, \Delta W_{\mathrm{a,E}}, \Delta G_{\mathrm{a,E}}, \Delta t_{\mathrm{w,E}}, \Delta G_{\mathrm{w,E}}\right]^T;\\
\xi_{\mathrm{tower}} &= \left[\xi_{t_{\mathrm{a,L}}}, \xi_{W_{\mathrm{a,L}}}, \xi_{t_{\mathrm{w,L}}}, 0\right]^T;
\end{aligned}
$$

$$
A_{\mathrm{tower}} = \begin{bmatrix}
\frac{X_{\mathrm{t},1}}{T_{\mathrm{t,ta}}} & \frac{X_{\mathrm{t},2}}{T_{\mathrm{t,ta}}} & \frac{X_{\mathrm{t},3}}{T_{\mathrm{t,ta}}} & 0\\
0 & \frac{Y_{\mathrm{t},1}}{T_{\mathrm{t,wa}}} & \frac{Y_{\mathrm{t},2}}{T_{\mathrm{t,wa}}} & 0\\
\frac{Z_{\mathrm{t},1}}{T_{\mathrm{t,tw}}} & \frac{Z_{\mathrm{t},2}}{T_{\mathrm{t,tw}}} & \frac{Z_{\mathrm{t},3}}{T_{\mathrm{t,tw}}} & 0\\
0 & 0 & \frac{M_{\mathrm{t},1}}{M_{\mathrm{w,pt}}} & \frac{M_{\mathrm{t},2}}{M_{\mathrm{w,pt}}}
\end{bmatrix};
B_{\mathrm{tower,a}} = \begin{bmatrix}
\frac{X_{\mathrm{t},4}}{T_{\mathrm{t,ta}}} & \frac{X_{\mathrm{t},6}}{T_{\mathrm{t,ta}}} & \frac{X_{\mathrm{t},7}}{T_{\mathrm{t,ta}}} & \frac{X_{\mathrm{t},5}}{T_{\mathrm{t,ta}}} & \frac{X_{\mathrm{t},8}}{T_{\mathrm{t,ta}}}\\
0 & \frac{Y_{\mathrm{t},4}}{T_{\mathrm{t,wa}}} & \frac{Y_{\mathrm{t},5}}{T_{\mathrm{t,wa}}} & \frac{Y_{\mathrm{t},3}}{T_{\mathrm{t,wa}}} & \frac{Y_{\mathrm{t},6}}{T_{\mathrm{t,wa}}}\\
\frac{Z_{\mathrm{t},4}}{T_{\mathrm{t,tw}}} & \frac{Z_{\mathrm{t},6}}{T_{\mathrm{t,tw}}} & \frac{Z_{\mathrm{t},7}}{T_{\mathrm{t,tw}}} & \frac{Z_{\mathrm{t},5}}{T_{\mathrm{t,tw}}} & \frac{Z_{\mathrm{t},8}}{T_{\mathrm{t,tw}}}\\
0 & 0 & 0 & 0 & \frac{M_{\mathrm{t},3}}{M_{\mathrm{w,pt}}}
\end{bmatrix};
$$

$$C_{\text{tower}} = \begin{bmatrix} 1 & 0 & 0 & 0 \\ 0 & 1 & 0 & 0 \\ 0 & 0 & 0 & 0 \\ 0 & 0 & 0 & 1 \\ 0 & 0 & 0 & 0 \end{bmatrix}; D_{\text{tower}} = \begin{bmatrix} 0 & 0 & 0 & 0 & 0 \\ 0 & 0 & 0 & 0 & 0 \\ 0 & 0 & 1 & 0 & 0 \\ 0 & 0 & 0 & 0 & 0 \\ 0 & 0 & 0 & 0 & 1 \end{bmatrix}.$$

2.2.3.2 Model Validation

(1) Experimental conditions

A counterflow wet-cooling tower was used for the model validation. The tower is of 1.5 m in diameter and 2.0 m in height. The total surface area of its fill is identified as 285.4 m^2. The test parameters include the following: ①temperature (±0.1 °C in absolute error) and humidity (±0.8 % in absolute error) of air inlet and outlet of cooling tower; ② cross-sectional velocity of air passing through the tower (±2 % of reading data); ③temperature (±0.1 °Cin absolute error) of water inlet and outlet of cooling tower; and ④ water flow rate (±0.5 % of reading data)

Experiments were made on the transient responses of exit air temperature and humidity of cooling tower and exit water temperature of fill and cooling tower when subjected to different disturbances under various initial conditions as shown in Table 2.10. Then, the experimental data were used for the model validation.

(2) Experimental results

For the experimental case I, the water flow rate had a sudden increase of 1.37 kg/s, while the other inlet variables were kept unchanged. The system matrixes

Table 2.10 Initial conditions for cooling tower model validation

Initial conditions	Cases		
	Case I	Case II	Case III
Inlet air temperature $(t_{a,E})_o$ (°C)	32.4	33.1	34.0
Exit air temperature $(t_{a,L})_o$ (°C)	34.3	34.1	34.8
Inlet air humidity $(W_{a,E})_o$ (g/kg dryair)	18.5	19.4	22.4
Exit air humidity $(W_{a,L})_o$ (g/kg dryair)	20.4	21.4	23.8
Airflow rate $(G_a)_o$ (kg/s)	12.62	12.62	12.62
Inlet water temperature $(t_{w,E})_o$ (°C)	40.8	38.8	38.2
Exit water temperature of fill $(t_{w,L})_o$ (°C)	34.5	33.2	32.7
Water flow rate $(G_w)_o$ (kg/s)	3.31	3.31	3.31
Exit water temperature of tower $(t'_{w,L})_o$ (°C)	34.1	32.8	32.3
Mass of water in the sink of tower M_{sump} (kg)	88.5	88.5	88.5

Perturbation for case 1: G_w increases 1.37 kg/s; perturbation for case II: G_a increases 5.60 kg/s; perturbations for case III are shown in Fig. 2.38

of cooling tower ($A_{\text{tower}}, B_{\text{tower}}$) under the initial conditions of experimental case I for the model calculation are counted as follows:

$$A_{\text{tower}} = \begin{bmatrix} -12.0343 & 0.0251 & 2.4203 & 0 \\ 0.0000 & -9.5964 & 0.0002 & 0.0000 \\ 0.5702 & 0.1313 & -3.1097 & 0.0000 \\ 0.0000 & 0.0000 & 0.0374 & -0.0374 \end{bmatrix};$$

$$B_{\text{tower}} = \begin{bmatrix} 7.1580 & 0.0251 & -0.6777 & 2.4203 & 0.0000 \\ 0.0000 & 9.5959 & -0.0013 & 0.0002 & 0.0000 \\ 0.5702 & 0.1313 & -0.2615 & 1.7810 & 3.6122 \\ 0.0000 & 0.0000 & 0.0000 & 0.0000 & 0.0011 \end{bmatrix}.$$

Figure 2.18 compares experimental dada and model results on the transient responses of exit air and water states under the initial conditions and perturbations of case I. The results manifest that the exit air and water temperature of cooling tower will rise as the water flow rate increases, while the impact of water flow rate on the exit air humidity is very small. The response time of exit water temperature of fill is much shorter than that of exit water temperature of tower (or tower's sink), and this is because the quantity of water in the sink is much larger than that in the fill of tower (as well known, a larger mass results in a larger thermal inertia). For the experimental case I, the average error (AE) of model results on the transient

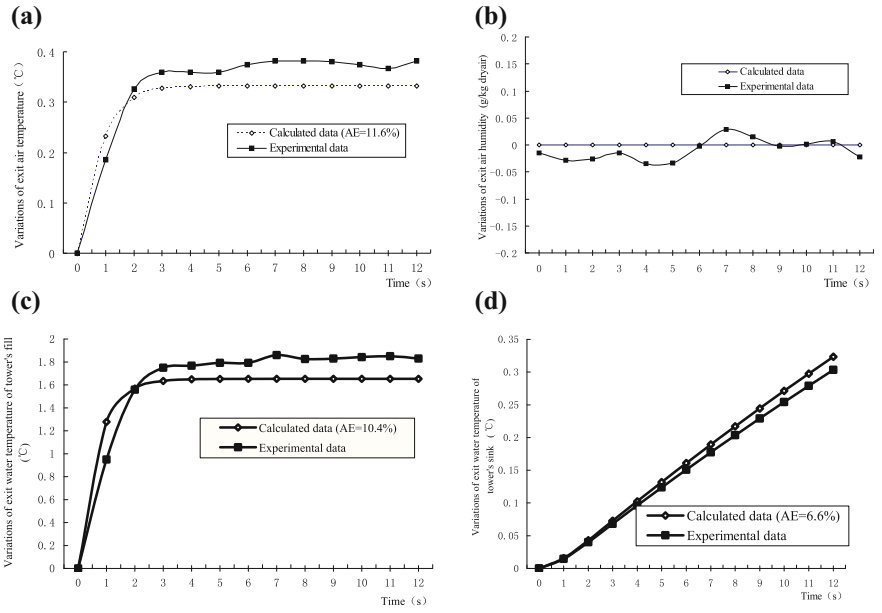

Fig. 2.18 Thermal responses of cooling water tower under the initial conditions and perturbations of case I (calculated results vs. experimental data). **a** Transient response of exit air temperature. **b** Transient response of exit air humidity. **c** Transient response of exit water temperature of tower's fill. **d** Transient response of exit water temperature of tower's sink

response of exit air temperature, exit air humidity, and exit water temperature of fill as well as that of cooling tower's sink is estimated as about 11.6, 10.4, and 6.7 %, respectively.

For the experimental case II, the airflow rate had a sudden increase of 5.60 kg/s while the other inlet variables were kept unchanged. The corresponding system matrixes of cooling tower ($A_{\text{tower}}, B_{\text{tower}}$) under the initial conditions of experimental case II are calculated as follows:

$$A_{\text{tower}} = \begin{bmatrix} -18.0200 & 0.3440 & 8.1797 & 0.0000 \\ 0.0000 & -9.5993 & 0.0023 & 0.0000 \\ 1.9699 & 1.8013 & -5.6933 & 0.0000 \\ 0.0000 & 0.0000 & 0.0374 & -0.0374 \end{bmatrix};$$

$$B_{\text{tower}} = \begin{bmatrix} 1.1722 & 0.3440 & 0.8738 & 8.1797 & 0.0000 \\ 0.0000 & 8.1797 & 0.0013 & 0.0023 & 0.0000 \\ 1.9699 & 1.8013 & -1.4503 & -0.8044 & 30.6488 \\ 0.0000 & 0.0000 & 0.0000 & 0.0000 & 0.0045 \end{bmatrix}.$$

The experimental and simulated results on the variations of response parameters of the cooling tower under the initial conditions and perturbations of case II are shown in Fig. 2.19. As shown in Fig. 2.19, the exit air temperature and the exit

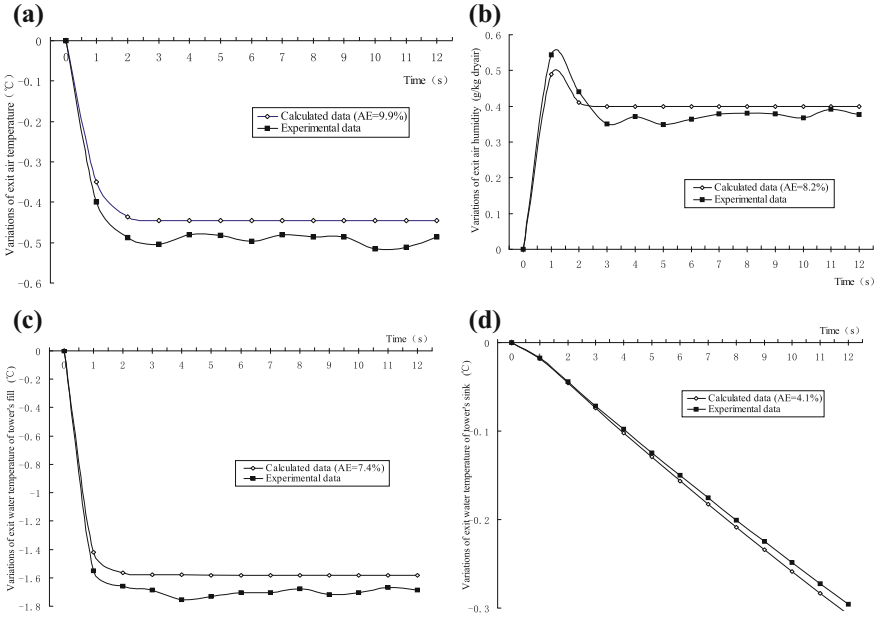

Fig. 2.19 Thermal responses of cooling water tower under the initial conditions and perturbations of case II (calculated results vs. experimental data). **a** Transient response of exit air temperature. **b** Transient response of exit air humidity. **c** Transient response of exit water temperature of tower's fill. **d** Transient response of exit water temperature of tower's sink

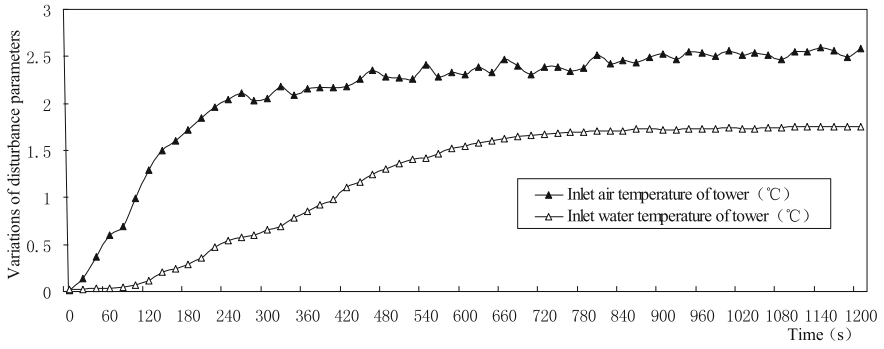

Fig. 2.20 Variations of disturbance parameters for experimental case III

water temperature of the cooling tower's fill and sink tend to decrease as the airflow rate has a step increase, while it is opposite for the exit air humidity. For the experimental case II, the average error (AE) of model results on the transient response of exit air temperature and exit water temperature of fill as well as that of cooling tower's sink is estimated as about 9.9, 8.2, 7.4, and 4.1 %, respectively.

To further validate the cooling tower's model, the perturbation parameters increase gradually under the initial conditions of experimental case III. The variations of the perturbation parameters are shown in Fig. 2.20, and the system matrixes of the cooling tower corresponding to the initial conditions of experimental case III are as follows:

$$A_{\text{tower}} = \begin{bmatrix} -16.4952 & 0.0079 & 4.1736 & 0.0000 \\ 0.0000 & -10.9671 & 0.0001 & 0.0000 \\ 0.6516 & 0.0488 & -7.1269 & 0.0000 \\ 0.0000 & 0.0000 & 0.0299 & -0.0299 \end{bmatrix};$$

$$B_{\text{tower}} = \begin{bmatrix} 9.2031 & 0.0057 & -0.8149 & 2.7824 & 0.0000 \\ 0.0000 & 13.7087 & -0.0015 & 0.0038 & 0.0000 \\ 0.6516 & 0.0300 & -0.2504 & 1,9525 & 1.2299 \\ 0.0000 & 0.0000 & 0.0000 & 0.0000 & 0.0036 \end{bmatrix}.$$

Figure 2.21 compares the simulated results with the experimental data on the transient responses of the concerned parameters under the initial conditions and perturbations of experimental case III. The model results are shown to be of fairly good consistency with the experimental data. The average error (AE) of model results on the transient response of exit air temperature, exit air humidity, and exit water temperature of fill as well as that of cooling tower's sink is about 9.2, 17.2, 10.2, and 11.6 %, respectively.

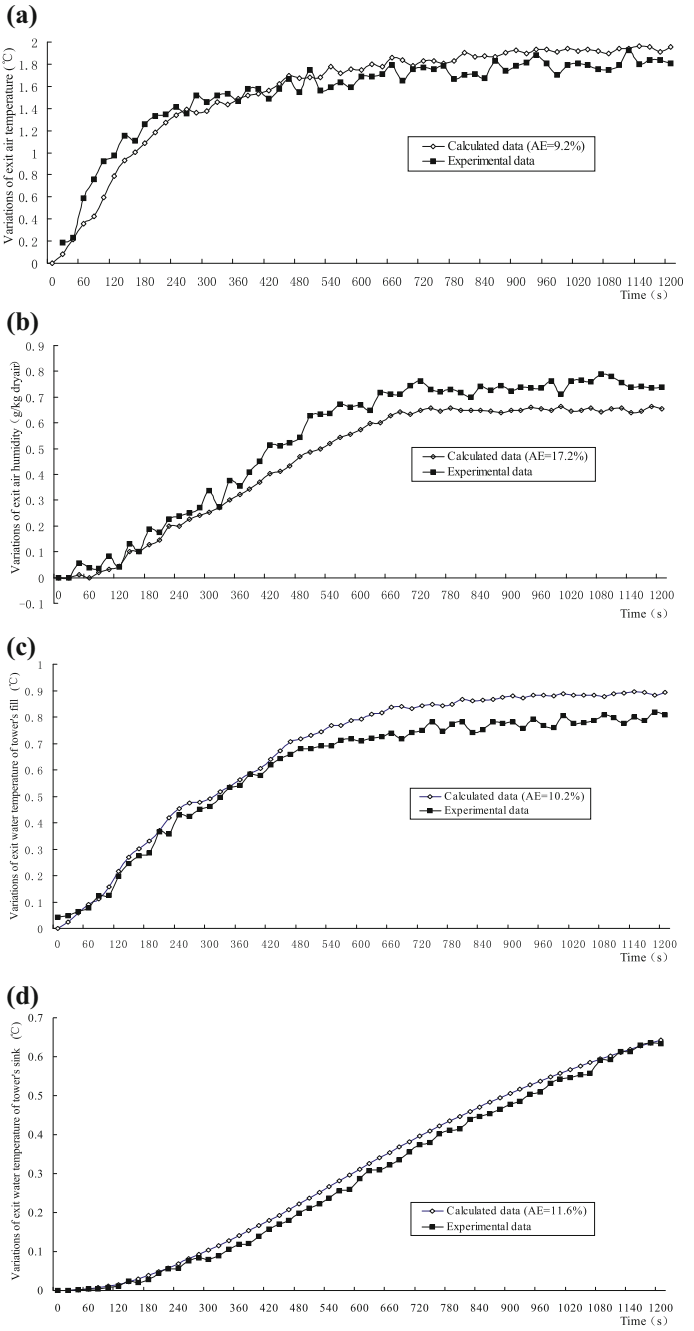

Fig. 2.21 Thermal responses of cooling water tower under the initial conditions and perturbations of case III (calculated results vs. experimental data). **a** Transient response of exit air temperature. **b** Transient response of exit air humidity. **c** Transient response of exit water temperature of tower's fill. **d** Transient response of exit water temperature of tower's sink

2.2.4 Duct (Pipe) and Fan (Pump)

Air and water systems transmit and distribute cooling or heating energy through duct and pipe work systems. They are important components of an air-conditioning system, typically including air ducts, water pipes, fans, and pumps. For central air-conditioning systems, the pipes and ducts are normally long, and the heat loss due to the pipes and ducts cannot be neglected during the thermal simulations of the whole air-conditioning system. Meanwhile, the transmission and distribution components connect the air-conditioning equipments, e.g., water-to-air heat exchanger, chiller, and cooling tower, which have been modeled in the state-space form. For the convenience of system modeling, the transmission and distribution components are required to be modeled in the state-space form.

2.2.4.1 Straight Air Duct Modeling

1) Assumptions and fundamental equations

Figure 2.22 shows the schematic diagram for straight air duct, and the main assumptions for modeling are as follows:

- Moisture air is treated as a mixture of ideal gases;
- Thermophysical parameters of air on the transversal surface of duct adopt lumped ones;
- Air temperature and humidity change linearly from inlet to outlet of the duct;
- External surface of duct's thermal insulation is non-condensing as the cooling air passes through the duct.

According to the first law of energy and mass conservation, the following equations can be obtained for the straight air duct.

(1) *Mass equation for moist air passing through straight air duct*

$$G_{\mathrm{da,L}} = G_{\mathrm{da,E}} = G_{\mathrm{da}} \tag{2.104}$$

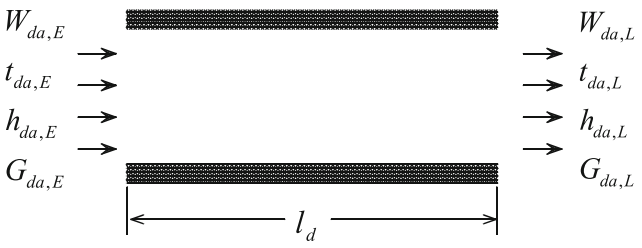

Fig. 2.22 Schematic diagram for straight air duct

(2) *Energy equation for moist air passing through straight air duct*

• In the case of condensation on the interior surface of duct,

$$\frac{1}{2}\rho_{\mathrm{a}}A_{\mathrm{d}}l_{\mathrm{d}}\frac{\mathbf{d}(h_{\mathrm{da,L}}+h_{\mathrm{da,E}})}{\mathbf{d}\tau}=G_{\mathrm{da,E}}(h_{\mathrm{da,E}}-h_{\mathrm{da,L}})+a_{\mathrm{da}}A_{\mathrm{da}}\left(t_{\mathrm{dg}}-\frac{t_{\mathrm{da,E}}+t_{\mathrm{da,L}}}{2}\right)+q_{\mathrm{r}}\lambda_{\mathrm{m}}A_{\mathrm{da}}\left(W_{\mathrm{db}}-\frac{W_{\mathrm{da,E}}+W_{\mathrm{da,L}}}{2}\right) \tag{2.105}$$

• In the case of non-condensation on the interior surface of duct,

$$\frac{1}{2}\rho_{\mathrm{a}}A_{\mathrm{d}}l_{\mathrm{d}}\frac{\mathbf{d}(h_{\mathrm{da,L}}+h_{\mathrm{da,E}})}{\mathbf{d}\tau}=G_{\mathrm{da,E}}(h_{\mathrm{da,E}}-h_{\mathrm{da,L}})+a_{\mathrm{da}}A_{\mathrm{da}}\left(t_{\mathrm{dg}}-\frac{t_{\mathrm{da,E}}+t_{\mathrm{da,L}}}{2}\right) \tag{2.106}$$

(3) *Mass equation for air humidity passing through straight air duct*

• In the case of condensation on the interior surface of duct,

$$\frac{1}{2}\rho_{\mathrm{a}}A_{\mathrm{d}}l_{\mathrm{d}}\frac{\mathbf{d}(W_{\mathrm{da,L}}+W_{\mathrm{da,E}})}{\mathbf{d}\tau}=G_{\mathrm{da,E}}(W_{\mathrm{da,E}}-W_{\mathrm{da,L}})+\lambda_{\mathrm{m}}A_{\mathrm{da}}\left(W_{\mathrm{db}}-\frac{W_{\mathrm{da,E}}+W_{\mathrm{da,L}}}{2}\right) \tag{2.107}$$

• In the case of non-condensation on the interior surface of duct,

$$W_{\mathrm{da,L}}=W_{\mathrm{da,E}} \tag{2.108}$$

(4) *Energy equation for duct wall*

• In the case of condensation on the interior surface of duct,

$$c_{\mathrm{dg}}M_{\mathrm{dg}}\frac{\mathbf{d}t_{\mathrm{dg}}}{\mathbf{d}\tau}=\frac{l_{\mathrm{d}}}{R_{\mathrm{dg}}}(t_{\mathrm{env}}-t_{\mathrm{dg}})+a_{\mathrm{da}}A_{\mathrm{di}}\left(\frac{t_{\mathrm{da,E}}+t_{\mathrm{da,L}}}{2}-t_{\mathrm{dg}}\right)+q_{\mathrm{r}}\lambda_{\mathrm{m}}A_{\mathrm{di}}\left(\frac{W_{\mathrm{da,E}}+W_{\mathrm{da,L}}}{2}-W_{\mathrm{db}}\right) \tag{2.109}$$

• In the case of non-condensation on the interior surface of duct,

$$c_{\mathrm{dg}}M_{\mathrm{dg}}\frac{\mathbf{d}t_{\mathrm{dg}}}{\mathbf{d}\tau}=\frac{l_{\mathrm{d}}}{R_{\mathrm{dg}}}(t_{\mathrm{env}}-t_{\mathrm{dg}})+a_{\mathrm{da}}A_{\mathrm{di}}\left(\frac{t_{\mathrm{da,E}}+t_{\mathrm{da,L}}}{2}-t_{\mathrm{dg}}\right) \tag{2.110}$$

2) State-space representation

As illustrated in previous text, the saturated air humidity (W_{db}) near the wet wall surface of duct in the case of condensation can be approximately expressed by:

$$W_{db} \approx \beta_1 t_{dg} \tag{2.111}$$

where β_1 is a constant coefficient.

Through linearization, Eqs. (2.104) through (2.110) can be converted as follows:

• In the case of condensation on the interior surface of duct,

$$T_{d,ta}\frac{\mathbf{d}\Delta t_{da,L}}{\mathbf{d}\tau} = X_{dwet,1}\Delta t_{da,L} + X_{dwet,2}\Delta W_{da,L} + X_{dwet,3}\Delta t_{dg} + X_{dwet,4}\Delta t_{da,E} + X_{dwet,5}W_{da,E} + X_{dwet,6}\Delta G_{da,E} + \xi_{t,dweta} \tag{2.112}$$

$$T_{d,wa}\frac{\mathbf{d}\Delta W_{da,L}}{\mathbf{d}\tau} = Y_{dwet,1}\Delta W_{da,L} + Y_{dwet,2}\Delta t_{dg} + Y_{dwet,3}\Delta W_{da,E} + Y_{dwet,4}\Delta G_{da,E} + \xi_{w,dweta} \tag{2.113}$$

$$T_{d,dg}\frac{\mathbf{d}\Delta t_{dg}}{\mathbf{d}\tau} = Z_{dwet,1}\Delta t_{da,L} + Z_{dwet,2}\Delta W_{da,L} + Z_{dwet,3}\Delta t_{dg} + Z_{dwet,4}\Delta t_{da,E} + Z_{dwet,5}\Delta W_{da,E} + Z_{dwet,6}\Delta G_{da,E} \tag{2.114}$$

$$\Delta G_{da,L} = \Delta G_{da,E} \tag{2.115}$$

• In the case of non-condensation on the interior surface of duct,

$$T_{d,ta}\frac{\mathbf{d}\Delta t_{da,L}}{\mathbf{d}\tau} = X_{ddry,1}\Delta t_{da,L} + X_{ddry,2}\Delta t_{dg} + X_{ddry,3}\Delta t_{da,E} + X_{ddry,4}\Delta G_{da,E} + \xi_{t,ddrya} \tag{2.116}$$

$$T_{d,dg}\frac{\mathbf{d}\Delta t_{dg}}{\mathbf{d}\tau} = Z_{ddry,1}\Delta t_{da,L} + Z_{ddry,2}\Delta t_{dg} + Z_{ddry,3}\Delta t_{da,E} + Z_{ddry,4}\Delta G_{da,E} \tag{2.117}$$

$$\Delta W_{da,L} = \Delta W_{da,E} \tag{2.118}$$

$$\Delta G_{da,L} = \Delta G_{da,E} \tag{2.119}$$

Coefficients in Eqs. (2.112) through (2.117) are listed in Table 2.11

Equations (2.112) through (2.119) can be expressed by the state-space representation as follows:

$$\dot{x}_{zduct} = A_{zduct} \cdot x_{zduct} + B_{zduct} \cdot u_{zduct} + \xi_{zduct} \tag{2.120}$$

$$y_{zduct} = C_{zduct} \cdot x_{zduct} + D_{zduct} \cdot u_{zduct} \tag{2.121}$$

Table 2.11 Coefficients in Eqs. (2.112) through (2.117)

Equation No.	Coefficient expression
Eq. (2.112)	$T_{\mathrm{d,ta}} = \frac{1}{2}\rho_{\mathrm{a}} c_{\mathrm{a}} A_{\mathrm{d}} l_{\mathrm{d}}$; $X_{\mathrm{dwet},1} = -c_{\mathrm{a}}(G_{\mathrm{da,E}})_{\mathrm{o}} - \frac{A_{\mathrm{da}}}{2}(a_{\mathrm{da}})_{\mathrm{o}}$; $X_{\mathrm{dwet},2} = X_{\mathrm{dwet},5} = -\frac{q_{\mathrm{r}}-\beta_2}{2} A_{\mathrm{da}}(\lambda_{\mathrm{m}})_{\mathrm{o}}$; $X_{\mathrm{dwet},3} = A_{\mathrm{da}}(a_{\mathrm{da}})_{\mathrm{o}} + \beta_1(q_{\mathrm{r}} - \beta_2) A_{\mathrm{da}}(\lambda_{\mathrm{m}})_{\mathrm{o}}$; $X_{\mathrm{dwet},4} = c_{\mathrm{a}}(G_{\mathrm{da,E}})_{\mathrm{o}} - \frac{A_{\mathrm{da}}}{2}(a_{\mathrm{da}})_{\mathrm{o}}$; $X_{\mathrm{dwet},6} = c_{\mathrm{a}}(t_{\mathrm{da,E}} - t_{\mathrm{da,L}})_{\mathrm{o}} + A_{\mathrm{da}}\left[t_{\mathrm{dg}} - \frac{t_{\mathrm{da,E}} + t_{\mathrm{da,L}}}{2}\right]_{\mathrm{o}} \left(\frac{\partial a_{\mathrm{da}}}{\partial G_{\mathrm{da,E}}}\right)_{\mathrm{o}}$ $+ A_{\mathrm{da}}(q_{\mathrm{r}} - \beta_2)\left[\beta_1 t_{\mathrm{dg}} - \frac{W_{\mathrm{da,E}} + W_{\mathrm{da,L}}}{2}\right]_{\mathrm{o}} \left(\frac{\partial \lambda_{\mathrm{m}}}{\partial G_{\mathrm{da,E}}}\right)_{\mathrm{o}}$ $\xi_{\mathrm{t,dweta}} = -T_{\mathrm{d,ta}} \frac{d\Delta t_{\mathrm{da,E}}}{d\tau}$
Eq. (2.113)	$T_{\mathrm{d,wa}} = \frac{1}{2}\rho_{\mathrm{a}} A_{\mathrm{d}} l_{\mathrm{d}}$; $Y_{\mathrm{dwet},1} = -(G_{\mathrm{da,E}})_{\mathrm{o}} - \frac{A_{\mathrm{da}}}{2}(\lambda_{\mathrm{m}})_{\mathrm{o}}$; $Y_{\mathrm{dwet},2} = \beta_1 A_{\mathrm{da}}(\lambda_{\mathrm{m}})_{\mathrm{o}}$; $Y_{\mathrm{dwet},3} = (G_{\mathrm{da,E}})_{\mathrm{o}} - \frac{A_{\mathrm{da}}}{2}(\lambda_{\mathrm{m}})_{\mathrm{o}}$; $Y_{\mathrm{dwet},4} = (W_{\mathrm{da,E}} - W_{\mathrm{da,L}})_{\mathrm{o}}$ $+ A_{\mathrm{da}}\left[\beta_1 t_{\mathrm{dg}} - \frac{W_{\mathrm{da,E}} + W_{\mathrm{da,L}}}{2}\right]_{\mathrm{o}} \left(\frac{\partial \lambda_{\mathrm{m}}}{\partial G_{\mathrm{da,E}}}\right)_{\mathrm{o}}$; $\xi_{\mathrm{w,dweta}} = -T_{\mathrm{d,wa}} \frac{d\Delta W_{\mathrm{da,E}}}{d\tau}$
Eq. (2.114)	$T_{\mathrm{d,dg}} = c_{\mathrm{dg}} M_{\mathrm{dg}}$; $Z_{\mathrm{dwet},1} = Z_{\mathrm{dwet},4} = \frac{A_{\mathrm{da}}}{2}(a_{\mathrm{da}})_{\mathrm{o}}$; $Z_{\mathrm{dwet},2} = Z_{\mathrm{dwet},5} = \frac{A_{\mathrm{da}}}{2} q_{\mathrm{r}}(\lambda_{\mathrm{m}})_{\mathrm{o}}$; $Z_{\mathrm{dwet},3} = -A_{\mathrm{di}}(a_{\mathrm{da}})_{\mathrm{o}} - \frac{l_{\mathrm{d}}}{R_{\mathrm{dg}}} - q_{\mathrm{r}}\beta_1 A_{\mathrm{da}}(\lambda_{\mathrm{m}})_{\mathrm{o}}$; $Z_{\mathrm{dwet},6} = A_{\mathrm{da}} q_{\mathrm{r}}\left[\frac{W_{\mathrm{da,E}} + W_{\mathrm{da,L}}}{2} - \beta_1 t_{\mathrm{dg}}\right]_{\mathrm{o}} \left(\frac{\partial \lambda_{\mathrm{m}}}{\partial G_{\mathrm{da,E}}}\right)_{\mathrm{o}}$ $+ A_{\mathrm{da}}\left[\frac{t_{\mathrm{da,E}} + t_{\mathrm{da,L}}}{2} - t_{\mathrm{dg}}\right]_{\mathrm{o}} \left(\frac{\partial a_{\mathrm{da}}}{\partial G_{\mathrm{da,E}}}\right)_{\mathrm{o}}$
Eq. (2.116)	$T_{\mathrm{d,ta}} = \frac{1}{2}\rho_{\mathrm{a}} c_{\mathrm{a}} A_{\mathrm{d}} l_{\mathrm{d}}$; $X_{\mathrm{ddry},1} = -c_{\mathrm{a}}(G_{\mathrm{da,E}})_{\mathrm{o}} - \frac{A_{\mathrm{da}}}{2}(a_{\mathrm{da}})_{\mathrm{o}}$; $X_{\mathrm{ddry},2} = A_{\mathrm{da}}(a_{\mathrm{da}})_{\mathrm{o}}$; $X_{\mathrm{ddry},3} = c_{\mathrm{a}}(G_{\mathrm{da,E}})_{\mathrm{o}} - \frac{A_{\mathrm{da}}}{2}(a_{\mathrm{da}})_{\mathrm{o}}$; $X_{\mathrm{ddry},4} = c_{\mathrm{a}}(t_{\mathrm{da,E}} - t_{\mathrm{da,L}})_{\mathrm{o}}$ $+ A_{\mathrm{di}}\left[t_{\mathrm{dg}} - \frac{t_{\mathrm{da,E}} + t_{\mathrm{da,L}}}{2}\right]_{\mathrm{o}} \left(\frac{\partial a_{\mathrm{da}}}{\partial G_{\mathrm{da,E}}}\right)_{\mathrm{o}}$; $\xi_{\mathrm{t,ddrya}} = -T_{\mathrm{d,ta}} \frac{d\Delta t_{\mathrm{da,E}}}{d\tau}$
Eq. (2.117)	$T_{\mathrm{d,dg}} = c_{\mathrm{dg}} M_{\mathrm{dg}}$; $Z_{\mathrm{ddry},1} = Z_{\mathrm{ddry},3} = \frac{A_{\mathrm{da}}}{2}(a_{\mathrm{da}})_{\mathrm{o}}$; $Z_{\mathrm{ddry},2} = -A_{\mathrm{da}}(a_{\mathrm{da}})_{\mathrm{o}} - \frac{l_{\mathrm{d}}}{R_{\mathrm{dg}}}$; $X_{\mathrm{tar},1} = c_{\mathrm{a}}(G_{\mathrm{a,i}} - G_{\mathrm{a,leal}})_{\mathrm{o}}$

The standard form of state-space equation corresponding to Eqs. (2.120) and (2.121) is written as follows:

$$\overset{dot}{X}_{\mathrm{zduct}} = A_{\mathrm{zduct}} X_{\mathrm{zduct}} + B_{\mathrm{zduct}} u_{\mathrm{zduct}} \tag{2.122}$$

$$y_{\mathrm{zduct}} = C_{\mathrm{zduct}} X_{\mathrm{zduct}} + D_{\mathrm{zduct}} u_{\mathrm{zduct}} - C_{\mathrm{zduct}} A_{\mathrm{zduct}}^{-1} \xi_{\mathrm{zduct}} \tag{2.123}$$

where $X_{\mathrm{zduct}} = x_{\mathrm{zduct}} + A_{\mathrm{zduct}}^{-1} \xi_{\mathrm{zduct}}$;

For the case of condensation on the interior surface of duct,

$$x_{\text{zduct}} = [\Delta t_{\text{da,L}}, \Delta W_{\text{da,L}}, \Delta t_{\text{dg}}]^T; y_{\text{zduct}} = [\Delta t_{\text{da,L}}, \Delta W_{\text{da,L}}, \Delta G_{\text{da,L}}]^T;$$
$$u_{\text{zduct}} = [\Delta t_{\text{da,E}}, \Delta W_{\text{da,E}}, \Delta G_{\text{da,E}}]^T; \xi_{\text{zduct}} = [\xi_{\text{t,dweta}}, \xi_{\text{w,dweta}}, 0]^T;$$
$$A_{\text{zduct}} = \begin{bmatrix} \frac{X_{\text{dwet,1}}}{T_{\text{d,ta}}} & \frac{X_{\text{dwet,2}}}{T_{\text{d,ta}}} & \frac{X_{\text{dwet,3}}}{T_{\text{d,ta}}} \\ 0 & \frac{Y_{\text{dwet,1}}}{T_{\text{d,wa}}} & \frac{Y_{\text{dwet,2}}}{T_{\text{d,wa}}} \\ \frac{Z_{\text{dwet,1}}}{T_{\text{d,dg}}} & \frac{Z_{\text{dwet,2}}}{T_{\text{d,dg}}} & \frac{Z_{\text{dwet,3}}}{T_{\text{d,dg}}} \end{bmatrix}; B_{\text{zduct}} = \begin{bmatrix} \frac{X_{\text{dwet,4}}}{T_{\text{d,ta}}} & \frac{X_{\text{dwet,5}}}{T_{\text{d,ta}}} & \frac{X_{\text{dwet,6}}}{T_{\text{d,ta}}} \\ 0 & \frac{Y_{\text{dwet,3}}}{T_{\text{d,wa}}} & \frac{Y_{\text{dwet,4}}}{T_{\text{d,wa}}} \\ \frac{Z_{\text{dwet,4}}}{T_{\text{d,dg}}} & \frac{Z_{\text{dwet,5}}}{T_{\text{d,dg}}} & \frac{Z_{\text{dwet,6}}}{T_{\text{d,dg}}} \end{bmatrix};$$
$$C_{\text{zduct}} = \begin{bmatrix} 1 & 0 & 0 \\ 0 & 1 & 0 \\ 0 & 0 & 0 \end{bmatrix}; D_{\text{zduct}} = \begin{bmatrix} 0 & 0 & 0 \\ 0 & 0 & 0 \\ 0 & 0 & 1 \end{bmatrix}.$$

For the case of non-condensation on the interior surface of duct,

$$x_{\text{zduct}} = [\Delta t_{\text{da,L}}, \Delta t_{\text{dg}}]^T; y_{\text{zduct}} = [\Delta t_{\text{da,L}}, \Delta W_{\text{da,L}}, \Delta G_{\text{da,L}}]^T;$$
$$u_{\text{zduct}} = [\Delta t_{\text{da,E}}, \Delta W_{\text{da,E}}, \Delta G_{\text{da,E}}]^T; \xi_{\text{zduct}} = [\xi_{\text{t,ddrya}} 0]^T;$$
$$A_{\text{zduct}} = \begin{bmatrix} \frac{X_{\text{ddry,1}}}{T_{\text{d,ta}}} & \frac{X_{\text{ddry,2}}}{T_{\text{d,ta}}} \\ \frac{Z_{\text{ddry,1}}}{T_{\text{d,dg}}} & \frac{Z_{\text{ddry,2}}}{T_{\text{d,dg}}} \end{bmatrix}; B_{\text{zduct}} = \begin{bmatrix} \frac{X_{\text{ddry,3}}}{T_{\text{d,ta}}} & 0 & \frac{X_{\text{ddry,4}}}{T_{\text{d,ta}}} \\ \frac{Z_{\text{ddry,3}}}{T_{\text{d,dg}}} & 0 & \frac{Z_{\text{ddry,4}}}{T_{\text{d,dg}}} \end{bmatrix}; C_{\text{zduct}} = \begin{bmatrix} 1 & 0 \\ 0 & 0 \\ 0 & 0 \end{bmatrix}; D_{\text{zduct}} = \begin{bmatrix} 0 & 0 & 0 \\ 0 & 1 & 0 \\ 0 & 0 & 1 \end{bmatrix}.$$

3) Model validation

A straight air duct is used to validate the state-space model. The main physical parameters of the duct are shown in Table 2.12. The test parameters include the following: ① inlet and outlet air temperature and humidity (precision: ±0.1 °C in temperature; ±0.8 % in relative humidity); ② duct wall temperature (precision: ±0.2 °C); ③ airflow rate (precision: ±2 % of reading data).

In most cases, water condensation is not allowed in the air duct. So, the experiments were performed under the non-condensation situation. Initial conditions for the model validation are as follows: The inlet and outlet air temperature are 29.3 and 29.5 °C, respectively; the inlet and outlet air humidity are both 20.3 g/(kg dry air); the duct wall temperature is 30.0 °C; the airflow rate is 0.20 kg/s.

Figure 2.24 compares model results with the experimental data on the transient responses of exit air temperature to perturbations as shown in Fig. 2.23. The average error (AE) of straight air duct model in this case is estimated as about 13.8 %.

Table 2.12 Structural parameters of the experimental duct

Length of duct l_{d} (m)	3.25	Width of duct W_{d} (m)	0.87
Height of duct H_{d} (m)	0.25	Specific heat of duct c_{dg} (J/(kg°C))	620
Density of duct material ρ_{d} (kg/m^3)	7800	Thickness of duct wall δ_{d} (m)	0.001

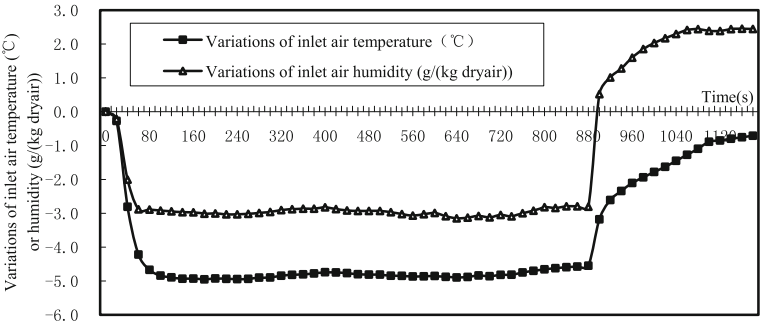

Fig. 2.23 Perturbations of inlet air temperature and humidity (measured data)

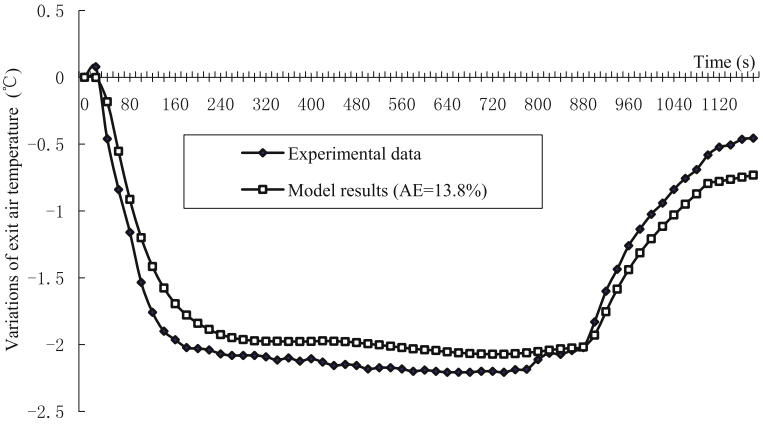

Fig. 2.24 Transient response of exit air temperature to perturbations as shown in Fig. 2.23 (calculated results vs. experimental data)

2.2.4.2 Straight Water Pipe Modeling

1) Fundamental equations

The assumptions for the straight water pipe modeling are basically the same as that for the straight air duct modeling. The schematic diagram for straight water pipe is given in Fig. 2.25, and corresponding equations are obtained as follows:

(1) *Mass equation for water passing through straight water pipe*

$$G_{\mathrm{zpw,L}} = G_{\mathrm{zpw,E}} = G_{\mathrm{zpw}} \tag{2.124}$$

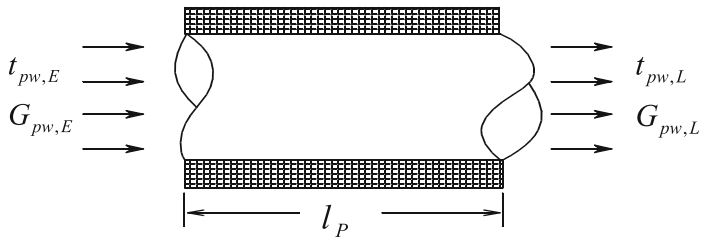

Fig. 2.25 Schematic diagram for straight water pipe

(2) *Energy equation for water passing through straight water pipe*

$$\frac{1}{2}\rho_{\mathrm{w}}c_{\mathrm{w}}A_{\mathrm{p}}l_{\mathrm{p}}\frac{\mathbf{d}(t_{\mathrm{pw,L}}+t_{\mathrm{pw,E}})}{\mathbf{d}\tau}=G_{\mathrm{pw,E}}(t_{\mathrm{pw,E}}-t_{\mathrm{pw,L}})+a_{\mathrm{pw}}A_{\mathrm{pi}}\left(t_{\mathrm{pg}}-\frac{t_{\mathrm{pw,E}}+t_{\mathrm{pw,L}}}{2}\right) \tag{2.125}$$

(3) *Energy equation for pipe wall*

$$c_{\mathrm{pg}}M_{\mathrm{pg}}\frac{\mathbf{d}t_{\mathrm{pg}}}{\mathbf{d}\tau}=\frac{l_{\mathrm{p}}}{R_{\mathrm{pg}}}(t_{\mathrm{env}}-t_{\mathrm{pg}})+a_{\mathrm{pw}}A_{\mathrm{pi}}\left(\frac{t_{\mathrm{pw,E}}+t_{\mathrm{pw,L}}}{2}-t_{\mathrm{pg}}\right) \tag{2.126}$$

2) State-space representation

Through linearization, Eqs. (2.124) through (2.126) can be written as follows:

$$T_{\mathrm{p,tw}}\frac{\mathbf{d}\Delta t_{\mathrm{pw,L}}}{\mathbf{d}\tau}=X_{\mathrm{p,1}}\Delta t_{\mathrm{pw,L}}+X_{\mathrm{p,2}}\Delta t_{\mathrm{pg}}+X_{\mathrm{p,3}}\Delta t_{\mathrm{pw,E}}+X_{\mathrm{p,4}}\Delta G_{\mathrm{pw,E}}+\xi_{\mathrm{tpw,L}} \tag{2.127}$$

$$T_{\mathrm{p,pg}}\frac{\mathbf{d}\Delta t_{\mathrm{pg}}}{\mathbf{d}\tau}=Y_{\mathrm{p,1}}\Delta t_{\mathrm{pw,L}}+Y_{\mathrm{p,2}}\Delta t_{\mathrm{pg}}+Y_{\mathrm{p,3}}\Delta t_{\mathrm{pw,E}}+Y_{\mathrm{p,4}}\Delta G_{\mathrm{pw,E}} \tag{2.128}$$

$$\Delta G_{\mathrm{pw,L}}=\Delta G_{\mathrm{pw,E}} \tag{2.129}$$

Coefficients in Eqs. (2.127) and (2.128) are listed in Table 2.13.

Thus, the state-space model for the straight-through pipe can be expressed by Eqs. (2.130) and (2.131).

$$\dot{X}_{\mathrm{zpipe}}=A_{\mathrm{zpipe}}X_{\mathrm{zpipe}}+B_{\mathrm{zpipe}}u_{\mathrm{zpipe}} \tag{2.130}$$

$$y_{\mathrm{zpipe}}=C_{\mathrm{zpipe}}X_{\mathrm{zpipe}}+D_{\mathrm{zpipe}}u_{\mathrm{zpipe}}-C_{\mathrm{zpipe}}A_{\mathrm{zpipe}}^{-1}\xi_{\mathrm{zpipe}} \tag{2.131}$$

Table 2.13 Coefficients in Eqs. (2.127) and (2.128)

Equation No.	Coefficient expression
Eq. (2.127)	$T_{\mathrm{p,tw}}=\frac{1}{2}\rho_{\mathrm{w}}c_{\mathrm{w}}A_{\mathrm{p}}l_{\mathrm{p}}$; $X_{\mathrm{p},1}=-(G_{\mathrm{pw,E}})_{\mathrm{o}}-\frac{A_{\mathrm{pi}}}{2}(a_{\mathrm{pw}})_{\mathrm{o}}$; $X_{\mathrm{p},2}=A_{\mathrm{pi}}(a_{\mathrm{pw}})_{\mathrm{o}}$; $X_{\mathrm{p},3}=(G_{\mathrm{pw,E}})_{\mathrm{o}}-\frac{A_{\mathrm{pi}}}{2}(a_{\mathrm{pw}})_{\mathrm{o}}$; $X_{\mathrm{p},4}=(t_{\mathrm{pw,E}}-t_{\mathrm{pw,L}})_{\mathrm{o}}+A_{\mathrm{pi}}\left(t_{\mathrm{pg}}-\frac{t_{\mathrm{pw,E}}+t_{\mathrm{pw,L}}}{2}\right)_{\mathrm{o}}\left(\frac{\partial a_{\mathrm{pw}}}{\partial G_{\mathrm{pw,E}}}\right)_{\mathrm{o}}$; $\xi_{\mathrm{tpw,L}}=-T_{\mathrm{p,tw}}\frac{d_{\mathrm{tpw,E}}}{d\tau}$
Eq. (2.128)	$T_{\mathrm{p,pg}}=c_{\mathrm{pg}}M_{\mathrm{pg}}$; $Y_{\mathrm{p},1}=Y_{\mathrm{p},3}=\frac{A_{\mathrm{pi}}}{2}(a_{\mathrm{pw}})_{\mathrm{o}}$; $Y_{\mathrm{p},2}=-A_{\mathrm{pi}}(a_{\mathrm{pw}})_{\mathrm{o}}-\frac{l_{\mathrm{p}}}{R_{\mathrm{pg}}}$; $Y_{\mathrm{p},4}=A_{\mathrm{pi}}\left(\frac{t_{\mathrm{pw,E}}+t_{\mathrm{pw,L}}}{2}-t_{\mathrm{pg}}\right)_{\mathrm{o}}\left(\frac{\partial a_{\mathrm{pw}}}{\partial G_{\mathrm{pw,E}}}\right)_{\mathrm{o}}$

where

$$X_{\mathrm{zpipe}}=x_{\mathrm{zpipe}}+A_{\mathrm{zpipe}}^{-1}\xi_{\mathrm{zpipe}};\ x_{\mathrm{zpipe}}=[\Delta t_{\mathrm{pw,L}},\Delta t_{\mathrm{pg}}]^T;$$

$$y_{\mathrm{zpipe}}=[\Delta t_{\mathrm{pw,L}},\Delta G_{\mathrm{pw,L}}]^T;\ u_{\mathrm{zpipe}}=[\Delta t_{\mathrm{pw,E}},\Delta G_{\mathrm{pw,E}}]^T;\ \xi_{\mathrm{zpipe}}=[\xi_{\mathrm{tpw,L}},0]^T;$$

$$A_{\mathrm{zpipe}}=\begin{bmatrix}\frac{X_{\mathrm{p},1}}{T_{\mathrm{p,tw}}} & \frac{X_{\mathrm{p},2}}{T_{\mathrm{p,tw}}}\\ \frac{Y_{\mathrm{p},1}}{T_{\mathrm{p,pg}}} & \frac{Y_{\mathrm{p},2}}{T_{\mathrm{p,pg}}}\end{bmatrix};\ B_{\mathrm{zpipe}}=\begin{bmatrix}\frac{X_{\mathrm{p},3}}{T_{\mathrm{p,tw}}} & \frac{X_{\mathrm{p},4}}{T_{\mathrm{p,tw}}}\\ \frac{Y_{\mathrm{p},3}}{T_{\mathrm{p,pg}}} & \frac{Y_{\mathrm{p},4}}{T_{\mathrm{p,pg}}}\end{bmatrix};\ C_{\mathrm{zpipe}}=\begin{bmatrix}1 & 0\\ 0 & 0\end{bmatrix};\ D_{\mathrm{zpipe}}=\begin{bmatrix}0 & 0\\ 0 & 1\end{bmatrix}.$$

3) Model validation

A straight water pipe is used for the model validation. The key physical information on the experimental water pipe is given in Table 2.14.

The test parameters include the following: ① inlet and outlet water temperature (precision: ±0.2 °C in temperature); ② pipe wall temperature (precision: ±0.2 °C); and ③ water flow rate (precision: 0.2 level). Initial conditions for model validation are as follows: the inlet and outlet water temperature are 26.2 and 27.4 °C, respectively; the pipe wall temperature is 29.4 °C; and the water flow rate is 0.205 kg/s.

Figure 2.27 shows the experimental data and model results on the transient response of exit water temperature to the perturbations of inlet water temperature as shown in Fig. 2.26. The average error (AE) of model results compared with the experimental data is estimated as 7.4 % in this case.

Table 2.14 Key physical information on the experimental water pipe

Length of water pipe l_{p} (m)	7.0	Inner diameter of water pipe D_{p} (m)	0.02
Specific heat of water pipe c_{pg} (J/(kg °C))	1569	Density of pipe material ρ_{pg} (kg/m^3)	1083
Thickness of water pipe δ_{p} (m)	0.005		

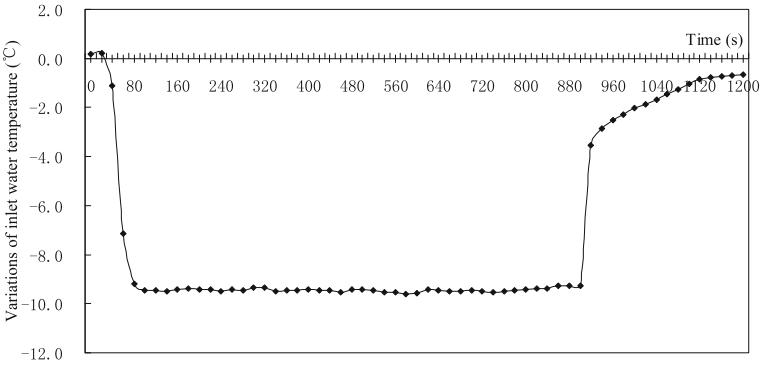

Fig. 2.26 Perturbations of inlet water temperature (measured data)

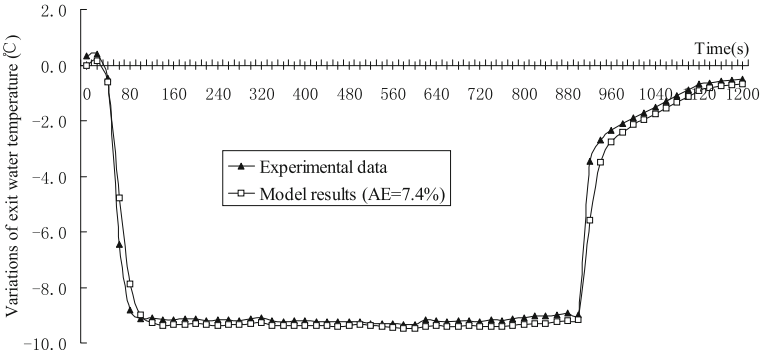

Fig. 2.27 Transient response of exit water temperature to perturbations as shown in Fig. 2.26 (calculated results vs. experimental data)

2.2.4.3 Three-Way Duct/Pipe Modeling

Three-way ducts or pipes are important links in the air duct or water pipe system in an air-conditioning system. Normally, the three-way duct or pipe has two types: One is confluent flow and the other is split flow (see Figs. 2.28 and 2.29). Since it takes very short time for fluid passing through the three-way duct or pipe, thermal loss of fluid caused by the three-way duct or pipe can be neglected.

(1) Three-way air duct

For the confluent flow, the following equations come into existence:

$$G_{\mathrm{da3,L}} = G_{\mathrm{da1,E}} + G_{\mathrm{da2,E}} \tag{2.132}$$

$$G_{\mathrm{da3,L}} W_{\mathrm{da3,L}} = G_{\mathrm{da1,E}} W_{\mathrm{da1,E}} + G_{\mathrm{da2,E}} W_{\mathrm{da2,E}} \tag{2.133}$$

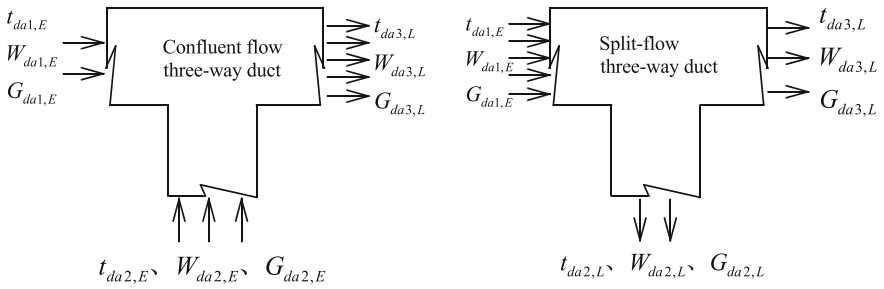

Fig. 2.28 Schematic diagram for three-way air duct

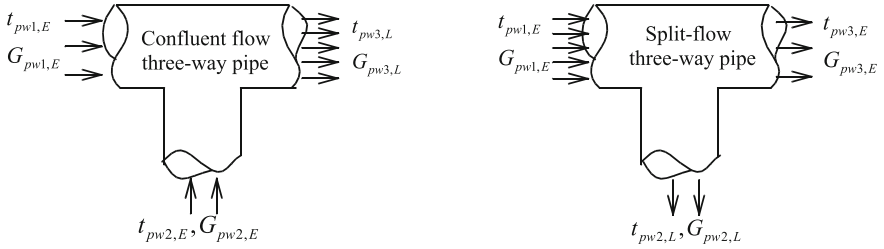

Fig. 2.29 Schematic diagram for three-way water pipe

$$G_{\mathrm{da3,L}} t_{\mathrm{da3,L}} = G_{\mathrm{da1,E}} t_{\mathrm{da1,E}} + G_{\mathrm{da2,E}} t_{\mathrm{da2,E}} \tag{2.134}$$

For the split flow, we have the following equations:

$$t_{\mathrm{da2,L}} = t_{\mathrm{da1,E}} \tag{2.135}$$

$$W_{\mathrm{da2,L}} = W_{\mathrm{da1,E}} \tag{2.136}$$

$$G_{\mathrm{da2,L}} = \kappa_{\mathrm{a}} G_{\mathrm{da1,E}} \tag{2.137}$$

$$t_{\mathrm{da3,L}} = t_{\mathrm{da1,E}} \tag{2.138}$$

$$W_{\mathrm{da3,L}} = W_{\mathrm{da1,E}} \tag{2.139}$$

$$G_{\mathrm{da3,L}} = (1 - \kappa_{\mathrm{a}}) G_{\mathrm{da1,E}} \tag{2.140}$$

Then, the dynamic relationships between the inlet variables and the outlet ones of the three-way air duct can be expressed by Eq. (2.141).

$$y_{\mathrm{sduct}} = D_{\mathrm{sduct}} \cdot u_{\mathrm{sduct}} \tag{2.141}$$

where for the confluent flow,

$$y_{\text{sduct}} = \left[\Delta t_{\text{da3,L}}, \Delta W_{\text{da3,L}}, \Delta G_{\text{da3,L}}\right]^T; u_{\text{sduct}} = \left[u_{\text{sduct,1}}, u_{\text{sduct,2}}\right]^T;$$
$$u_{\text{sduct,1}} = \left[\Delta t_{\text{da1,E}}, \Delta W_{\text{da1,E}}, \Delta G_{\text{da1,E}}\right]^T; u_{\text{sduct,2}} = \left[\Delta t_{\text{da2,E}}, \Delta W_{\text{da2,E}}, \Delta G_{\text{da2,E}}\right]^T;$$
$$D_{\text{sduct}} = \left[D_{\text{da1,E}}, D_{\text{da2,E}}\right];$$

$$D_{\text{da1,E}} = \begin{bmatrix} \frac{(G_{\text{da1,E}})_{\text{o}}}{(G_{\text{da3,L}})_{\text{o}}} & 0 & \frac{[(t_{\text{da1,E}})_{\text{o}} - (t_{\text{da3,L}})_{\text{o}}]}{(G_{\text{da3,L}})_{\text{o}}} \\ 0 & \frac{(G_{\text{da1,E}})_{\text{o}}}{(G_{\text{da3,L}})_{\text{o}}} & \frac{[(W_{\text{da1,E}})_{\text{o}} - (W_{\text{da3,L}})_{\text{o}}]}{(G_{\text{da3,L}})_{\text{o}}} \\ 0 & 0 & 1 \end{bmatrix};$$

$$D_{\text{da2,E}} = \begin{bmatrix} \frac{(G_{\text{da2,E}})_{\text{o}}}{(G_{\text{da3,L}})_{\text{o}}} & 0 & \frac{[(t_{\text{da2,E}})_{\text{o}} - (t_{\text{da3,L}})_{\text{o}}]}{(G_{\text{da3,L}})_{\text{o}}} \\ 0 & \frac{(G_{\text{da2,E}})_{\text{o}}}{(G_{\text{da3,L}})_{\text{o}}} & \frac{[(W_{\text{da2,E}})_{\text{o}} - (W_{\text{da3,L}})_{\text{o}}]}{(G_{\text{da3,L}})_{\text{o}}} \\ 0 & 0 & 1 \end{bmatrix};$$

and for the split flow,

$$y_{\text{sduct}} = \left[y_{\text{sduct,2}}, y_{\text{sduct,3}}\right]^T; u_{\text{sduct}} = \left[\Delta t_{\text{da1,E}}, \Delta W_{\text{da1,E}}, \Delta G_{\text{da1,E}}\right]^T;$$
$$y_{\text{sduct,2}} = \left[\Delta t_{\text{da2,L}}, \Delta W_{\text{da2,L}}, \Delta G_{\text{da2,L}}\right]^T; y_{\text{sduct,3}} = \left[\Delta t_{\text{da3,L}}, \Delta W_{\text{da3,L}}, \Delta G_{\text{da3,L}}\right]^T;$$
$$D_{\text{sduct}} = \begin{bmatrix} D_{\text{fda12,E}} \\ D_{\text{fda13,E}} \end{bmatrix}; D_{\text{fda12,E}} = \begin{bmatrix} 1 & 0 & 0 \\ 0 & 1 & 0 \\ 0 & 0 & \kappa_{\text{a}} \end{bmatrix}; D_{\text{fda13,E}} = \begin{bmatrix} 1 & 0 & 0 \\ 0 & 1 & 0 \\ 0 & 0 & 1 - \kappa_{\text{a}} \end{bmatrix}.$$

(2) Three-way water pipe

For the confluent flow, the following equations can be obtained:

$$G_{\text{pw3,L}} = G_{\text{pw1,E}} + G_{\text{pw2,E}} \tag{2.142}$$

$$G_{\text{pw3,L}} t_{\text{pw3,L}} = G_{\text{pw1,E}} t_{\text{pw1,E}} + G_{\text{pw2,E}} t_{\text{pw2,E}} \tag{2.143}$$

For the split flow, we have the following equations:

$$t_{\text{pw2,L}} = t_{\text{pw1,E}} \tag{2.144}$$

$$G_{\text{pw2,L}} = \kappa_{\text{w}} G_{\text{pw1,E}} \tag{2.145}$$

$$t_{\text{pw3,L}} = t_{\text{pw1,E}} \tag{2.146}$$

$$G_{\text{pw3,L}} = (1 - \kappa_{\text{w}}) G_{\text{pw1,E}} \tag{2.147}$$

Likewise, the dynamic relationships between the inlet variables and the outlet ones of the three-way air duct can be expressed by:

$$y_{\text{spipe}} = D_{\text{spipe}} \cdot u_{\text{spipe}} \tag{2.148}$$

where

for the confluent flow,

$$y_{\text{spipe}} = \left[\Delta t_{\text{pw3,L}}, \Delta G_{\text{pw3,L}}\right]^T; u_{\text{spipe}} = \left[\Delta t_{\text{pw1,E}}, \Delta G_{\text{pw1,E}}, \Delta t_{\text{pw2,E}}, \Delta G_{\text{pw2,E}}\right]^T;$$
$$D_{\text{spipe}} = \begin{bmatrix} \frac{(G_{\text{pw1,E}})_{\text{o}}}{(G_{\text{pw3,L}})_{\text{o}}} & \frac{[(t_{\text{pw1,E}})_{\text{o}} - (t_{\text{pw3,L}})_{\text{o}}]}{(G_{\text{pw3,L}})_{\text{o}}} & \frac{(G_{\text{pw2,E}})_{\text{o}}}{(G_{\text{pw3,L}})_{\text{o}}} & \frac{[(t_{\text{pw2,E}})_{\text{o}} - (t_{\text{pw3,L}})_{\text{o}}]}{(G_{\text{pw3,L}})_{\text{o}}} \\ 0 & 1 & 0 & 1 \end{bmatrix};$$

and for the split flow,

$$y_{\text{spipe}} = \left[\Delta t_{\text{pw2,L}}, \Delta G_{\text{pw2,L}}, \Delta t_{\text{pw3,L}}, \Delta G_{\text{pw3,L}}\right]^T; u_{\text{sduct}} = \left[\Delta t_{\text{pw1,E}}, \Delta G_{\text{pw1,E}}\right]^T;$$
$$D_{\text{spipe}} = \begin{bmatrix} 1 & 0 \\ 0 & \kappa_{\text{w}} \\ 1 & 0 \\ 0 & 1-\kappa_{\text{w}} \end{bmatrix}.$$

2.2.4.4 Fan and Pump

Fan and pump are key power equipments for fluid transportation in an air-conditioning system. They are also the main control objects in a variable air volume (VAV) or variable water volume (VWV) air-conditioning system. The fan or pump is normally driven by an alternating current motor, as shown in Fig. 2.30.

Assuming that input electric voltage of motor be U_{m}, and electric resistance and inductance and rotary inertia of motor be R_{a}, L_{a} and J_{m}, respectively, we have the following equations [16]:

(1) *Angular speed equation*

$$\frac{\mathbf{d}\theta_{\text{m}}}{\mathbf{d}\tau} = \omega_{\text{m}} \tag{2.149}$$

where θ_{m} is angular displacement, rad; ω_{m} is angular velocity, rad/s.

(2) *Voltage equation*

$$L_{\text{a}}\frac{\mathbf{d}i_{\text{a}}}{\mathbf{d}\tau} = -R_{\text{a}}i_{\text{a}} - K_{\text{v}}\omega_{\text{m}} + U_{\text{m}} \tag{2.150}$$

where i_{a} is electric current, A; K_{v} is coefficient of counterpotential, V s/rad;

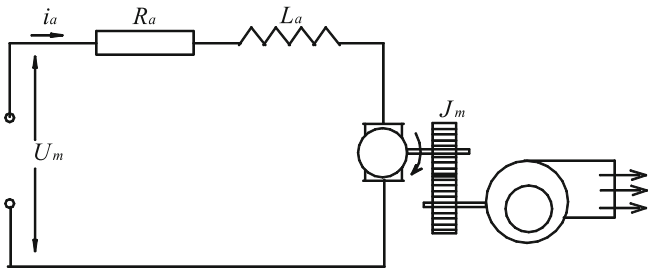

Fig. 2.30 Schematic diagram for fan/pump's motor

(3) *Moment equation*

$$J_{\mathrm{m}}\frac{\mathbf{d}\omega_{\mathrm{m}}}{\mathbf{d}\tau}=K_{\mathrm{m}}i_{\mathrm{a}}-B_{\mathrm{m}}\omega_{\mathrm{m}}-F_{\mathrm{l}} \tag{2.151}$$

where J_{m} is rotary inertia of motor, kg m^2; K_{m} is coefficient of torsion torque, N m rad/A; B_{m} is equivalent friction coefficient, kg m^2/s^2; and F_{l} is load of motor, kg m^2 rad/s^2.

The load of motor, F_{l}, is the function dependent on the outlet pressure of fan or pump ($P_{\mathrm{f/p}}$) and fluid flow rate ($G_{\mathrm{f/p}}$) as follows:

$$F_{\mathrm{l}}\omega_{\mathrm{m}}\eta_{\mathrm{f/p}}=\frac{G_{\mathrm{f/p}}P_{\mathrm{f/p}}}{\rho_{\mathrm{a/w}}} \tag{2.152}$$

$$G_{\mathrm{f/p}}=\chi_{\mathrm{f/p,G}}\chi_{\mathrm{n}}\rho_{\mathrm{a/w}}d_{\mathrm{f/p}}^2b_{\mathrm{f/p}}n_{\mathrm{m}} \tag{2.153}$$

$$P_{\mathrm{f/p}}=\chi_{\mathrm{f/p,P}}\chi_{\mathrm{n}}^2\rho_{\mathrm{a/w}}d_{\mathrm{f/p}}^2n_{\mathrm{m}}^2 \tag{2.154}$$

Thus, Eq. (2.151) can be written as follows:

$$J_{\mathrm{m}}\frac{\mathbf{d}\omega_{\mathrm{m}}}{\mathbf{d}\tau}=K_{\mathrm{m}}i_{\mathrm{a}}-B_{\mathrm{m}}\omega_{\mathrm{m}}-\frac{\varepsilon_{\mathrm{G}}\varepsilon_{\mathrm{P}}\omega_{\mathrm{m}}^2}{(2\pi)^3\eta_{\mathrm{f/p}}} \tag{2.155}$$

where $\varepsilon_{\mathrm{G}}=\chi_{\mathrm{f/p,G}}\chi_{\mathrm{n}}\rho_{\mathrm{a/w}}d_{\mathrm{f/p}}^2b_{\mathrm{f/p}}$, $\varepsilon_{\mathrm{P}}=\chi_{\mathrm{f/p,P}}\chi_{\mathrm{n}}^2\rho_{\mathrm{a/w}}d_{\mathrm{f/p}}^2$, $\omega_{\mathrm{m}}=2\pi n_{\mathrm{m}}$

(4) *Power equation*

$$N_{\mathrm{m}}=\alpha_{\mathrm{m}}U_{\mathrm{m}}i_{\mathrm{a}} \tag{2.156}$$

where N_{m} is power of motor, W; $\alpha_{\mathrm{m}}=\sqrt{3}\phi_{\mathrm{m}}$, φ_{m} is power factor.

Through linearization, Eqs. (2.149), (2.150), (2.151), (2.153), and (2.156) can be changed into incremental form as follows:

$$\frac{\mathbf{d}\Delta\theta_{\mathrm{m}}}{\mathbf{d}\tau}=\Delta\omega_{\mathrm{m}} \tag{2.157}$$

$$L_{\mathrm{a}}\frac{\mathbf{d}\Delta i_{\mathrm{a}}}{\mathbf{d}\tau}=-R_{\mathrm{a}}\Delta i_{\mathrm{a}}-K_{\mathrm{v}}\Delta\omega_{\mathrm{m}}+\Delta U_{\mathrm{m}} \tag{2.158}$$

$$J_{\mathrm{m}}\frac{\mathbf{d}\Delta\omega_{\mathrm{m}}}{\mathbf{d}\tau}=K_{\mathrm{m}}\Delta i_{\mathrm{a}}-\left[B_{\mathrm{m}}+\frac{2\varepsilon_{\mathrm{G}}\varepsilon_{\mathrm{P}}\omega_{\mathrm{m}}}{(2\pi)^3\eta_{\mathrm{f/p}}}\right]_{\mathrm{o}}\Delta\omega_{\mathrm{m}} \tag{2.159}$$

$$\Delta G_{\mathrm{f/p}}=\frac{(\varepsilon_{\mathrm{G}})_{\mathrm{o}}}{2\pi}\Delta\omega_{\mathrm{m}} \tag{2.160}$$

$$\Delta N_{\mathrm{m}}=\alpha_{\mathrm{m}}(U_{\mathrm{m}})_{\mathrm{o}}\Delta i_{\mathrm{a}}+\alpha_{\mathrm{m}}(i_{\mathrm{a}})_{\mathrm{o}}\Delta U_{\mathrm{m}} \tag{2.161}$$

Assume that the inlet air conditions of fan equal to the outlet ones, i.e.,

$$\Delta t_{\mathrm{fan,L}}=\Delta t_{\mathrm{fan,E}} \tag{2.162}$$

$$\Delta W_{\mathrm{fan,L}}=\Delta W_{\mathrm{fan,E}} \tag{2.163}$$

$$\Delta G_{\mathrm{fan,L}}=\Delta G_{\mathrm{fan,E}}=\Delta G_{\mathrm{f/p}}=\frac{(\varepsilon_{\mathrm{G}})_{\mathrm{o}}}{2\pi}\Delta\omega_{\mathrm{m}} \tag{2.164}$$

Choosing $\Delta\theta_{\mathrm{m}},\Delta\omega_{\mathrm{m}}$ and Δi_{a} as state-space variables, $\Delta t_{\mathrm{fan,E}},\Delta W_{\mathrm{fan,E}},\Delta G_{\mathrm{fan,E}}$ and ΔU_{m} as input ones, and $\Delta t_{\mathrm{fan,L}},\Delta W_{\mathrm{fan,L}},\Delta G_{\mathrm{fan,L}}$ and ΔN_{m} as output ones, the state-space model for fan is expressed by Eqs. (2.165) and (2.166)

$$\dot{x}_{\mathrm{fan}}=A_{\mathrm{fan}}\cdot x_{\mathrm{fan}}+B_{\mathrm{fan}}\cdot u_{\mathrm{fan}} \tag{2.165}$$

$$y_{\mathrm{fan}}=C_{\mathrm{fan}}\cdot x_{\mathrm{fan}}+D_{\mathrm{fan}}\cdot u_{\mathrm{fan}} \tag{2.166}$$

where

$$x_{\mathrm{fan}}=[\Delta\theta_{\mathrm{m}},\Delta i_{\mathrm{a}},\Delta\omega_{\mathrm{m}}]^T;\ y_{\mathrm{fan}}=[\Delta t_{\mathrm{fan,L}},\Delta W_{\mathrm{fan,L}},\Delta G_{\mathrm{fan,L}},\Delta N]^T;$$

$$u_{\mathrm{fan}}=[\Delta t_{\mathrm{fan,E}},\Delta W_{\mathrm{fan,E}},\Delta G_{\mathrm{fan,E}},\Delta U_{\mathrm{m}}]^T;$$

$$A_{\mathrm{fan}}=\begin{bmatrix}0 & 0 & 1\\ 0 & -\frac{R_{\mathrm{a}}}{L_{\mathrm{a}}} & -\frac{K_{\mathrm{v}}}{L_{\mathrm{a}}}\\ 0 & \frac{K_{\mathrm{m}}}{J_{\mathrm{m}}} & -\left(\frac{B_{\mathrm{m}}}{J_{\mathrm{m}}}+\frac{2\varepsilon_{\mathrm{G}}\varepsilon_{\mathrm{P}}\omega_{\mathrm{m}}}{(2\pi)^3J_{\mathrm{m}}\eta_{\mathrm{f/p}}}\right)_{\mathrm{o}}\end{bmatrix};$$

$$B_{\mathrm{fan}}=[B_{\mathrm{fan,a}},B_{\mathrm{fan,U}}];\ C_{\mathrm{fan}}=\begin{bmatrix}C_{\mathrm{fan,a}}\\ C_{\mathrm{fan,U}}\end{bmatrix};\ D_{\mathrm{fan}}=\begin{bmatrix}D_{\mathrm{fan,a}}\\ D_{\mathrm{fan,U}}\end{bmatrix};$$

$$B_{\text{fan,a}} = \begin{bmatrix} 0 & 0 & 0 \\ 0 & 0 & 0 \\ 0 & 0 & 0 \end{bmatrix}; B_{\text{fan,U}} = \begin{bmatrix} 0 \\ 1/L_{\text{a}} \\ 0 \end{bmatrix}; C_{\text{fan,a}} = \begin{bmatrix} 0 & 0 & 0 \\ 0 & 0 & 0 \\ 0 & 0 & (\varepsilon_{\text{G}})_{\text{o}}/2\pi \end{bmatrix};$$

$$C_{\text{fan,U}} = [0 \quad a_{\text{m}}(U_{\text{m}})_{\text{o}} \quad 0]; D_{\text{fan,a}} = \begin{bmatrix} 1 & 0 & 0 & 0 \\ 0 & 1 & 0 & 0 \\ 0 & 0 & 0 & 0 \end{bmatrix}; D_{\text{fan,U}} = [0 \quad 0 \quad 0 \quad a_{\text{m}}(i_{\text{a}})_{\text{o}}].$$

Likewise, the state-space model for pump is written as follows:

$$\dot{x}_{\text{pump}} = A_{\text{pump}} \cdot x_{\text{pump}} + B_{\text{pump}} \cdot u_{\text{pump}} \tag{2.167}$$

$$y_{\text{pump}} = C_{\text{pump}} \cdot x_{\text{pump}} + D_{\text{pump}} \cdot u_{\text{pump}} \tag{2.168}$$

where

$$x_{\text{pump}} = [\Delta\theta_{\text{m}}, \Delta i_{\text{a}}, \Delta\omega_{\text{m}}]^T; y_{\text{pump}} = [\Delta t_{\text{pump,L}}, \Delta G_{\text{pump,L}}, \Delta N]^T;$$

$$u_{\text{pump}} = [\Delta t_{\text{pump,E}}, \Delta G_{\text{pump,E}}, \Delta U_{\text{m}}]^T;$$

$$A_{\text{pump}} = \begin{bmatrix} 0 & 0 & 1 \\ 0 & -\frac{R_{\text{a}}}{L_{\text{a}}} & -\frac{K_{\text{v}}}{L_{\text{a}}} \\ 0 & \frac{K_{\text{m}}}{J_{\text{m}}} & -\left(\frac{B_{\text{m}}}{J_{\text{m}}} + \frac{2\varepsilon_{\text{G}}\varepsilon_{\text{P}}\omega_{\text{m}}}{(2\pi)^3 J_{\text{m}}\eta_{\text{f/p}}}\right)_{\text{o}} \end{bmatrix};$$

$$B_{\text{pump}} = [B_{\text{pump,w}}, B_{\text{pump,U}}]; C_{\text{pump}} = \begin{bmatrix} C_{\text{pump,w}} \\ C_{\text{pump,U}} \end{bmatrix}; D_{\text{pump}} = \begin{bmatrix} D_{\text{pump,w}} \\ D_{\text{pump,U}} \end{bmatrix};$$

$$B_{\text{pump,w}} = \begin{bmatrix} 0 & 0 \\ 0 & 0 \\ 0 & 0 \end{bmatrix}; B_{\text{pump,U}} = \begin{bmatrix} 0 \\ 1/L_{\text{a}} \\ 0 \end{bmatrix}; C_{\text{pump,w}} = \begin{bmatrix} 0 & 0 & 0 \\ 0 & 0 & (\varepsilon_{\text{G}})_{\text{o}}/2\pi \end{bmatrix};$$

$$C_{\text{pump,U}} = [0 \quad a_{\text{m}}(U_{\text{m}})_{\text{o}} \quad 0]; D_{\text{pump,w}} = \begin{bmatrix} 1 & 0 & 0 \\ 0 & 0 & 0 \end{bmatrix}; D_{\text{pump,U}} = [0 \quad 0 \quad a_{\text{m}}(i_{\text{a}})_{\text{o}}].$$

2.2.5 Air-Conditioned Room Modeling

Although air-conditioned room itself is not part of an air-conditioning system, its model is indispensable for the simulation or analysis of the air-conditioning system because the ultimate objective of an air-conditioning system is to keep an anticipated thermal environment indoors. In this section, a state-space model for air-conditioned room is established. The room model can be used to analyze thermal response characteristics of air in a room.

2.2.5.1 Model Development [17]

1) Assumptions

The following assumptions are made for the room model development:

① Room is separated into three typical zones, i.e., the air-supply, the work, and the air-return zone, as shown in Fig. 2.31. Each air zone is fully mixed and is described by one state.
② The surface temperature of each inner and external wall is all described with a lumped value. The heat transfer from the external walls only affects the air in the work zone, and there is no heat and mass transfer between the air-supply and the air-return zones.
③ In the air-supply zone, light bulbs are the only heat sources defined by a constant surface temperature during the transient response simulation. No moisture sources exist in the air-supply zone.
④ In the work zone, the heat sources are mainly electrical appliances and people indoors, and the moisture sources are evaporative water from the skin and from the respiration of human indoors. The surface temperature of all the heat sources is assumed to be constant during the dynamic response simulation.
⑤ There are no heat and moisture sources in the air-return zone.
⑥ The radiant heat transfer between walls and objects in the room is negligible. The convective heat transfer coefficients between the walls or the heat sources and the adjacent air are considered to be constant during the dynamic response simulation.

2) Basic equations

Based on the above assumptions, the following equations for each indoor air zone can be obtained according to the principle of energy and mass conservation.

(1) *For the air-supply zone*

$$\rho_{\mathrm{a}} V_{\mathrm{a,s}} \frac{\mathbf{d}h_{\mathrm{a,s}}}{\mathbf{d}\tau} = G_{\mathrm{a}}(h_{\mathrm{a,i}} - h_{\mathrm{a,s}}) + \Delta Q_{\mathrm{a,s}} \tag{2.169}$$

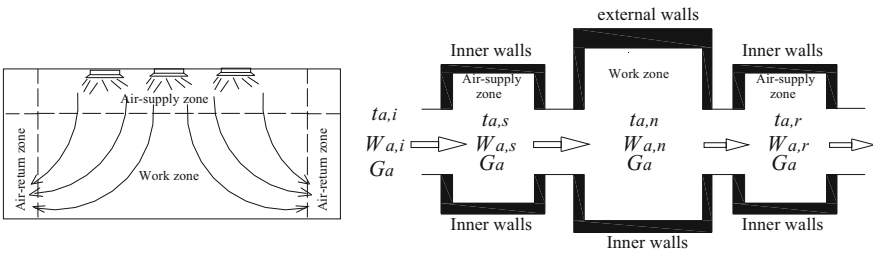

Fig. 2.31 Schematic diagram for air-conditioned room

$$\rho_{\mathrm{a}} V_{\mathrm{a,s}} \frac{\mathbf{d}W_{\mathrm{a,s}}}{\mathbf{d}\tau} = G_{\mathrm{a}}(W_{\mathrm{a,i}} - W_{\mathrm{a,s}}) \tag{2.170}$$

$$c_{\mathrm{riw,s}} \rho_{\mathrm{riw}} V_{\mathrm{riw,s}} \frac{\mathbf{d}t_{\mathrm{riw,s}}}{\mathbf{d}\tau} = a_{\mathrm{riw,s}} A_{\mathrm{riw,s}} (t_{\mathrm{a,s}} - t_{\mathrm{riw,s}}) \tag{2.171}$$

(2) *For the work zone*

$$\rho_{\mathrm{a}} V_{\mathrm{a,n}} \frac{\mathbf{d}h_{\mathrm{a,n}}}{\mathbf{d}\tau} = G_{\mathrm{a}}(h_{\mathrm{a,s}} - h_{\mathrm{a,n}}) + \Delta Q_{\mathrm{a,n}} \tag{2.172}$$

$$\rho_{\mathrm{a}} V_{\mathrm{a,n}} \frac{\mathbf{d}W_{\mathrm{a,n}}}{\mathbf{d}\tau} = G_{\mathrm{a}}(W_{\mathrm{a,s}} - W_{\mathrm{a,n}}) + \Delta M_{\mathrm{Wa,n}} \tag{2.173}$$

$$c_{\mathrm{riw,n}} \rho_{\mathrm{riw}} V_{\mathrm{riw,n}} \frac{\mathbf{d}t_{\mathrm{riw,n}}}{\mathbf{d}\tau} = a_{\mathrm{riw,n}} A_{\mathrm{riw,n}} (t_{\mathrm{a,n}} - t_{\mathrm{riw,n}}) \tag{2.174}$$

$$c_{\mathrm{rew,n}} \rho_{\mathrm{rew}} V_{\mathrm{rew,n}} \frac{\mathbf{d}t_{\mathrm{rew,n}}}{\mathbf{d}\tau} = a_{\mathrm{rew,n}} A_{\mathrm{rew,n}} (t_{\mathrm{a,n}} - t_{\mathrm{rew,n}}) + \frac{\lambda_{\mathrm{rew}} A_{\mathrm{rew,n}}}{\delta_{\mathrm{rew}}} (t_{\mathrm{rew,o}} - t_{\mathrm{rew,n}}) \tag{2.175}$$

(3) *For the air-return zone*

$$\rho_{\mathrm{a}} V_{\mathrm{a,r}} \frac{\mathbf{d}h_{\mathrm{a,r}}}{\mathbf{d}\tau} = G_{\mathrm{a}}(h_{\mathrm{a,n}} - h_{\mathrm{a,r}}) + \Delta Q_{\mathrm{a,r}} \tag{2.176}$$

$$\rho_{\mathrm{a}} V_{\mathrm{a,r}} \frac{\mathbf{d}W_{\mathrm{a,r}}}{\mathbf{d}\tau} = G_{\mathrm{a}}(W_{\mathrm{a,n}} - W_{\mathrm{a,r}}) \tag{2.177}$$

$$c_{\mathrm{riw,r}} \rho_{\mathrm{riw}} V_{\mathrm{riw,r}} \frac{\mathbf{d}t_{\mathrm{riw,r}}}{\mathbf{d}\tau} = a_{\mathrm{riw,r}} A_{\mathrm{riw,r}} (t_{\mathrm{a,r}} - t_{\mathrm{riw,r}}) \tag{2.178}$$

3) Key parameters

The enthalpy of air in different zones can be calculated by Eq. (2.179).

$$h_{\mathrm{a}} = c_{\mathrm{a}} t_{\mathrm{a}} + \beta_2 W_{\mathrm{a}} \tag{2.179}$$

where β_2 equals to 2.5×10^6.

Energy gain rate of the air in the air-supply zone, $\Delta Q_{\mathrm{a,s}}$, consists of the following three parts: (1) heat gain rate from the internal walls, $\Delta Q_{\mathrm{a,s,1}}$; (2) heat gain rate from the adjacent air zone (the work zone), $\Delta Q_{\mathrm{a,s,2}}$; and (3) heat gain rate from the indoor heat sources, $\Delta Q_{\mathrm{a,s,3}}$.

$$\Delta Q_{\mathrm{a,s,1}} = a_{\mathrm{riw,s}} A_{\mathrm{riw,s}} (t_{\mathrm{riw,s}} - t_{\mathrm{a,s}}) \tag{2.180}$$

$$\Delta Q_{\mathrm{a,s,2}} = a_{\mathrm{as-an}} A_{\mathrm{as-an}} (t_{\mathrm{a,n}} - t_{\mathrm{a,s}}) \tag{2.181}$$

$$\Delta Q_{\mathrm{a,s,3}} = a_{\mathrm{rq,s}} A_{\mathrm{rq,s}} (t_{\mathrm{rq,s}} - t_{\mathrm{a,s}}) \tag{2.182}$$

Energy gain rate of the air in the work zone, $\Delta Q_{\mathrm{a,n}}$, consists of the following four parts: ① heat gain rate from the internal and external walls, $\Delta Q_{\mathrm{a,n,1}}$; ② heat gain rate from the adjacent air zones, $\Delta Q_{\mathrm{a,n,2}}$; ③heat gain rate from the indoor heat sources, $\Delta Q_{\mathrm{a,n,3}}$; and ④ heat gain rate due to the exhaled air from the occupants, $\Delta Q_{\mathrm{a,n,4}}$.

$$\Delta Q_{\mathrm{a,n,1}} = a_{\mathrm{riw,n}} A_{\mathrm{riw,n}} (t_{\mathrm{riw,n}} - t_{\mathrm{a,n}}) + a_{\mathrm{rew,n}} A_{\mathrm{rew,n}} (t_{\mathrm{rew,n}} - t_{\mathrm{a,n}}) \tag{2.183}$$

$$\Delta Q_{\mathrm{a,n,2}} = a_{\mathrm{as-an}} A_{\mathrm{as-an}} (t_{\mathrm{a,s}} - t_{\mathrm{a,n}}) + a_{\mathrm{an-ar}} A_{\mathrm{an-ar}} (t_{\mathrm{a,r}} - t_{\mathrm{a,n}}) \tag{2.184}$$

$$\Delta Q_{\mathrm{a,n,3}} = \sum_{i=1}^{k} \left[a_{\mathrm{rq,n}} A_{\mathrm{rq,n}}^{(i)} \left(t_{\mathrm{rq,n}}^{(i)} - t_{\mathrm{a,n}} \right) \right] \tag{2.185}$$

$$\Delta Q_{\mathrm{a,n,4}} = G_{\mathrm{res}} (h_{\mathrm{exhale}} - h_{\mathrm{a,n}}) \tag{2.186}$$

In the work zone, there are different kinds of indoor heat sources with different surface temperatures. The superscript 'i' in Eq. (2.185) stands for the ith indoor heat source. The enthalpy of the exhaled air, h_{exhale}, is related to the temperature (t_{exhale}) and humidity ratio (W_{exhale}) of the exhaled air. For typical indoor environments ($t_{\mathrm{a,n}} = 25\,^{\circ}\mathrm{C}$), the exhaled temperature and humidity ratio are given in terms of ambient conditions [8]:

$$t_{\mathrm{exhale}} = 32.6 + 0.066 t_{\mathrm{a,n}} \tag{2.187}$$

$$W_{\mathrm{exhale}} = 0.02933 + 0.2 W_{\mathrm{a,n}} \tag{2.188}$$

Please note that the unit of $W_{\mathrm{a,n}}$ in Eq. (2.188) is kg/(kg dry air). The pulmonary ventilation rate, G_{res}, is primarily a function of metabolic rate as follows [8]:

$$G_{\mathrm{res}} = C_{\mathrm{res}} E_{\mathrm{body}} A_{\mathrm{rq,n}}^{(1)} \tag{2.189}$$

where C_{res} is a proportionality constant (1.43×10^{-6}kg/J); E_{body} is metabolic rate, W/m$_2$; and $A_{\mathrm{rq,n}}^{(1)}$ is body surface area of occupant indoors (m^2), which is calculated by Eq. (2.190) [8].

$$A_{\mathrm{rq,n}}^{(1)} = 0.202 M_{\mathrm{body}}^{0.425} H_{\mathrm{body}}^{0.725} \tag{2.190}$$

where M_{body} and H_{body} are the weight and the height of the occupant.

Moisture gain rate of the air in the work zone, $\Delta M_{\mathrm{Wa,n}}$, is calculated by:

$$\Delta M_{\mathrm{Wa,n}} = G_{\mathrm{res}}(W_{\mathrm{exhale}} - W_{\mathrm{a,n}}) = C_{\mathrm{res}} E_{\mathrm{body}} A_{\mathrm{rq,n}}^{(1)}(0.02933 - 0.8W_{\mathrm{a,n}}) \quad (2.191)$$

Energy gain rate of the air in the air-return zone, $\Delta Q_{\mathrm{a,r}}$, consists of two parts: (1) heat gain rate from the internal walls, $\Delta Q_{\mathrm{a,r,1}}$; and (2) heat gain rate from the adjacent air zone (the work zone), $\Delta Q_{\mathrm{a,r,2}}$.

$$\Delta Q_{\mathrm{a,r,1}} = a_{\mathrm{riw,r}} A_{\mathrm{riw,r}}(t_{\mathrm{riw,r}} - t_{\mathrm{a,r}}) \quad (2.192)$$

$$\Delta Q_{\mathrm{a,r,2}} = a_{\mathrm{an-ar}} A_{\mathrm{an-ar}}(t_{\mathrm{a,n}} - t_{\mathrm{a,r}}) \quad (2.193)$$

The external surface temperature of external walls, $t_{\mathrm{rew,o}}$, is affected by the ambient air temperature and solar radiation intensity on the walls, which can be calculated by:

$$t_{\mathrm{rew,o}} = t_{\mathrm{a,out}} + \alpha_{\rho,rew} I_{\mathrm{sol}} / a_{\mathrm{rew,o}} \quad (2.194)$$

The division of the room air volume into air zones ($V_{\mathrm{a,s}}, V_{\mathrm{a,n}}, V_{\mathrm{a,r}}$) can be determined based on the airflow pattern and the steady-state temperature field calculated with the CFD method [18, 19]. Meanwhile, the actual situations should be fully considered in the division of the indoor air zones. Normally, the work zone is less than 2.0 m in height.

The other critical parameters of the zonal model include the heat transfer coefficients between the air and the internal surface of the room walls ($a_{\mathrm{riw,s}}$, $a_{\mathrm{riw,n}}$, $a_{\mathrm{riw,r}}$),the indoor heat sources ($a_{\mathrm{rq,s}}$, $a_{\mathrm{rq,n}}$), and the heat transfer coefficients between two adjacent air zones ($a_{\mathrm{an-ar}}$ and $a_{\mathrm{as-an}}$). Basically, these heat transfer coefficients are originally obtained from the relevant literature [20, 21] and need to be adjusted according to the comparisons of the calculated results and the experimental data.

4) State-space representation

Through linearization, Eqs. (2.169)–(2.178) can be written as follows:

$$T_{\mathrm{tas}} \frac{\mathbf{d}\Delta t_{\mathrm{a,s}}}{\mathbf{d}\tau} = X_{\mathrm{tas,1}}\Delta t_{\mathrm{a,s}} + X_{\mathrm{tas,2}}\Delta t_{\mathrm{a,i}} + X_{\mathrm{tas,3}}\Delta t_{\mathrm{riw,s}} + X_{\mathrm{tas,4}}\Delta t_{\mathrm{a,n}} + X_{\mathrm{tas,5}}\Delta G_{\mathrm{a,i}} \quad (2.195)$$

$$T_{\mathrm{was}} \frac{\mathbf{d}\Delta W_{\mathrm{a,s}}}{\mathbf{d}\tau} = X_{\mathrm{was,1}}\Delta W_{\mathrm{a,s}} + X_{\mathrm{was,2}}\Delta W_{\mathrm{a,i}} + X_{\mathrm{was,3}}\Delta G_{\mathrm{a,i}} \quad (2.196)$$

$$T_{triws} \frac{\mathbf{d}\Delta t_{\mathrm{riw,s}}}{\mathbf{d}\tau} = X_{triws,1}\Delta t_{\mathrm{a,s}} + X_{triws,2}\Delta t_{\mathrm{riw,s}} \quad (2.197)$$

$$T_{\text{tan}}\frac{\mathbf{d}\Delta t_{\text{a,n}}}{\mathbf{d}\tau}=X_{\text{tan},1}\Delta t_{\text{a,s}}+X_{\text{tan},2}\Delta t_{\text{a,n}}+X_{\text{tan},3}\Delta t_{\text{riw,n}}+X_{\text{tan},4}\Delta t_{\text{rew,n}}+X_{\text{tan},5}\Delta t_{\text{a,r}}+X_{\text{tan},6}\Delta G_{\text{a,i}}+\sum_{i=1}^{k}\left[X_{\text{tan},7}^{(i)}\Delta A_{\text{rq,n}}^{(i)}\right] \tag{2.198}$$

$$T_{\text{wan}}\frac{\mathbf{d}\Delta W_{\text{a,n}}}{\mathbf{d}\tau}=X_{\text{wan},1}\Delta W_{\text{a,s}}+X_{\text{wan},2}\Delta W_{\text{a,n}}+X_{\text{wan},3}\Delta G_{\text{a,i}}+X_{\text{wan},4}\Delta A_{\text{rq,n}}^{(1)} \tag{2.199}$$

$$T_{\text{triwn}}\frac{\mathbf{d}\Delta t_{\text{riw,n}}}{\mathbf{d}\tau}=X_{\text{triwn},1}\Delta t_{\text{a,n}}+X_{\text{triwn},2}\Delta t_{\text{riw,n}} \tag{2.200}$$

$$T_{\text{trewn}}\frac{\mathbf{d}\Delta t_{\text{rew,n}}}{\mathbf{d}\tau}=X_{\text{trewn},1}\Delta t_{\text{a,n}}+X_{\text{trewn},2}\Delta t_{\text{rew,n}}+X_{\text{trewn},3}\Delta t_{\text{a,out}}+X_{\text{trewn},4}\Delta I_{\text{sol}} \tag{2.201}$$

$$T_{\text{tar}}\frac{\mathbf{d}\Delta t_{\text{a,r}}}{\mathbf{d}\tau}=X_{\text{tar},1}\Delta t_{\text{a,n}}+X_{\text{tar},2}\Delta t_{\text{a,r}}+X_{\text{tar},3}\Delta t_{\text{riw,r}}+X_{\text{tar},4}\Delta G_{\text{a,i}} \tag{2.202}$$

$$T_{\text{war}}\frac{\mathbf{d}\Delta W_{\text{a,r}}}{\mathbf{d}\tau}=X_{\text{war},1}\Delta W_{\text{a,n}}+X_{\text{war},2}\Delta W_{\text{a,r}}+X_{\text{war},3}\Delta G_{\text{a,i}} \tag{2.203}$$

$$T_{\text{triwr}}\frac{\mathbf{d}\Delta t_{\text{riw,r}}}{\mathbf{d}\tau}=X_{\text{triwr},1}\Delta t_{\text{a,r}}+X_{\text{triwr},2}\Delta t_{\text{riw,r}} \tag{2.204}$$

The coefficients in Eqs. (2.195)–(2.204) are listed in Table 2.15.
Thus, the state-space model for air-conditioned room can be written as follows:

$$\dot{x}_{\text{room}}=A_{\text{room}}\cdot x_{\text{room}}+B_{\text{room}}\cdot u_{\text{room}} \tag{2.205}$$

$$y_{\text{room}}=C_{\text{room}}x_{\text{room}} \tag{2.206}$$

where

$$x_{room}=[\Delta t_{a,s}\ \ \Delta W_{a,s}\ \ \Delta t_{riw,s}\ \ \Delta t_{a,n}\ \ \Delta W_{a,n}\ \ \Delta t_{riw,n}\ \ \Delta t_{rew,n}\ \ \Delta t_{a,r}\ \ \Delta W_{a,r}\ \ \Delta t_{riw,r}]^T;$$
$$y_{room}=[\Delta t_{a,s}、\ \Delta W_{a,s}、\ \Delta t_{a,n}、\ \Delta W_{a,n}、\ \Delta t_{a,r}、\ \Delta W_{a,r}]^T;$$
$$u_{room}=[\Delta t_{a,i}\ \ \Delta W_{a,i}\ \ \Delta G_{a,i}\ \ \Delta A^{(1)}{}_{rq,n}\ \ \Delta A^{(2)}{}_{rq,n}\ \ \Delta A^{(i)}{}_{rq,n}\ \ \Delta t_{a,out}\ \ \Delta I_{\text{sol}}]^T;$$

$$A_{room}=\begin{bmatrix}
X_{tas,1}/T_{tas} & 0 & X_{tas,3}/T_{tas} & X_{tas,4}/T_{tas} & 0 & 0 & 0 & 0 & 0 & 0\\
0 & X_{was,1}/T_{was} & 0 & 0 & 0 & 0 & 0 & 0 & 0 & 0\\
X_{triws,1}/T_{triws} & 0 & X_{triws,2}/T_{triws} & 0 & 0 & 0 & 0 & 0 & 0 & 0\\
X_{tan,1}/T_{tan} & 0 & 0 & X_{tan,2}/T_{tan} & 0 & X_{tan,3}/T_{tan} & X_{tan,4}/T_{tan} & X_{tan,5}/T_{tan} & 0 & 0\\
0 & X_{wan,1}/T_{wan} & 0 & 0 & X_{wan,2}/T_{wan} & 0 & 0 & 0 & 0 & 0\\
0 & 0 & 0 & X_{triwn,1}/T_{triwn} & 0 & X_{triwn,2}/T_{triwn} & 0 & 0 & 0 & 0\\
0 & 0 & 0 & X_{trewn,1}/T_{trewn} & 0 & 0 & X_{trewn,2}/T_{trewn} & 0 & 0 & 0\\
0 & 0 & 0 & X_{tar,1}/T_{tar} & 0 & 0 & 0 & X_{tar,2}/T_{tar} & 0 & X_{tar,3}/T_{tar}\\
0 & 0 & 0 & 0 & X_{war,1}/T_{war} & 0 & 0 & 0 & X_{war,2}/T_{war} & 0\\
0 & 0 & 0 & 0 & 0 & 0 & 0 & X_{triwr,1}/T_{triwr} & 0 & X_{triwr,2}/T_{triwr}
\end{bmatrix}$$

Table 2.15 Coefficients in Eqs. (2.195) through (2.204)

Equation No.	Coefficient expression
Eq. (2.195)	$T_{\text{tas}} = c_{\text{a}}\rho_{\text{a}}V_{\text{a,s}}$; $X_{\text{tas},1} = -(c_{\text{a}}G_{\text{a}} + a_{\text{riw,s}}A_{\text{riw,s}} + a_{\text{as-an}}A_{\text{as-an}} + a_{\text{rq,s}}A_{\text{rq,s}})_{\text{o}}$; $X_{\text{tas},2} = c_{\text{a}}(G_{\text{a}})_{\text{o}}$; $X_{\text{tas},3} = a_{\text{riw,s}}A_{\text{riw,s}}$; $X_{\text{tas},4} = a_{\text{as-an}}A_{\text{as-an}}$; $X_{\text{tas},5} = c_{\text{a}}(t_{\text{a,i}} - t_{\text{a,s}})_{\text{o}}$
Eq. (2.196)	$T_{\text{was}} = \rho_{\text{a}}V_{\text{a,s}}$; $X_{\text{was},1} = -(G_{\text{a}})_{\text{o}}$; $X_{\text{was},2} = (G_{\text{a}})_{\text{o}}$; $X_{\text{was},3} = (W_{\text{a,i}} - W_{\text{a,s}})_{\text{o}}$
Eq. (2.197)	$T_{triws} = c_{\text{riw,s}}\rho_{\text{riw}}V_{\text{riw,s}}$; $X_{\text{triws},1} = a_{\text{riw,s}}A_{\text{riw,s}}$; $X_{\text{triws},2} = -a_{\text{riw,s}}A_{\text{riw,s}}$
Eq. (2.198)	$T_{\text{tan}} = c_{\text{a}}\rho_{\text{a}}V_{\text{a,n}}$; $X_{\text{tan},1} = c_{\text{a}}(G_{\text{a}})_{\text{o}} + a_{\text{as-an}}A_{\text{as-an}}$; $X_{\text{tan},2} = -\left[\begin{array}{l} c_{\text{a}}(G_{\text{a}})_{\text{o}} + 0.934c_{\text{a}}C_{\text{res}}E_{\text{body}}A^{(1)}_{\text{rq,n}} + a_{\text{riw,n}}A_{\text{riw,n}} \\ \quad + a_{\text{rew,n}}A_{\text{rew,n}} + a_{\text{as-an}}A_{\text{as-an}} + a_{\text{an-ar}}A_{\text{an-ar}} + \sum_{i=1}^{k}\left[a_{\text{rq,n}}(A^{(i)}_{\text{rq,n}})_{\text{o}}\right] \end{array}\right]$; $X_{\text{tan},3} = a_{\text{riw,n}}A_{\text{riw,n}}$; $X_{\text{tan},4} = a_{\text{rew,n}}A_{\text{rew,n}}$; $X_{\text{tan},5} = a_{\text{an-ar}}A_{\text{an-ar}}$; $X_{\text{tan},6} = c_{\text{a}}(t_{\text{a,s}} - t_{\text{a,n}})_{\text{o}}$; $X^{(i)}_{\text{tan},7} = a_{\text{rq,n}}\left[t^{(i)}_{\text{rq,n}} - t_{\text{a,n}}\right]_{\text{o}}$
Eq. (2.199)	$T_{\text{wan}} = \rho_{\text{a}}V_{\text{a,n}}$; $X_{\text{wan},1} = (G_{\text{a}})_{\text{o}}$; $X_{\text{wan},2} = \left[-0.8C_{\text{res}}E_{\text{body}}A^{(1)}_{\text{rq,n}} - G_{\text{a}}\right]_{\text{o}}$; $X_{\text{wan},3} = (W_{\text{a,s}} - W_{\text{a,n}})_{\text{o}}$; $X_{\text{wan},4} = C_{\text{res}}E_{\text{body}}(0.02933 - 0.8W_{\text{a,n}})_{\text{o}}$
Eq. (2.200)	$T_{\text{triwn}} = c_{\text{riw,n}}\rho_{\text{riw}}V_{\text{riw,n}}$; $X_{\text{triwn},1} = a_{\text{riw,n}}A_{\text{riw,n}}$; $X_{\text{triwn},2} = -a_{\text{riw,n}}A_{\text{riw,n}}$
Eq. (2.201)	$T_{\text{trewn}} = c_{\text{rew,n}}\rho_{\text{rew}}V_{\text{rew,n}}$; $X_{\text{trewn},1} = a_{\text{rew,n}}A_{\text{rew,n}}$; $X_{\text{trewn},2} = -a_{\text{rew,n}}A_{\text{rew,n}} - \lambda_{\text{rew}}A_{\text{rew,n}}/\delta_{\text{rew}}$; $X_{\text{trewn},3} = \lambda_{\text{rew}}A_{\text{rew,n}}/\delta_{\text{rew}}$; $X_{\text{trewn},4} = \alpha_{\rho,rew}\lambda_{\text{rew}}A_{\text{rew,n}}/(a_{\text{rew,o}}\delta_{\text{rew}})$
Eq. (2.202)	$T_{\text{tar}} = c_{\text{a}}\rho_{\text{a}}V_{\text{a,r}}$; $X_{\text{tar},1} = c_{\text{a}}(G_{\text{a}})_{\text{o}} + a_{\text{an-ar}}A_{\text{an-ar}}$; $X_{\text{tar},2} = -[a_{\text{riw,r}}A_{\text{riw,r}} + c_{\text{a}}(G_{\text{a}})_{\text{o}} + a_{\text{an-ar}}A_{\text{an-ar}}]$; $X_{\text{tar},3} = a_{\text{riw,r}}A_{\text{riw,r}}$; $X_{\text{tar},4} = c_{\text{a}}(t_{\text{a,n}} - t_{\text{a,r}})_{\text{o}}$
Eq. (2.203)	$T_{\text{war}} = \rho_{\text{a}}V_{\text{a,r}}$; $X_{\text{tar},1} = c_{\text{a}}(G_{\text{a}})_{\text{o}} + a_{\text{an-ar}}A_{\text{an-ar}}$; $X_{\text{war},1} = (G_{\text{a}})_{\text{o}}$; $X_{\text{war},2} = -(G_{\text{a}})_{\text{o}}$; $X_{\text{war},3} = (W_{\text{a,n}} - W_{\text{a,r}})_{\text{o}}$
Eq. (2.204)	$T_{\text{triwr}} = c_{\text{riw,r}}\rho_{\text{riw}}V_{\text{riw,r}}$; $X_{\text{triwr},1} = a_{\text{riw,r}}A_{\text{riw,r}}$; $X_{\text{triwr},2} = -a_{\text{riw,r}}A_{\text{riw,r}}$

$$B_{room} = \begin{bmatrix} X_{tas,2}/T_{tas} & 0 & X_{tas,5}/T_{tas} & 0 & 0 & 0 & 0 & 0 & 0 \\ 0 & X_{was,2}/T_{was} & X_{was,3}/T_{was} & 0 & 0 & 0 & 0 & 0 & 0 \\ 0 & 0 & 0 & 0 & 0 & 0 & 0 & 0 & 0 \\ 0 & 0 & X_{\text{tan},6}/T_{\text{tan}} & X^{(1)}{}_{\text{tan},7}/T_{\text{tan}} & X^{(2)}{}_{\text{tan},7}/T_{\text{tan}} & \cdots & X^{(i)}{}_{\text{tan},7}/T_{\text{tan}} & 0 & 0 \\ 0 & 0 & X_{\text{wan},3}/T_{\text{wan}} & X_{\text{wan},4}/T_{\text{wan}} & 0 & 0 & 0 & 0 & 0 \\ 0 & 0 & 0 & 0 & 0 & 0 & 0 & 0 & 0 \\ 0 & 0 & 0 & 0 & 0 & 0 & 0 & X_{trewn,3}/T_{trewn} & X_{trewn,4}/T_{trewn} \\ 0 & 0 & X_{tar,4}/T_{tar} & 0 & 0 & 0 & 0 & 0 & 0 \\ 0 & 0 & X_{war,3}/T_{war} & 0 & 0 & 0 & 0 & 0 & 0 \\ 0 & 0 & 0 & 0 & 0 & 0 & 0 & 0 & 0 \end{bmatrix}$$

$$C_{room} = \begin{bmatrix} 1 & 0 & 0 & 0 & 0 & 0 & 0 & 0 & 0 & 0 \\ 0 & 1 & 0 & 0 & 0 & 0 & 0 & 0 & 0 & 0 \\ 0 & 0 & 0 & 1 & 0 & 0 & 0 & 0 & 0 & 0 \\ 0 & 0 & 0 & 0 & 1 & 0 & 0 & 0 & 0 & 0 \\ 0 & 0 & 0 & 0 & 0 & 0 & 0 & 1 & 0 & 0 \\ 0 & 0 & 0 & 0 & 0 & 0 & 0 & 0 & 1 & 0 \end{bmatrix}$$

The matrix A_{room} in the state-space model contains different heat transfer coefficients which are affected by airflow rate and turbulence.

2.2.5.2 Model Validation

(1) Experimental system and conditions

To validate the room model, experiments have been conducted in a full-size air-conditioned room. The internal walls of the room are mainly made from bricks and limestone with a thickness of 16.8 cm. The air-handling system consists of a water-to-air surface heat exchanger, a ventilator, and air-supply/return ducts. Two air-supply diffusers are located in the upper space of the room for a favorable air distribution in the room. The supply air temperature can be controlled through adjusting supply water temperature of the heat exchanger.

The state-space model is validated experimentally mainly in terms of transient responses of air temperature in different zones and that of air humidity in the return air zone to perturbations of supply air temperature and humidity. According to the airflow patterns obtained by the standard $k-\varepsilon$ CFD model, the size of the air-supply, the work, and the air-return zone is identified as $348 \times 270 \times 70$, $348 \times 270 \times 180$ cm, and $80 \times 270 \times 180$ cm (length × width × height),

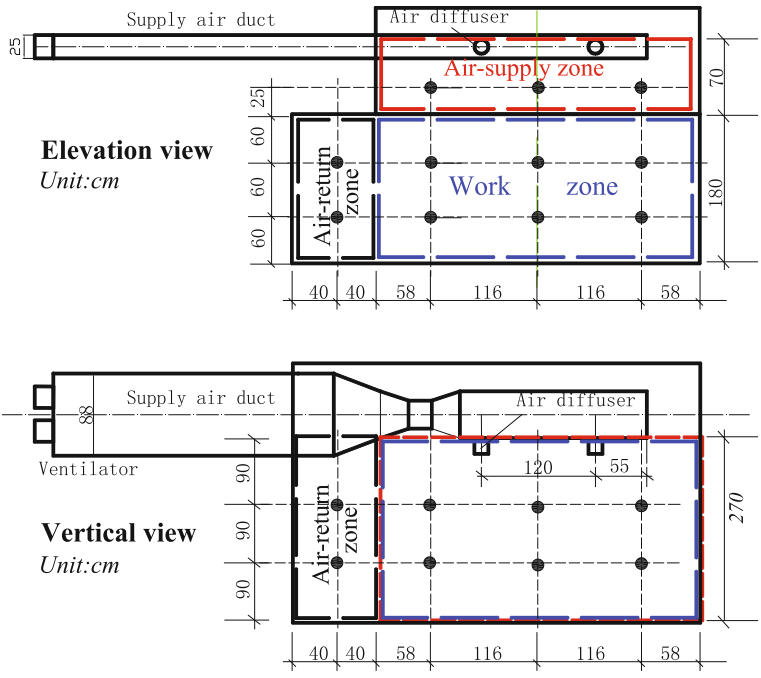

Fig. 2.32 Test room and detailed positions of temperature sensors

respectively, as shown in Fig. 2.23. The internal surface area of walls corresponding to the three zones is 13.72, 20.52, and 3.60 m^2 respectively. The contact area between the work zone and the air-supply zone and the air-return zone is 9.40 m^2 and 4.90 m^2, respectively. Figure 2.32 also shows detailed locations of thermocouples (measurement precision: ±0.1 °C) in the room. The measured air temperature of each zone is obtained through taking average value of all test points in corresponding zone. A humidity sensor (measurement precision: ±0.8 % of the humidity ratio) is placed in the air-return zone to observe the air humidity. The supply airflow rate is measured with a hot-wire anemometer with a measurement precision of ±0.015 m/s. Being one of the initial conditions, the internal surface temperatures of the walls are measured by thermocouples (measurement precision: ±0.1 °C) embedded in the internal surface of the walls. The heat sources in the air-supply zone are fluorescent lamps whose surface area is estimated as 0.3 m^2. In the work zone, there are two adults (total body surface area: 3.65 m^2) and a constant-temperature plate heater (surface area: 0.28 m^2). An infrared thermometer (measurement precision: ±0.2 °C) is used to measure surface temperature of the indoor heat sources. The surface temperature was measured to be 39.6, 35.2, and 43.9 °C, respectively, for the lamps, the human bodies, and the plate heater during the dynamic response experiments.

Two experimental cases have been investigated for a time period of 2400 s. The initial conditions for the model validation (see Table 2.16) were obtained before the

Table 2.16 Initial conditions for the room model validation

Experimental cases	Case I	Case II
Parameters		
Air-supply temperature $(t_{a,i})_o$ (°C)	31.4	26.4
Air-supply humidity $(W_{a,i})_o$ (g/(kg dry air))	20.3	18.1
Air temperature in the air-supply zone $(t_{a,s})_o$ (°C)	32.1	28.0
Air humidity in the air-supply zone $(W_{a,s})_o$ (g/(kg dry air))	20.3	18.1
Internal surface temperature of walls in the air-supply zone $(t_{riw,s})_o$ (°C)	32.7	30.2
Air temperature in the work zone $(t_{a,n})_o$ (°C)	33.0	29.5
Air humidity in the work zone $(W_{a,n})_o$ (g/(kg dry air))	20.5	18.3
Internal surface temperature of walls in the work zone $(t_{riw,n})_o$ (°C)	33.2	30.6
Air temperature in the air-return zone $(t_{a,r})_o$ (°C)	33.1	29.9
Air humidity in the air-return zone $(W_{a,r})_o$ (g/(kg dry air))	20.5	18.3
Internal surface temperature of walls in the air-return zone $(t_{riw,r})_o$ (°C)	33.6	31.1
Supply airflow rate $(G_a)_o$ (kg/s)	0.15	0.20

Other parameters for the model calculation: c_a = 1005 J/(kg °C); c_{riw} = 1250 J/(kg °C); ρ_a = 1.18 kg/m^3; ρ_{riw} = 1800 kg/m^3; δ_{riw} = 0.22 m

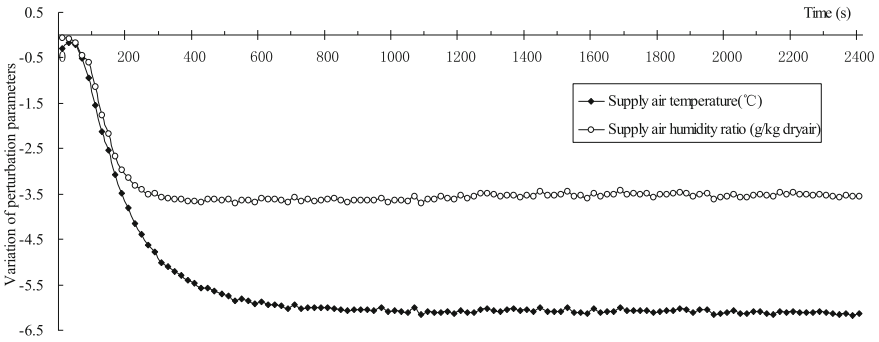

Fig. 2.33 Variation of perturbation parameters in the case I (measured data)

response experiments began. All the values of air temperature and humidity as well as wall surface temperatures were collected with a data acquisition system at a sample interval of two seconds.

(2) Experimental results

Experimental case I

Figure 2.33 shows the variation of perturbation parameters in the experimental case *I*, in which the supply air temperature and humidity ratio decrease till to steady value. The calculated and experimental results on the transient response of indoor air temperature and humidity in different air zones under the initial conditions of case *I* are shown in Figs. 2.34 and 2.35. In the model calculation, the convective heat transfer coefficients are taken as 9.2, 11.6 and 3.2 W/(m^2.K), respectively, for the room walls, the indoor heat sources, and the air layers between the adjacent indoor air zones. As shown in Figs. 2.34 and 2.35, the calculated response curves of the indoor air temperatures and humidity ratios are favorably consistent with the experimental ones, and the average errors of the calculated results compared with the experimental data are all lower than 10 % .

Experimental case II

Figure 2.36 shows the perturbations under the initial conditions of the case *II*, in which the supply air temperature and humidity ratio increase. The corresponding results on the response of the indoor air temperature and humidity in different air zones are shown in Figs. 2.37 and 2.38. In this case, the heat transfer coefficients of internal wall surface and indoor heat sources as well as the air layers between the adjacent indoor air zones are adjusted, respectively, as 10.7, 12.3, and 3.6 W/(m^2 K) for the model calculations, which are a little larger than that in the case *I* due to the higher supply airflow rate in the case *II* (0.20 kg/s). The average errors of the calculated results compared with the experimental data are no more than 12 % for the case *II*.

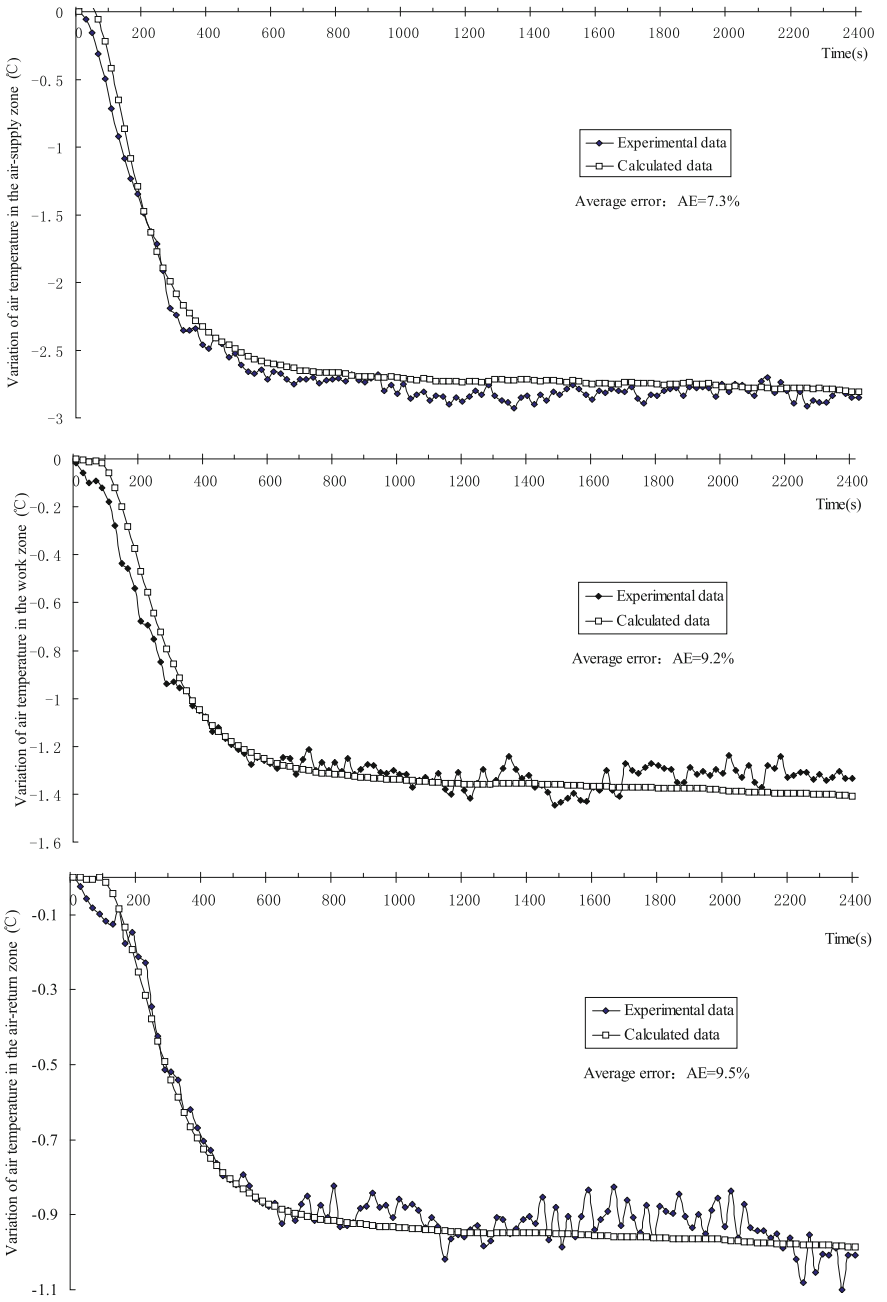

Fig. 2.34 Dynamic responses of air temperature in different zones in the case I (calculation vs. measurement)

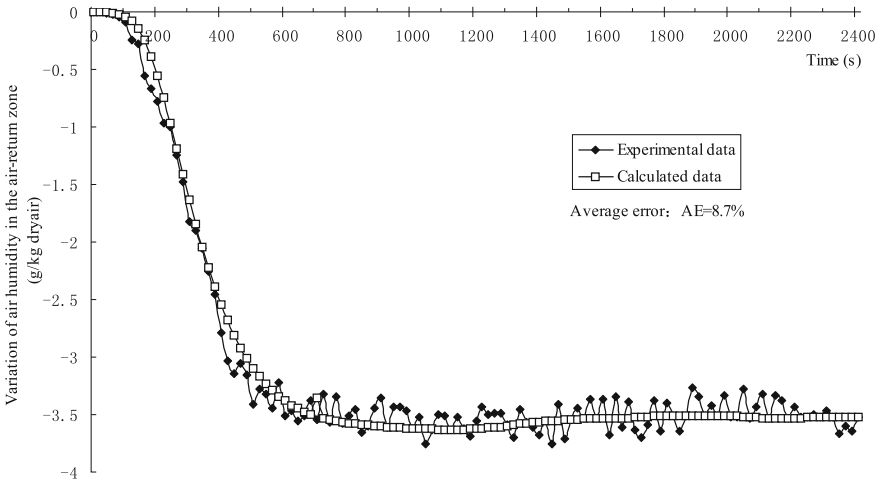

Fig. 2.35 Dynamic responses of air humidity in the air-return zone in the case I (calculation vs. measurement)

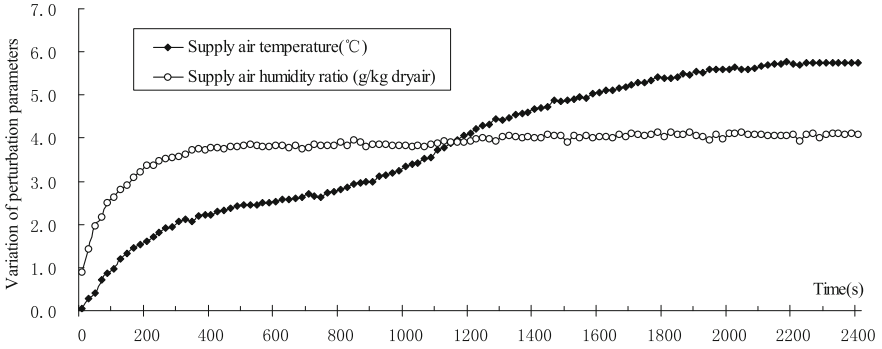

Fig. 2.36 Variation of perturbation parameters in the case II (measured data)

2.3 Modeling for HVAC System

2.3.1 Component Model Connection

HVAC system comprises of numerous components or subsystems. These components or subsystems are generally connected in parallel or series, as shown in Fig. 2.39.

In Fig. 2.39, the components S_1 and S_2 are expressed, respectively, by Eqs. (2.207) and (2.208)

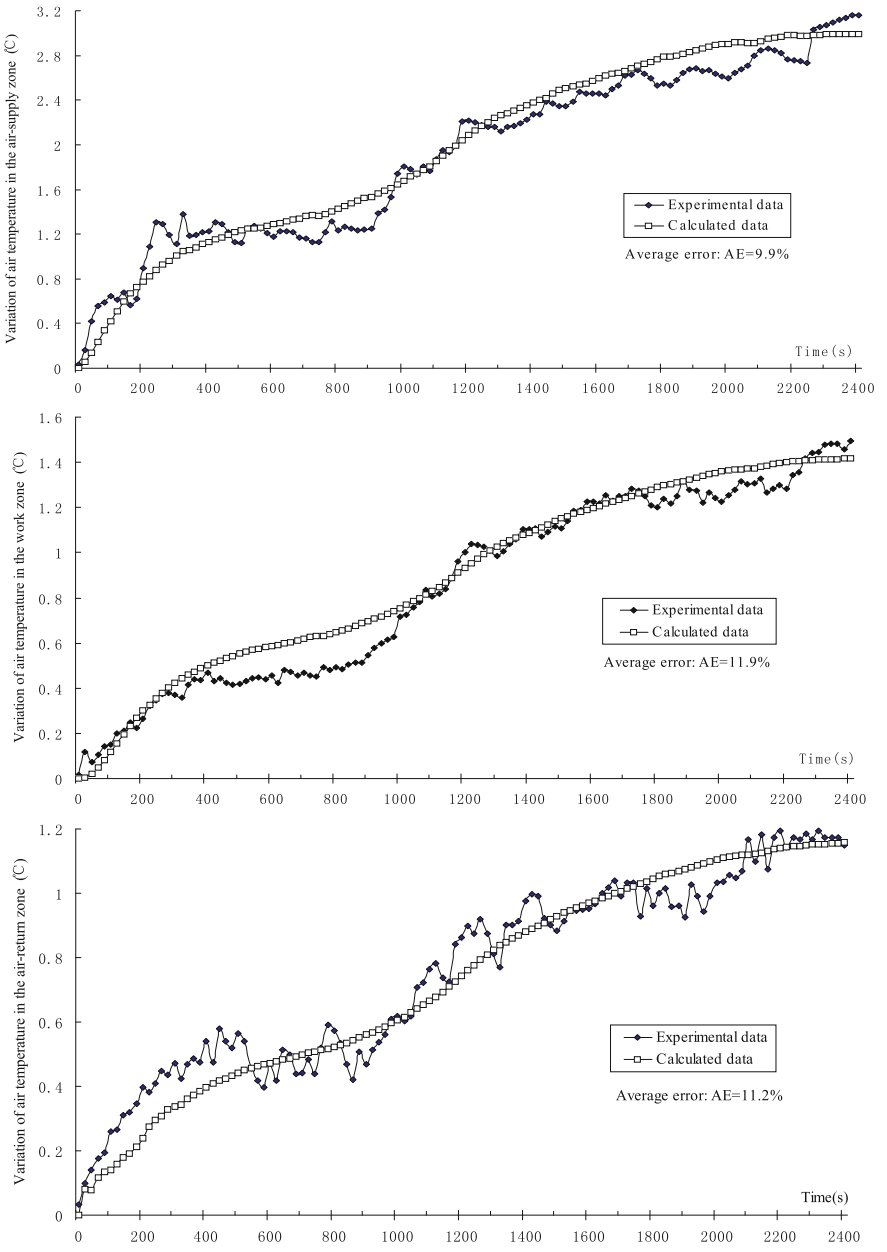

Fig. 2.37 Dynamic responses of air temperature in different zones in the case II (calculation vs. measurement)

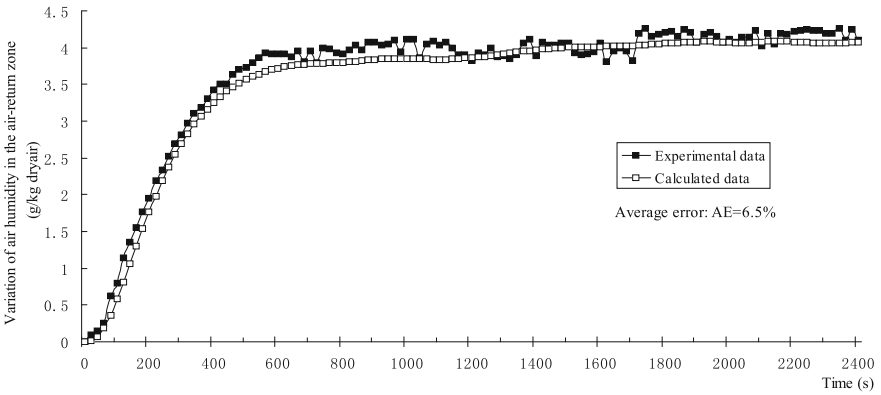

Fig. 2.38 Dynamic responses of air humidity in the air-return zone in the case II (calculation vs. measurement)

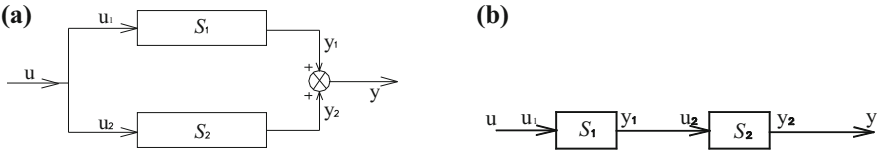

Fig. 2.39 Schematic diagram for the component model connection. **a** Parallel connection. **b** Series connection

$$\text{Component } S_1: \begin{cases} \dot{x}_1 = A_1 x_1 + B_1 u \\ y_1 = C_1 x_1 + D_1 u_1 \end{cases} \tag{2.207}$$

$$\text{Component } S_2: \begin{cases} \dot{x}_2 = A_2 x_2 + B_2 u_2 \\ y_2 = C_2 x_2 + D_2 u_2 \end{cases} \tag{2.208}$$

2.3.1.1 Parallel Connection

When the type of output parameters and dimensions of the two subsystems are simultaneously **homogeneous**, the various parameters in the combined system output vector $\boldsymbol{y}$ is equal to the sum of corresponding parameter values of output vector y_1 for subsystem S_1 and output vector y_2 for subsystem S_2, i.e.,

$$[y] = [y_1] + [y_2] \tag{2.209}$$

In such case, the state-space equation of combined system in parallel connection (Fig. 2.39a) is described as follows:

$$\begin{bmatrix} \dot{x}_1 \\ \dot{x}_2 \end{bmatrix} = \begin{bmatrix} A_1 & 0 \\ 0 & A_2 \end{bmatrix} \cdot \begin{bmatrix} x_1 \\ x_2 \end{bmatrix} + \begin{bmatrix} B_1 & 0 \\ 0 & B_2 \end{bmatrix} \cdot \begin{bmatrix} u_1 \\ u_2 \end{bmatrix} \tag{2.209a}$$

$$y = [C_1 C_2] \cdot \begin{bmatrix} x_1 \\ x_2 \end{bmatrix} + [D_1 D_2] \cdot \begin{bmatrix} u_1 \\ u_2 \end{bmatrix} \tag{2.209b}$$

When the type of output parameters and dimensions of the two subsystems are not simultaneously homogeneous (i.e., not similar), the combined system output vector $\boldsymbol{y}$ is the union of output vectors y_1 and y_2 of subsystems S_1 and S_2, respectively, i.e.,

$$[y] = \begin{bmatrix} y_1 \\ y_2 \end{bmatrix} \tag{2.210}$$

In such case, the state-space model of the parallel system (Fig. 2.39a) can be obtained as follows:

$$\begin{bmatrix} \dot{x}_1 \\ \dot{x}_2 \end{bmatrix} = \begin{bmatrix} A_1 & 0 \\ 0 & A_2 \end{bmatrix} \cdot \begin{bmatrix} x_1 \\ x_2 \end{bmatrix} + \begin{bmatrix} B_1 & 0 \\ 0 & B_2 \end{bmatrix} \cdot \begin{bmatrix} u_1 \\ u_2 \end{bmatrix} \tag{2.211a}$$

$$[y] = \begin{bmatrix} C_1 & 0 \\ 0 & C_2 \end{bmatrix} \cdot \begin{bmatrix} x_1 \\ x_2 \end{bmatrix} + \begin{bmatrix} D_1 & 0 \\ 0 & D_2 \end{bmatrix} \cdot \begin{bmatrix} u_1 \\ u_2 \end{bmatrix}. \tag{2.211b}$$

2.3.1.2 Series Connection

The combined system in series connection (Fig. 2.39b) has input vector $u = u_1$ and output vector $y = y_2$; and the output vector y_1 of subsystem S_1 is equal to the input vector u_2 of subsystem S_2. Thus, we have

$$\dot{x}_1 = A_1 x_1 + B_1 u_1 \tag{2.212}$$

$$y_1 = C_1 x_1 + D_1 u_1 \tag{2.213}$$

$$\dot{x}_2 = A_2 x_2 + B_2 u_2 = A_2 x_2 + B_2 y_1 = A_2 x_2 + B_2 C_1 x_1 + B_2 D_1 u \tag{2.214}$$

$$y_2 = C_2 x_2 + D_2 u_2 = C_2 x_2 + D_2 y_1 = C_2 x_2 + D_2 C_1 x_1 + D_2 D_1 u \tag{2.215}$$

So, the combined system equation of series connection of S_1 and S_2 is as follows:

$$\begin{bmatrix} \dot{x}_1 \\ \dot{x}_2 \end{bmatrix} = \begin{bmatrix} A_1 & 0 \\ B_2C_1 & A_2 \end{bmatrix} \cdot \begin{bmatrix} x_1 \\ x_2 \end{bmatrix} + \begin{bmatrix} B_1 \\ B_2D_1 \end{bmatrix} \cdot u \tag{2.215}$$

$$y = \begin{bmatrix} D_2C_1 & C_2 \end{bmatrix} \cdot \begin{bmatrix} x_1 \\ x_2 \end{bmatrix} + D_2D_1u \tag{2.216}$$

2.3.2 State-Space Representation for HVAC System

Taking a general HVAC system (see Fig. 2.40) for example, in order to make the system be of hierarchy, the system can be divided into five subsystems: ① refrigeration system represented by S_{refri}; ② cooling coolant system represented by S_{conw} which consists of cooling coolant pump, cooling tower, and pipes; ③ chilled coolant system represented by S_{chw} which consists of chilled coolant pump and pipes; ④ air-handling system represented by S_{ahu} which consists of surface heat exchanger and supply air fan; ⑤ supply air system represented by $S_{\text{air,s}}$; and exhaust-return air system represented by $S_{\text{air,er}}$. Based on the above principle of model connection, we can get state-space model of the subsystems in the HVAC system.

2.3.2.1 Mathematical Dynamic Model of Cooling Coolant System (S_{conw})

$$\dot{X}_{\text{conw}} = A_{\text{conw}}X_{\text{conw}} + B_{\text{conw}}U_{\text{conw}} \tag{2.217}$$

$$Y_{\text{conw}} = C_{\text{zpipe,2}}x_{\text{zpipe,2}} + D_{\text{zpipe,2}}C_{\text{tower,w}}x_{\text{tower}} + R_3u_{\text{tower,w}} \tag{2.218}$$

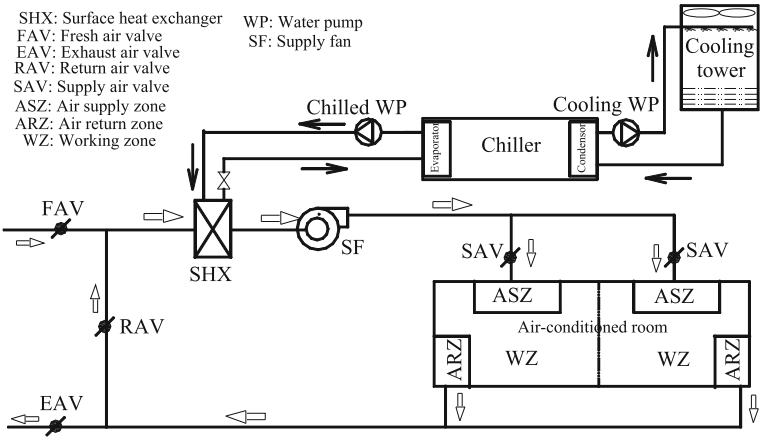

Fig. 2.40 Schematic diagram of a HVAC system

where

$$X_{\text{conw}} = [x_{\text{pump},1}, x_{\text{zpipe},1}, x_{\text{tower}}, x_{\text{zpipe},2}]^T; U_{\text{conw}} = [u_{\text{pump,w},1}, \Delta U_{\text{m}}, u_{\text{tower},1}, u_{\text{tower,w}}]^T;$$
$$Y_{\text{conw}} = y_{\text{zpipe},2};$$
$$A_{\text{conw}} = \begin{bmatrix} A_{\text{pump},1} & 0 & 0 & 0 \\ B_{\text{zpipe},1}C_{\text{pump,w},1} & A_{\text{zpipe},1} & 0 & 0 \\ B_{\text{tower,w}}D_{\text{zpipe},1}C_{\text{pump,w},1} & B_{\text{tower,w}}C_{\text{zpipe},1} & A_{\text{tower}} & 0 \\ 0 & 0 & B_{\text{zpipe},2}C_{\text{tower,w}} & A_{\text{zpipe},2} \end{bmatrix};$$
$$U_{\text{conw}} = \begin{bmatrix} B_{\text{pump,w},1} & B_{\text{pump,U},1} & 0 & 0 \\ R_1 & 0 & 0 & 0 \\ 0 & 0 & B_{\text{tower,a}} & 0 \\ 0 & 0 & 0 & R_2 \end{bmatrix};$$
$$R_1 = \begin{bmatrix} \left(\frac{X_{\text{p},3}}{T_{\text{p,tw}}}\right)_1 & 0 \\ \left(\frac{Y_{\text{p},3}}{T_{\text{p,pg}}}\right)_1 & 0 \end{bmatrix}; R_2 = \begin{bmatrix} 0 & \left(\frac{X_{\text{p},4}}{T_{\text{p,tw}}}\right)_2 \\ 0 & \left(\frac{Y_{\text{p},4}}{T_{\text{p,pg}}}\right)_2 \end{bmatrix}; R_3 = \begin{bmatrix} 0 & 0 \\ 0 & 1 \end{bmatrix}.$$

2.3.2.2 Mathematical Dynamic Model of Chilled Coolant System (S_{chw})

The chilled coolant system consists of water-to-air heat exchanger, pipes, and pump which are in series connection. The state-space model for the chilled coolant system (S_{chw}) can be written as follows:

$$\dot{X}_{\text{chw}} = A_{\text{chw}}X_{\text{chw}} + B_{\text{chw}}U_{\text{chw}} \tag{2.219}$$

$$Y_{\text{chw}} = C_{\text{zpipe},4}x_{\text{zpipe},4} + D_{\text{zpipe},4}C_{\text{coil,w}}x_{\text{coil}} + D_{\text{zpipe},4}R_5C_{\text{zpipe},3}x_{\text{zpipe},3} + D_{\text{zpipe},4}R_5D_{\text{zpipe},3}C_{\text{pump,w},2}x_{\text{pump},2} \tag{2.220}$$

where

$$X_{\text{chw}} = [x_{\text{pump},2}, x_{\text{zpipe},3}, x_{\text{coil}}, x_{\text{zpipe},4}]^T; U_{\text{chw}} = [u_{\text{pump,w},2}, \Delta U_{\text{m}}]^T; Y_{\text{chw}} = y_{\text{zpipe},4};$$
$$A_{\text{chw}} = \begin{bmatrix} A_{\text{pump},2} & 0 & 0 & 0 \\ B_{\text{zpipe},3}C_{\text{pump,w},2} & A_{\text{zpipe},3} & 0 & 0 \\ B_{\text{coil,w}}D_{\text{zpipe},3}C_{\text{pump,w}} & B_{\text{coil,w}}C_{\text{zpipe},3} & A_{\text{coil}} & 0 \\ B_{\text{zpipe},4}R_5D_{\text{zpipe},3}C_{\text{pump,w},2} & B_{\text{zpipe},4}R_5C_{\text{zpipe},3} & B_{\text{zpipe},4}C_{\text{coil,w}} & A_{\text{zpipe},4} \end{bmatrix};$$

$$B_{\text{chw}} = \begin{bmatrix} B_{\text{pump,w,2}} & B_{\text{pump,U,2}} \\ R_4 & 0 \\ 0 & 0 \\ 0 & 0 \end{bmatrix}; R_4 = \begin{bmatrix} \left(\frac{X_{\text{p,3}}}{T_{\text{p,tw}}}\right)_3 & 0 \\ \left(\frac{Y_{\text{p,3}}}{T_{\text{p,pg}}}\right)_3 & 0 \end{bmatrix}; R_5 = \begin{bmatrix} 0 & 0 \\ 0 & 1 \end{bmatrix}.$$

2.3.2.3 Mathematical Dynamic Model of Supply Air System ($S_{\text{air,s}}$)

$$\dot{\mathrm{X}}_{\text{air,s}} = A_{\text{air,s}} X_{\text{air,s}} + B_{\text{air,s}} U_{\text{air,s}} \tag{2.221}$$

$$Y_{\text{air,s}} = C_{\text{air,s}} X_{\text{air,s}} + D_{\text{air,s}} U_{\text{air,s}} \tag{2.222}$$

where

$$X_{\text{air,s}} = \left[x_{\text{zduct,1}}, x_{\text{zduct,2}}\right]^T; Y_{\text{air,s}} = \left[\left(y_{\text{sduct,2}}\right)_1, y_{\text{zduct,2}}\right]^T; U_{\text{air,s}} = u_{\text{zduct,1}};$$

$$A_{\text{air,s}} = \begin{bmatrix} A_{\text{zduct,1}} & 0 \\ B_{\text{zduct,2}}\left(C_{\text{fda13,E}}\right)_1 C_{\text{zduct,1}} & A_{\text{zduct,2}} \end{bmatrix}; B_{\text{air,s}} = \begin{bmatrix} B_{\text{zduct,1}} \\ B_{\text{zduct,2}}\left(C_{\text{fda13,E}}\right)_1 D_{\text{zduct,1}} \end{bmatrix};$$

$$C_{\text{air,s}} = \begin{bmatrix} \left(C_{\text{fda12,E}}\right) C_{\text{zduct,1}} & 0 \\ D_{\text{zduct,2}}\left(C_{\text{fda13,E}}\right)_1 C_{\text{zduct,1}} & C_{\text{zduct,2}} \end{bmatrix}; D_{\text{air,s}} = \begin{bmatrix} \left(C_{\text{fda12,E}}\right)_1 D_{\text{zduct,1}} \\ D_{\text{zduct,2}}\left(C_{\text{fda13,E}}\right)_1 D_{\text{zduct,1}} \end{bmatrix}.$$

2.3.2.4 Mathematical Dynamic Model of Exhaust-Return Air System ($S_{\text{air,Er}}$)

$$\dot{X}_{\text{air,er}} = A_{\text{air,er}} X_{\text{air,er}} + B_{\text{air,er}} U_{\text{air,er}} \tag{2.223}$$

$$Y_{\text{air,er}} = C_{\text{air,er}} X_{\text{air,er}} + D_{\text{air,er}} U_{\text{air,er}} \tag{2.224}$$

where

$$X_{\text{air,er}} = x_{\text{zduct,3}}; Y_{\text{air,er}} = \left[\left(y_{\text{sduct,2}}\right)_3, \left(y_{\text{sduct,3}}\right)_3\right]^T; U_{\text{air,er}} = \left(u_{\text{sduct}}\right)_2;$$

$$A_{\text{air,er}} = A_{\text{zduct,3}}; B_{\text{air,er}} = B_{\text{zduct,3}}\left(C_{\text{sduct}}\right)_2;$$

$$C_{\text{air,er}} = \left[\left(C_{\text{fda12,E}}\right)_3 C_{\text{zduct,3}}, \left(C_{\text{fda13,E}}\right)_3 C_{\text{zduct,3}}\right]^T;$$

$$C_{\text{air,er}} = \left[\left(C_{\text{fda12,E}}\right)_3 D_{\text{zduct,3}}\left(C_{\text{sduct}}\right)_2, \left(C_{\text{fda13,E}}\right)_3 D_{\text{zduct,3}}\left(C_{\text{sduct}}\right)_2\right]^T;$$

$$\left(u_{\text{sduct}}\right)_2 = \left[\left(u_{\text{sduct,1}}\right)_2, \left(u_{\text{sduct,2}}\right)_2\right]; \left(C_{\text{sduct}}\right)_2 = \left[\left(C_{\text{da1,E}}\right)_2, \left(C_{\text{da2,E}}\right)_2\right].$$

2.3.2.5 Mathematical Dynamic Model of Air-Handling System (S_{ahu})

$$\dot{X}_{ahu} = A_{ahu}X_{ahu} + B_{ahu}U_{ahu} \tag{2.225}$$

$$Y_{ahu} = C_{coil,a}x_{coil} + R_7C_{fan,a}x_{fan} + R_7R_6(C_{sduct})_4(u_{sduct})_4 \tag{2.226}$$

where

$$X_{ahu} = [x_{fan}, x_{coil}]^T; Y_{ahu} = y_{coil,a}; U_{ahu} = [\Delta U_m, u_{coil,w}, (u_{sduct})_4]^T;$$
$$(u_{sduct})_4 = [(u_{sduct,1})_4, (u_{sduct,2})_4]; (C_{sduct})_4 = [(C_{da1,E})_4, (C_{da2,E})_4];$$
$$A_{ahu} = \begin{bmatrix} A_{fan} & 0 \\ B_{coil,a}C_{fan,a} & A_{coil} \end{bmatrix}; B_{ahu} = \begin{bmatrix} B_{fan,U} & 0 & 0 \\ 0 & B_{coil,w} & B_{coil,a}R_6(C_{sduct})_4 \end{bmatrix}; R_6 = \begin{bmatrix} 1 & 0 & 0 \\ 0 & 1 & 0 \\ 0 & 0 & 0 \end{bmatrix};$$

Under dry condition: $R_7 = \begin{bmatrix} 0 & 0 & 0 \\ 0 & 1 & 0 \\ 0 & 0 & 1 \end{bmatrix}$; Under wet condition: $R_7 = \begin{bmatrix} 0 & 0 & 0 \\ 0 & 0 & 0 \\ 0 & 0 & 1 \end{bmatrix}$.

2.3.3 Case Study

2.3.3.1 System Model Description

On the basis of state-space models of components and connection principle, this section gives an example on the system model integration. The system considered in this study consists of a water-to-air surface heat exchanger, an outlet water pipe, and an outlet air duct. According to the actual situation, the water outlet pipe and air outlet duct are in parallel, and they are connected to the heat exchanger in series, as shown in Fig. 2.41.

According to the state-space representation of component models in the previous chapters, the state-space model of water-to-air surface heat exchanger can be represented by:

$$\dot{X}_{coil} = A_{coil}X_{coil} + B_{coil}u_{coil} \tag{2.227}$$

$$Y_{coil} = C_{coil}X_{coil} + D_{coil}u_{coil} - C_{coil}A_{coil}^{-1}\xi_{coil} \tag{2.228}$$

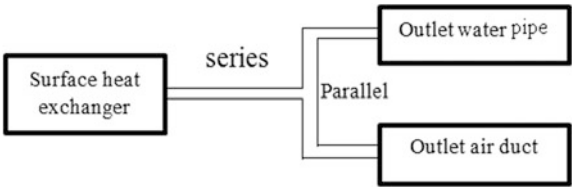

Fig. 2.41 Multi-component system in this case study

The state-space model for water pipe can be represented by:

$$\dot{X}_{\text{zpipe}} = A_{\text{zpipe}} X_{\text{zpipe}} + B_{\text{zpipe}} u_{\text{zpipe}} \tag{2.229}$$

$$Y_{\text{zpipe}} = C_{\text{zpipe}} X_{\text{zpipe}} + D_{\text{zpipe}} u_{\text{zpipe}} - C_{\text{zpipe}} A_{\text{zpipe}}^{-1} \xi_{\text{zpipe}} \tag{2.230}$$

The state-space model of air duct can be written as follows:

$$\dot{X}_{\text{zduct}} = A_{\text{zduct}} X_{\text{zduct}} + B_{\text{zduct}} u_{\text{zduct}} \tag{2.231}$$

$$Y_{\text{zduct}} = C_{\text{zduct}} X_{\text{zduct}} + D_{\text{zduct}} u_{\text{zduct}} - C_{\text{zduct}} A_{\text{zduct}}^{-1} \xi_{\text{zduct}} \tag{2.232}$$

To begin with, the state-space model of parallel connection of air duct and water pipe are obtained as follows:

$$\dot{X}_{\text{duct\&pipe}} = \begin{bmatrix} \dot{X}_{\text{zpipe}} \\ \dot{X}_{\text{zduct}} \end{bmatrix} = \dot{A}_{\text{duct\&pipe}} \begin{bmatrix} X_{\text{zpipe}} \\ X_{\text{zduct}} \end{bmatrix} + \dot{B}_{\text{duct\&pipe}} \begin{bmatrix} u_{\text{zpipe}} \\ u_{\text{zduct}} \end{bmatrix} \tag{2.233}$$

$$Y_{\text{duct\&pipe}} = \begin{bmatrix} Y_{\text{zpipe}} \\ Y_{\text{zduct}} \end{bmatrix} = \dot{C}_{\text{duct\&pipe}} \begin{bmatrix} X_{\text{zpipe}} \\ X_{\text{zduct}} \end{bmatrix} + \dot{D}_{\text{duct\&pipe}} \begin{bmatrix} u_{\text{zpipe}} \\ u_{\text{zduct}} \end{bmatrix} - \zeta_{\text{duct\&pipe}} \tag{2.234}$$

where

$$\begin{aligned} A_{\text{duct\&pipe}} &= \begin{bmatrix} A_{\text{zpipe}} & 0 \\ 0 & A_{\text{zduct}} \end{bmatrix}; B_{\text{duct\&pipe}} = \begin{bmatrix} B_{\text{zpipe}} & 0 \\ 0 & B_{\text{zduct}} \end{bmatrix}; C_{\text{duct\&pipe}} \\ &= \begin{bmatrix} C_{\text{zpipe}} & 0 \\ 0 & C_{\text{zduct}} \end{bmatrix}; D_{\text{duct\&pipe}} = \begin{bmatrix} D_{\text{zpipe}} & 0 \\ 0 & D_{\text{zduct}} \end{bmatrix}; \zeta_{\text{duct\&pipe}} \\ &= \begin{bmatrix} C_{\text{zpipe}} A_{\text{zpipe}}^{-1} \xi_{\text{zpipe}} \\ C_{\text{zduct}} A_{\text{zduct}}^{-1} \xi_{\text{zduct}} \end{bmatrix}. \end{aligned}$$

Then, the above state-space model in parallel is integrated with the water-to-air heat exchanger in series, and we have:

$$\dot{X}_{\text{sys}} = A_{\text{sys}}X_{\text{sys}} + B_{\text{sys}}\,\dot{u}_{\text{coil}} - \xi_{\text{Xsys}} \tag{2.235}$$

$$Y_{\text{sys}} = Y_{\text{duct\&pipe}} = C_{\text{sys}}\dot{X}_{\text{sys}} + D_{\text{sys}}\dot{u}_{\text{coil}} - \xi_{\text{Ysys}} \tag{2.236}$$

where

$$X_{\text{sys}} = \begin{bmatrix} X_{\text{coil}} \\ X_{\text{duct\&pipe}} \end{bmatrix}; A_{\text{sys}} = \begin{bmatrix} A_{\text{coil}} & 0 \\ B_{\text{duct\&pipe}}C_{\text{coil}} & A_{\text{duct\&pipe}} \end{bmatrix}; B_{\text{sys}} = \begin{bmatrix} B_{\text{coil}} \\ B_{\text{duct\&pipe}}D_{\text{coil}} \end{bmatrix};$$

$$C_{\text{sys}} = \begin{bmatrix} D_{\text{duct\&pipe}}C_{\text{coil}} & C_{\text{duct\&pipe}} \end{bmatrix}; D_{\text{sys}} = D_{\text{duct\&pipe}}D_{\text{coil}};$$

$$\xi_{\text{Xsys}} = \begin{bmatrix} 0 \\ B_{\text{duct\&pipe}}C_{\text{coil}}A_{\text{coil}}^{-1}\xi_{\text{coil}} \end{bmatrix}; \xi_{\text{Ysys}} = D_{\text{duct\&pipe}}C_{\text{coil}}A_{\text{coil}}^{-1}\xi_{\text{coil}} + \xi_{\text{duct\&pipe}};$$

For the convenience of calculation, the system model, i.e., Eqs. (2.235) and (2.236), needs to be transformed into a standard form as follows:

$$\dot{\overline{X_{sys}}} = A_{sys}\overline{X_{sys}} + B_{sys}u_{coil} \tag{2.237}$$

$$Y_{\text{sys}} = C_{\text{sys}}\overline{X_{\text{sys}}} + D_{\text{sys}}u_{\text{sys}} + \xi_{\text{sys}} \tag{2.238}$$

where $\overline{X_{\text{sys}}} = X_{\text{sys}} - A_{\text{sys}}^{-1}\xi_{\text{Xsys}}$; $\xi_{\text{sys}} = C_{\text{sys}}A_{\text{sys}}^{-1}\zeta_{\text{Xsys}} - \zeta_{\text{Ysys}}$.

2.3.3.2 System Model Validation

An experimental air-conditioning system is built for the system model validation. As shown in Fig. 2.42, the system mainly consists of a water-to-air surface heat exchanger, a heat pump (for chilled or hot water supply), a circulating water pump, fans, air ducts, and water pipes. The test instruments mainly include the temperature

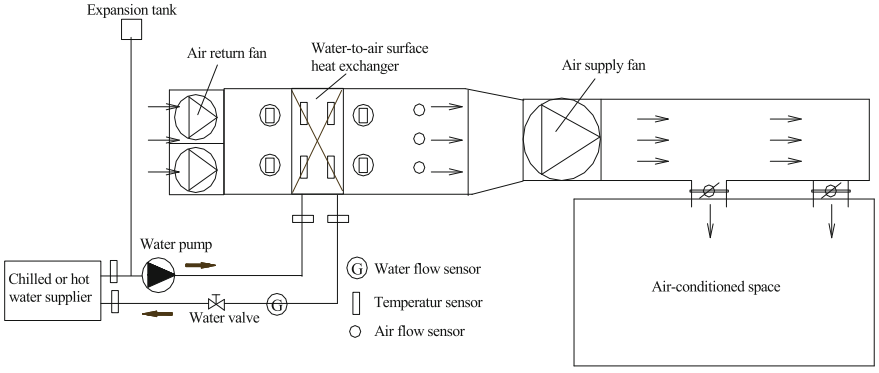

Fig. 2.42 Schematic diagram for the experimental system

Table 2.17 Initial conditions for system model validation

Initial conditions of parameters	Initial value
Inlet air temperature of surface heat exchanger, $(t_{a,E})_o$ (°C)	28.8
Inlet air humidity of surface heat exchanger, $(W_{a,E})_o$ (g/kg)	20.0
Airflow rate, $(G_a)_o$ (kg/s)	0.2002
Inlet water temperature of surface heat exchanger, $(t_{w,E})_o$ (°C)	29.1
Water flow rate, $(G_w)_o$ (kg/s)	0.930
External wall temperature of plate and fin pipe, $(t_g)_o$ (°C)	28.7
Wall temperature of air duct, $(t_{dg})_o$ (°C)	28.5
Exit air temperature of air duct, $(t_{da,L})_o$ (°C)	28.9
Exit air humidity of air duct, $(W_{da,L})_o$ (g/kg)	20.0
Wall temperature of water pipe, $(t_{pg})_o$ (°C)	29.4
Exit water temperature of water pipe, $(t_{pw,L})_o$ (°C)	27.5

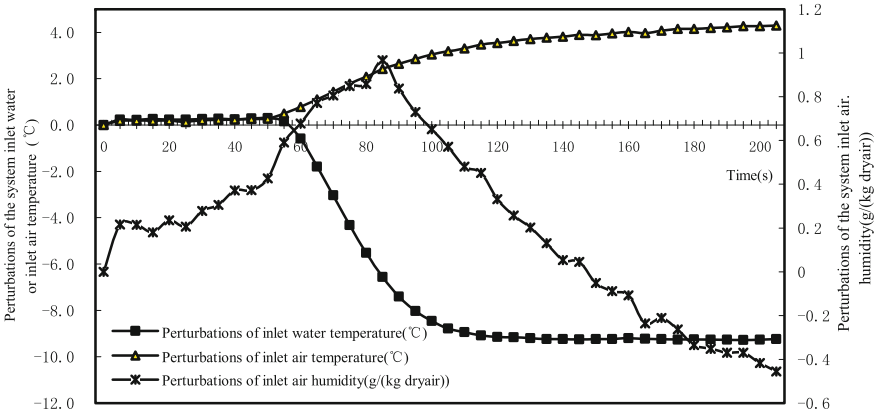

Fig. 2.43 Perturbations of inlet variables of the AHU system

sensors (measurement precision: ±0.1 °C), the water flow sensor (accuracy of measurement: 0.5 magnitude), and the hotwire anemometer (accuracy of measurement: ±2 % reading data).

The initial conditions (measured data) for the model validation are given in Table 2.17. The perturbations of inlet variables of the system are shown in Fig. 2.43. The experimental and calculated results of the change responses of the system exit variables are plotted in Fig. 2.44. As shown in Fig. 2.44, the calculated responses of the system exit variables under the perturbations of inlet variables have a favorable agreement with the experimental ones. The average error of the model calculation is estimated as 12.6, 22.2, and 9.5 %, respectively, for the response of the exit air temperature, the exit air humidity, and the exit water temperature of the system.

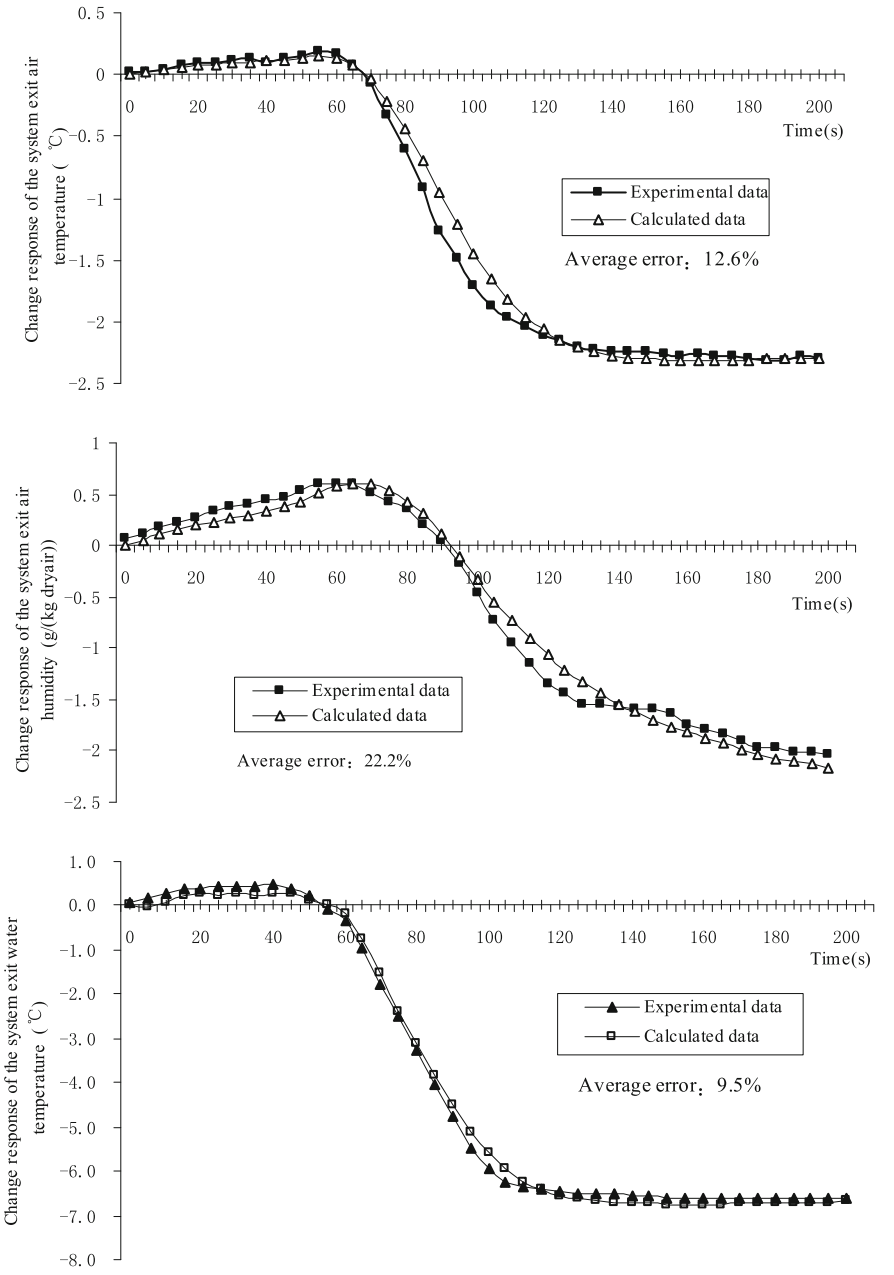

Fig. 2.44 Responses of exit variables of the AHU system (experimental vs. calculated)

References

1. Hangos, K.M., Lakner, R., Gerzson, M.: Intelligent Control Systems: An Introduction with Examples. Springer, Berlin (2001)
2. Hangos, K.M., Bokor, J., Szederkényi, G.: Analysis and Control of Nonlinear Process Systems. Springer, Berlin (2004)
3. Brogan, W.L.: Modern Control Theory (1st edn). Quantum Publishers Inc. (1974)
4. http://en.wikipedia.org/wiki/State-space_representation
5. ASHRAE. ASHRAE Handbook: Heating, Ventilating, and Air-conditioning Systems and Equipment (SI Edition). Atlanta (USA), GA (2004)
6. Yao, Y., Huang, M., Mo, J., Dai, S.: State-space model for transient behavior of water-to-air surface heat exchanger. Int. J. Heat Mass Transf. **66**(9), 173–192 (2013)
7. Vaisi, A., Talebi, S., Esmaeilpour, M.: Transient behavior simulation of fin-and-tube heat exchangers for the variation of the inlet temperatures of both fluids. Int. Commun. Heat Mass Transfer **38**(5), 951–957 (2011)
8. ASHRAE. ASHRAE Handbook—Fundamentals, Chap. 6. Atlanta (USA), GA (2005)
9. Yao, Y., Huang, M., Chen, J.: State-space model for dynamic behavior of vapor compression liquid chiller. Int. J. Refrig. **36**(8), 2128–2147 (2013)
10. Browne, M.W., Bansal, P.K.: An elemental NTU-ε model for vapour-compression liquid chillers. Int. J. Refrig. **24**(5), 612–627 (2001)
11. Chan, C.Y., Haselden, G.G.: Computer-based refrigerant thermodynamic properties, part 1: basic equations. Int. J. Refrig. **4**(1), 7–12 (1981)
12. Chan, C.Y., Haselden, G.G.: Computer-based refrigerant thermodynamic properties, part 2: program listings. Int. J. Refrig. **4**(1), 52–60 (1981)
13. Su, C.: Advanced Engineering Thermodynamics. Higher Education Press (HEP), Beijing (1987)
14. Lemmon, E.W., McLinden, M.O., Huber, M.L.: NIST Reference Fluid Thermodynamic and Transport Properties—REFPRO Users' Guide (version 7.0). National Institute of Standards and Technology (2002)
15. Zhang, X.M., Ren, Z.F.: Heat Transfer. China Architecture & Building Press, Beijing (2006)
16. Badescu, V.: Dynamic model of a complex system including PV cells, electric battery, electrical motor and water pump. Energy **28**, 1165–1181 (2003)
17. Yao, Y., Yang, K., Huang, M.: A state-space model for dynamic response of indoor air temperature and humidity. Build. Environ. **64**(6), 26–37 (2013)
18. Inard, C., Bouia, H., Dalicieux, P.: Prediction of air temperature distribution in buildings with a zonal model. Energy Build. **24**(2), 125–132 (1996)
19. Peng, X., van Paassen, A.H.C.: A state space model for predicting and controlling the temperature responses of indoor air zones. Energy Build. **28**(1), 197–203 (1998)
20. Liu, W., Lian, Z., Yao, Y.: Optimization on indoor air diffusion of floor-standing type room air-conditioners. Energy Build. **40**(2), 59–70 (2008)
21. Gao, J., Zhang, X., Zhao, J.N., Gao, F.S.: A heat transfer parameter at air interfaces in the BLOCK model for building thermal environment. Int. J. Therm. Sci. **49**(2), 463–470 (2010)

http://www.springer.com/978-3-662-53311-6

Modeling and Control in Air-conditioning Systems

Yao, Y.; Yu, Y.

2017, XXI, 479 p. 272 illus., 46 illus. in color., Hardcover
ISBN: 978-3-662-53311-6